



Derivation of Evaporative Resistance of Clothing from Its Thermal Resistance Measured on Dry Thermal Manikin

Dissertation Thesis

Study programme:

P3106 Textile Engineering

Study branch:

Textile Technics and Materials Engineering

Author:

Frederick Tungshing Fung, M.A.

Thesis Supervisor:

prof. Ing. Luboš Hes, DrSc.

Department of Textile Evaluation



Declaration

I hereby certify, I, myself, have written my dissertation as an original and primary work using the literature listed below and consulting it with my thesis supervisor and my thesis counsellor.

I acknowledge that my bachelor dissertation is fully governed by Act No. 121/2000 Coll., the Copyright Act, in particular Article 60 – School Work.

I acknowledge that the Technical University of Liberec does not infringe my copyrights by using my dissertation for internal purposes of the Technical University of Liberec.

I am aware of my obligation to inform the Technical University of Liberec on having used or granted license to use the results of my dissertation; in such a case the Technical University of Liberec may require reimbursement of the costs incurred for creating the result up to their actual amount.

At the same time, I honestly declare that the text of the printed version of my dissertation is identical with the text of the electronic version uploaded into the IS/STAG.

I acknowledge that the Technical University of Liberec will make my dissertation public in accordance with paragraph 47b of Act No. 111/1998 Coll., on Higher Education Institutions and on Amendment to Other Acts (the Higher Education Act), as amended.

I am aware of the consequences which may under the Higher Education Act result from a breach of this declaration.

September 10, 2021

Frederick Tungshing Fung, M.A.

Acknowledgment

First, I would like to thank **Prof. Ing. Luboš Hes, DrSc.** (my supervisor) for his tremendous dedication to teaching, effective instructions, and carefully listening to a non-scientific person like me.

Special thanks to **Doc. Ing. Vladimir Bajzik, Ph.D.** and **Prof. Dr. Unmar Roshan** for their detail-oriented guidance, advice and demonstrations to help me see a different light on the same matter.

I would also like to thank professors and technicians from universities and institutes that offered me ample time, patience, help, and advice during the Erasmus internship and the Mobility training. I am deeply appreciated and thankful for their generosity and hospitality.

Politechnika Łódzka - Lodz University of Technology (LUT)

Poland 10-11/2017 - *Faculty of Material Technologies and Textile Design (W4), Institute of Material Science of Textile and Polymer Composites*

Prof. Dr. Hab. Eng. Izabella Krucińska (Director of the Institute)

Dr. Hab. Eng. Zbigniew Draczyński (prof. university)

Dr. Inz. Ewa Skrzetuska and Dr. Inz. Agnieszka Komisarczyk
(Sweating thermal manikin laboratory assistance)

浙江纺织服装职业技术学院 - Zhejiang Fashion Institute of Technology (ZFIT) China 12-01/2017-2018 - *Textile College*

王瑄 - 紡織書院院長, Xuan Wang (Head of Textile College)

俞鑫 - 老師, Sisi Yu (Lecturer)

İstanbul Teknik Üniversitesi - Istanbul Technical University (ITU)

Turkey 06-07/2018 - *Faculty of Textile Technologies and Design, Textile Engineer*

Prof. Dr. Fatma Kalaoglu

Pelin Altay, Doctoral student

Lund University (LU)

Sweden 08-10/2019 - *Thermal Environment Laboratory, Division of Ergonomics and Aerosol Technology, Department of Design Sciences, Faculty of Engineering*

Associate Prof. Chuansi Gao

Amitava Halder, Doctoral student

University of Mauritius (UOM)

Mauritius, Faculty of Engineering, Department of Applied Sustainability and Enterprise Development (DASED)

Prof. Dr. Unmar Roshan

Technická univerzita v Liberci – Technical University of Liberec (TUL)

Czech Republic 2016-2021- Faculty of Textile Engineering:

Department of Technologies and Structures

Ing. Gabriela Krupincová, Ph.D

Study Department

Bohumila Keilová and Ing. Hana Musilová, Ph.D.

Erasmus plus and Mobility

Ing. Pavla Tesinova, Ph.D. and Ing. Radka Přeučilová

I.T. Technician

Petr Kulhánek, Petr Kavan, Ing. Michal Chotěbor, Ing. Michal Martinka

Department of Evaluation

Prof. Ing. Luboš Hes, DrSc. (my supervisor)

Doc. Ing. Vladimír Bajzik, Ph.D.

A big thank you to **my brothers and sisters** for their endless support, good wishes and encouragement.

*Last, I want to thank my dear **Lord** which art in heaven; looking after me since the beginning of time, guiding me to walk on the right path, enlightening my heart when I am confused and helping me relentlessly when I in needs.*

Thank you all.

God bless you all.

Abbreviations

2D	stands for two-dimensional
3D	stands for three-dimensional
ANOVA	stands for Analysis of Variance
Cot	stands for cotton
CV	stands for coefficient of variances
Eq	stands for equation
<i>Gr</i>	stands for Grashof number, a dimensionless number
H	stands for horizontal
ISO	stands for an independent, non-governmental international organization for standardization that develops standards to ensure the quality, safety, and efficiency of products, services, and systems
<i>L</i>	stands for the length/thickness
Pes	stands for polyester
PP	stands for polypropylene
<i>Pr</i>	stands for the Prandtl number, a dimensionless number
<i>Ra</i>	stands for the Rayleigh number, a dimensionless number
SGHP	stands for the sweating guarded hotplate apparatus
<i>T</i>	stands for the ambient temperature
V	stands for vertical
Vs	stands for versus - is the abbreviation to compare
<i>p-value</i>	stands for probability value, is the resultant value from a null hypothesis significance testing

Symbols

Symbol	Description	Unit
A	is the area	$[m^2]$
D_p	is the pressure diffusivity	$[Pa/s]$
Dp	is the water vapor thermal diffusivity	$[W/m.Pa]$
DP	is the water vapor diffusion permeability/ coefficient	$[kg/m.Pa.s]$
DP_{eff}	is the effective vapor diffusion permeability	$[kg/m.Pa.s]$
dp	is the amount of pressure per unit volume	$[kg/m^3]$
HL_t	is the total heat loss	$[W]$
L	is the heat needed for evaporation of water	$[J/kg]$
P_a	is the testing pressure	$[Pa]$
P_o	is the ambient water vapor pressure in the climatic chamber	$[Pa]$
PP_o	is the partial pressure of the water vapor in the measuring channel of the Permetest skin model	$[Pa]$
P_s	is the saturated water vapor pressure of the thermal manikin wet-skin	$[Pa]$
PP_s	is the partial pressure of the saturated water vapor above the hotplate of the Permetest skin model	$[Pa]$
q_{et}	is the heat flow passing through the measuring head of Permetest covered by the tested sample	$[W/m^2]$
q_{etg}	is the total heat including the boundary layer, the air-gap distance rings and the sample from Permetest skin model	$[W/m^2]$
q_{eto}	is the heat flow from the bared measuring head of Permetest without the air-gap distance rings nor sample	$[W/m^2]$
R_{ct}	is the thermal resistance	$[m^2.K/W]$
Rct_{eff}	is the effective thermal resistance including the thermal resistance of the air gap and the material	$[m^2.K/W]$
Rct_f	is the thermal resistance of the material	$[m^2.K/W]$
Rct_g	is the thermal resistance of the air gap	$[m^2.K/W]$
Rct_m	is the thermal resistance of the boundary layer	$[m^2.K/W]$
Rct_o	is the thermal resistance of the boundary layer above the measuring surface of the Permetest skin model	$[m^2.mK/W]$

Rct_s	is the surface boundary layer of the thermal manikin	$[m^2 \cdot K/W]$
Rct_t	is the total thermal resistance including the thermal resistance of the boundary layer, the air gap and the material	$[m^2 \cdot K/W]$
R_{et}	is the water vapor resistance	$[m^2 \cdot Pa/W]$
\bar{R}_{et}	is the arithmetic mean of the actual R_{et} test results	$[m^2 \cdot Pa/W]$
Ret_{eff}	is the effective evaporative resistance including the evaporative resistance of the air gap and the material	$[m^2 \cdot Pa/W]$
Ret_f	is the evaporative resistance of the material	$[m^2 \cdot Pa/W]$
Ret_g	is the evaporative resistance of the air gap	$[m^2 \cdot Pa/W]$
Ret_g^*	is the evaporative resistance of the air gap when it relates to the water vapor diffusion permeability	$[m^2 \cdot Pa \cdot s/kg]$
Ret_m	is the evaporative resistance of the boundary layer	$[m^2 \cdot Pa/W]$
Ret_o	is the evaporative resistance of the boundary layer above the measuring surface of the Permetest skin model	$[m^2 \cdot Pa/W]$
Ret_s	is the evaporative resistance of the wet skin of the thermal manikin	$[m^2 \cdot Pa/W]$
Ret_t	is the total evaporative resistance including the evaporative resistance of the boundary layer, the air gap and the material	$[m^2 \cdot Pa/W]$
R_v	is water vapor gas constant which is	4615 $[J/kg \cdot K]$
R^2	is the symbol of the coefficient of determination	--
T_s	is the temperature of the thermal manikin shell	$[K]$
TP_s	is the surface temperature of the measuring head of the Permetest skin model	$[mK]$
T_o	is the ambient temperature of the climatic chamber for the thermal manikin	$[K]$
TP_o	is the ambient temperature in the measuring channel of the Permetest skin model	$[mK]$
\bar{V}	is the arithmetic mean of the calculated test results	$[mK]$
r	is the symbol of coefficient correlation	--
h	is the thickness	$[m]$
λ	is the thermal conductivity of the air	$[W/m \cdot K]$
g	is the acceleration due to the Earth's gravity which is	9.81 $[m/s^2]$
β	is the thermal expansion coefficient	$[K]$
a	is thermal diffusivity	$[m^2/s]$
ν	is the kinematic viscosity	$[m^2/s]$

Table of Contents

Prohlášení.....	iii
Declaration.....	iv
Acknowledgment.....	v
Abbreviations.....	vii
Symbols.....	viii
Table of Contents.....	x
Abstract.....	1
Abstrakt.....	2
大綱簡介.....	3
1. Introduction.....	4
2. Objectives of Research.....	12
3. Review of the Current State of Problem.....	14
4. Experiments and Results.....	16
4.1 Analysis of Air Gap Sizes Related to Free Convection and the Water Vapor Transfer in Air Gaps in Clothing.....	16
4.1.1 Air Gap Sizes Related to Free Convection.....	16
4.1.2 Water Vapor Transfer in Air Gaps in Clothing.....	20
4.2 Materials and Apparatuses.....	23
4.2.1 Method of Calculating Fabric Porosity.....	25
4.2.2 Method of Calculating Fabric Drapability.....	26
4.3 R _{ct} /R _{et} – Methods.....	36
4.3.1 Thermal Manikin – Samples.....	36
4.3.1.1 Thermal Manikin Clothing Samples by Molding Method.....	36
4.3.2 Thermal Manikin - Climatic Chamber and Experiment Procedures.....	41
4.3.3 Thermal Manikin - R _{ct} Results.....	43
4.3.4 Thermal Manikin - R _{et} Results.....	45
4.3.5 Vertically Oriented Permetest Skin Model – Samples.....	47
4.3.6 Vertically Oriented Permetest Skin Model – Climatic Chamber and Experiment Procedures.....	47
4.3.7 Vertically Oriented Permetest Skin Model – R _{ct} Results.....	50

4.3.8 Vertically Oriented Permetest Skin Model – R_{et} Results.....	53
4.4 Analysis of Thermal Manikin and Permetest Skin Model (Vertical Orientation).....	56
4.4.1 Correlation coefficient (r) -- The Thermal Manikin and the Vertically Oriented Permetest skin model.....	56
4.4.2 R^2 - Regression between the Thermal Manikin and the Vertically Oriented Permetest skin model.....	56
4.4.3 Two-way ANOVA -- The Thermal Manikin and the Vertically Oriented Permetest skin model.....	57
4.5 R_{ct}/R_{et} on Horizontally/Vertically Oriented Permetest Skin Model.....	58
4.5.2 Climatic Chamber and Experiment Procedures.....	58
4.5.3 Results.....	62
4.6 Analysis of the H/V Oriented Permetest Skin Mode.....	65
4.6.1 The Correlation Coefficient (r) of the Vertically and the Horizontally Oriented Permetest Results from Seven Tested Materials.....	65
4.6.2 R^2 - Regression between the Vertically and the Horizontally Oriented Permetest Results from Seven Tested Materials.....	67
4.6.3 Two-way ANOVA with five repetitions results from Vertically and Horizontally Oriented Permetest from Seven Materials.....	67
4.7 Determination for the Best Fit Equation Models for the R_{ct}/R_{et} Data from the H/V Oriented Permetest Skin Model Results.....	68
5. Evaluation of Results.....	71
5.1 Validation.....	74
6. Conclusion.....	81
7. Future Scope of Work.....	82
8. References.....	83
9. List of Tables.....	89
10. List of Figures.....	91
11. List of Publications by the Author.....	94
List of Publications in Research Journals.....	94
List of Publications in International Conferences.....	95
Research Projects.....	95
12. Appendices.....	96
Appendix 1- Images of devices.....	96
Appendix 2 – Porosity Information of Seven Fabrics.....	97

Appendix 3 - Drapability Information of Seven Fabrics	99
Appendix 4 – Fibre properties	102
Appendix 5 – Sensirion software samples.....	104
Appendix 6 – Picolog software sample	105
Appendix 7 – Sensirion and Picolog resultant sample	106
Appendix 8 - Original Data from Thermal Manikin	107
Appendix 9 - Original Data from Permetest Skin Model.....	109
Appendix 10 - Original Data from the Vertical/Horizontal Permetest Skin Model.....	113

Abstract

Sweating thermal manikin is considered the best machine for testing thermal insulation (R_{ct}) and evaporative resistance (R_{et}) of clothing because manikin's human form can be put on the ready-to-wear garment for testing in a 360-degree environment. It does not like the sweating guarded hot plate (SGHP), so-called skin model; the testing material has to be in a two-dimensional format. However, the sweating thermal manikin cost is very expensive and not commonly owned by research institutes or clothing companies. To solve this issue, a dry thermal manikin (non-sweating, more affordable and popular among many research institutes) is used together with the Permetest skin model to predict the R_{et} for the clothing. The research aims to use the R_{ct} result from a dry thermal manikin and the correlation of the vertically oriented skin model (Permetest) to develop a model equation that can calculate the R_{et} without using the wet thermal manikin.

Four popular clothing materials were chosen (cotton, polyester and their blends plus polypropylene as counter sample) and sewn into shirts in different sizes equivalent to different air gap sizes. Shirts were tested on the dry manikin. Results were analyzed and correlated to the results of the same materials and same air gap distances in a vertically oriented skin model (Permetest). Then, by choosing the best-fit line for all the resultant data from the experiments as the basic equations to develop the final model equation to predict the R_{et} of the clothing without using the sweating thermal manikin.

Keywords: *Sweating thermal manikin, Permetest skin model, Vertical-horizontal orientation, Evaporative resistance, Clothing comfort, Air gap size, Correlation coefficient*

Abstrakt

Potící se tepelný manekýn je považován za nejlepší zařízení pro testování tepelné izolace (R_{ct}) a výparného odporu (R_{et}) oděvů, protože na manekýna ve formě lidské postavy lze snadno obléci trojrozměrný konfekční oděv při jeho testování. Tuto možnost neposkytuje tepelný model lidské kůže – skin model, neboť zkoušený materiál se zde nachází dvourozměrném formátu. Náklady na pořízení tepelného manekýna s možností pocení jsou však velmi vysoké a proto tato zařízení jsou jen zřídka instalovány ve výzkumných ústavech nebo oděvních společnostech. Ke stanovení R_{et} u zkoušených oděvů je v této práci použit suchý tepelný manekýn (cenově dostupnější a oblíbený v mnoha výzkumných ústavech) společně s českým tepelným modelem lidské kůže (skin modelem) Permetest. Výzkum v této práci si klade za cíl použít výsledek R_{ct} ze suchého tepelného manekýna a korelaci vertikálně orientovaného modelu kůže (Permetest) k vytvoření modelové rovnice, která umožní výpočet R_{et} bez použití potícího se tepelného manekýna.

K experimentům byly vybrány čtyři oblíbené oděvní materiály (bavlna, polyester a jejich směsi plus polypropylen) a použity k výrobě do košil v různých velikostech odpovídajících různým velikostem vzduchové mezery. Košile byly testovány na suchém manekýnu. Výsledky byly analyzovány a korelovány se stejnými materiály a stejnými šířkami vzduchových mezer ve vertikálně orientovaném skin modelu. Poté byly nalezeny nejvhodnější závislosti pro všechna data potřebná pro sestavení základních rovnic sloužících k prezentaci finální modelové rovnice umožňující cílový výpočet a predikci výparného odporu R_{et} oblečení bez použití potícího se tepelného manekýna.

Klíčová slova: *potící se tepelný manekýn, Permetest skin model, oděvní komfort, výparný odpor, tepelný odpor, vertikálně-horizontální orientace vzduchových mezer.*

大綱簡介

會出汗的人體模型衣物測驗器被認為是測試服裝隔熱性 (R_{ct}) 和抗蒸發性 (R_{et}) 的最佳機器。因為它的人形模式，成衣或其他衣物可以直接放在人體模型上進行 360 度環境的測試。它不同於出汗防護熱板 (SGHP)，一種又稱為皮膚模型的測驗器；測試材料必須是平面形式。然而，人體模型衣物測驗器成本非常昂貴，並不為研究機構或服裝公司所共有。不出汗的人體模型衣物測驗器 (乾的，不出汗) 就是用來解決這個問題的另類方法；因它價格更實惠，深受眾多研究機構歡迎，配合 Permetest 皮膚模型來預測服裝的 R_{et} 。此項研究旨在利用乾的人體模型的 R_{ct} 結果和垂直定向皮膚模型 (Permetest) 的相關性來開發一個模型方程，可以在不使用濕的人體模型的情況下計算 R_{et} 。

測驗過程選擇了四種常用的服裝材料包括棉、滌綸及其混紡，再加上聚丙烯作為對照樣品，縫製成不同尺寸的襯衫，尺寸的大小相當於不同的氣隙尺寸大小。襯衫在乾的人體模型上進行了測試。又在垂直定向的皮膚模型中對相同材料和相同氣隙距離的測試結果進行分析和關聯，並通過選擇所有數據的最佳擬合線作為基本方程來開發最終模型方程來預測服裝的 R_{et} 。

關鍵詞：出汗機械人模型, Permetest 皮膚模型, 垂直-水平方向, 蒸發阻力, 服裝舒適度, 氣隙大小, 相關係數

1. Introduction

Clothing comfort consists of three main aspects: psychological, thermophysiological, and neurophysiological comfort [1-2]. In the thermophysiological comfort, thermal insulation (R_{ct}) and evaporative resistance (R_{et}) are two important parameters that influence the body heat balance during various activities. These two parameters are most commonly measured by thermal manikin (*Figure 1-2*) and sweating guarded hot plate so-called skin model (*Figure 3*).

Thermal manikin [3-5] is an anatomically correct, human-like robot that the whole body is divided into segments which are the heat zones, and the heat can be controlled and adjusted using a computer program to simulate human body heat to test the heat transfers from the manikin body through clothing system to the environment. Using thermal manikin for clothing measurement is standardized in ISO 15831: 2004 [6]. Thermal manikins have two major types: dry and wet (built-in sweating system) thermal manikins. The sweating thermal manikin models have small holes embedded in particular segments connected to the water pump inside the manikin to secrete water to simulate the human body's sweating glands. Some models of thermal manikins can perform simple movements like cycling and walking to simulate activities [7-8]. Thermal manikin (dry/wet) is considered the most accurate apparatus to measure heat and mass transfer for the clothing system because of the human form. It can measure the radiation, conduction and convection in 360 degrees in real life [9]. However, when testing the R_{et} , even following the international standard of procedures, the 4mm thick wet-skin (made of a material containing a microporous structure that evaporates the water vapor to simulate human sweating) put on the sweating thermal manikin because of the evaporation of the surface temperature is difficult to control, it is always lower than the manikin shell temperature [10]. Also, the sweating holes only built-in areas like chest, back, some parts of legs and arms, and it takes a long time for water to spread out on the wet-skin. The direct contact of wet skin on clothing may moisten and influences the water vapor permeability of the clothing, decrease the evaporative resistance [11-12] and lower the accuracy of the repeatability and lab-to-lab data comparison.

Furthermore, scientists are still debating whether to use heat loss or mass loss method to measure (the mass loss method was removed from the newest version of the ASTM standard [13]), the condensation on the inside of low permeable clothing is causing over/under-estimation of the results and so on [14-15]. Also, the long hours of preparation and observing time for each test and the maintenance fee of sweating thermal manikins are relatively more expensive than the dry thermal manikin (non-sweating thermal manikins). Dry thermal manikins are often simpler to use, more affordable and used in more places worldwide.



Figure 1. Sweating thermal manikin-Newton



Figure 2. Newton in wet-suit and walking mode

Sweating guarded hotplate (SGHP) - a skin model (*Figure 2*) is an apparatus with a hotplate installed in an enclosed space. Heat is released from the porous hotplate simulating human skin and through a permeable membrane to the material put on the hotplate to test for the R_{ct}/R_{et} by sensors installed inside the closed environment. Results will then be collected and shown on the computer program connected to the skin model [16-17]. The procedure of testing materials on SGHP is standardized in ISO 11092: 2014 [18]. The hotplate skin model has a long history of being used to determine R_{ct}/R_{et} of materials [19], yet; it can only test materials in two-dimensional form and on a flat surface in a particular size; also, the flatness, the range of temperature and the insulation of the hotplate are still challenging the developers for improvement.



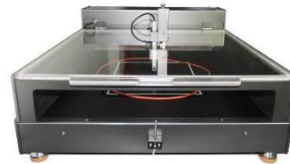
Figure 3. Sweating guarded hot plate and software



Figure 4. Permetest skin model

Permetest (*Figure 4*) is an alternative kind of skin model which is also standardized in ISO 11092. However, its portable size and the versatile vertically or horizontally oriented measuring method make it stand out among other skin models. Also, its non-destructive measure, fabric or garment can be tested without cutting, and the quick testing result only takes a few minutes for preparation time. The only disadvantages of the machine are limited in the thickness of garment/fabric layers, from 0-16 mm, and the constant monitoring of the water level is needed when testing on R_{et} of the materials. *Tables 1* and *Table 2* are presenting the comparison of the sweating thermal manikin, sweating guarded hotplate and Permetest skin model.

Table 1. Properties comparison among the sweating thermal manikin, sweating guarded hotplate and Permetest skin model



Instrument	Sweating Thermal Manikin	Sweating Guarded Hotplate	Permetest Skin Model
Shape	Human form	Rectangular form	Rectangular form
Dimension (approx.)	Height-170cm, Chest-94cm, Waist-88cm	Length-77cm, Width-67cm, Height-43cm	Length-54cm, Width-23cm, Height-13cm
Weight	Unknown	62 kg	7 kg
Materials	Plastic form shell and metallic frame for body parts and joints. Wet-skin for R_{et} test is 4mm thick material containing a microporous structure	Metal	Metal
Body Movements	Yes	No	No
Heat zones Control	Yes	No	No
Total heated measured area	1.774 m ²	645 cm ²	50.265 cm ²
Measuring Method	3D – Ready-to-wear garments	2D – Flat surface of textile or garments (cut size)	2D – Flat surface of textile or garments (non-destructive)
Sample Thickness	From 0 mm up	0 – 50 mm	0 – 16 mm
Preparation Time	One day	One day	15 to 30 minutes
Measuring Time	1 hour or more	1 hour or more	1 to 5 minutes in each measurement in average

Table 2. The sweating thermal manikin is in wet-skin (in blue) prepared for water vapor resistance tests and sweating guarded hotplate is put inside the climatic chamber before any sample testing; and Permetest skin model is in the vertical orientation



ISO Standard	15831	11092	11092
Price	Very Expensive	Expensive	Affordable
Climatic Chamber	Needed	Needed	No
Orientation Versatility	Possible	Impossible	Possible
Rct/Ret Measurement	Yes	Yes	Yes
Principle of Instrument	To measure total heat loss between the manikin shell temperature and the ambient temperature through the air gap and the test sample garment	To measure the power required to maintain the flat hotplate measurement area at a constant temperature	To measure the power needed to keep the flat hotplate measurement area at a constant temperature
Other Problems	-Wet skin (4mm thick) temperature is difficult to control when measuring R_{et} -Costly maintenance fee -A large climatic chamber needed	-Problem when measuring samples with an air gap, the center area will drape -Uneven temperature on a hotplate -Uneven smoothness/thickness of hotplate	-Limited water reservoir for R_{et} measure -Limited sample height, only 16mm -Only a small area is tested

Either sweating thermal manikin or any skin models follows the Fourier's law. Fourier's law is the law of heat conduction, and it states that "the heat flux resulting from thermal conduction is proportional to the magnitude of the temperature gradient and opposite to it in sign" [20]. When in a one-dimensional, steady-state with no heat generated, this observation may be expressed as Eq (1):

$$\dot{q}_x = -\lambda(dT/dx) \quad (1)$$

where \dot{q}_x is the heat flux [W/m^2], dT/dx is the temperature gradient [K/m] and the minus sign confirms heat flows from higher to lower temperature. λ is the thermal conductivity of the material [$\text{W}/\text{m}\cdot\text{K}$]. When Fourier's law is combined with the principle of conservation of energy, it becomes the essential reference for analyzing thermal conduction problems. Newton's law of cooling*¹ Eq (2) is a discrete analogue of Fourier's law and Fick's laws of diffusion*² Eq (3-4) are its concentration and pressure analogues [21].

$$Q = \alpha \cdot A(T_s - T_\infty) \quad (2)$$

where Q is the heat flow rate from the body to the ambient fluid area [W], α is the heat transfer coefficient [$\text{W}/\text{m}^2\cdot\text{K}$], A is the surface area where the heat transfer takes place [m^2], T_s and T_∞ are the body and ambient temperature respectively [K].

$$m^* = -D_c(dc/dx) \quad (3)$$

$$m^* = -D_p(dp/dx) \quad (4)$$

where m^* is the amount of substance that will flow through a unit area during a unit time interval [$\text{mol}/\text{m}^2 \cdot \text{s}$], D_c is the concentration diffusivity [m^2/s], D_p is the pressure diffusivity [Pa/s], dc is the amount of substance per unit volume [mol/m^3], dp is the amount of pressure per unit volume [kg/m^3], dx is the distance/length [m]. Also, one-dimensional heat transfer through fabric or other materials by conduction is governed by Fourier's Law of thermal conduction as in Eq (1) [22-23].

**¹Newton's law of cooling states that the rate of heat loss of a body is directly proportional to the difference in the temperatures between the body and its surroundings [from Wikipedia].*

**²Fick's law of diffusion states that the diffusion rate is proportional to both the surface area and concentration/ pressure difference and is inversely proportional to the thickness of the membrane [from Wikipedia].*

2. Objectives of Research

Knowing the relationship/correlation of the dry thermal manikin and the hotplate skin model is important when there is a need to test garment systems with difficult access to the sweating thermal manikin; the correlation can solve the immediate problem plus saving time and cost of labor.

However, in a standard operation regime, the hotplate skin model serves to determine the R_{ct}/R_{et} of a single-layered fabric placed horizontally and flat on the porous measuring surface, which simulates the human skin. When there is a need to test garment systems with vertical gaps using a standard skin model, serious problems arise; for example, the testing surface area is usually large. The tests involving air gaps are practically impossible because textile material will drape/deform around the center area. The effective air gap gets reduced, then the measurement suffers from a big error. Moreover, vertical measurements are also impossible in standard skin models. Their large size in the vertical direction will cause an uneven distribution of water within the apparatus's porous measuring plate. On the contrary, the Permetest skin model (*Figure 3*) has a small diameter (8 cm) testing plate and a slightly curved surface to allow a very secure and close contact with material even with an air gap distance of up to 16 mm and still keeps the material flat for testing. The portable size of Permetest also gives it the advantage of turning a horizontally (H) oriented test into a vertically (V) oriented test in a second.

The research aims to develop an equation that can calculate the evaporative resistance (R_{et}) result by using the data obtained from the dry thermal manikin and the correlation of R_{ct}/R_{et} of the vertically oriented Permetest skin model. The research is divided into two major parts:

First part: Analysis of Air Gap Sizes Related to Free Convection and the Water Vapor Transfer in Air Gaps in Clothing

Second part: Experiments, Results and Analysis for the Thermal Manikin and the Vertical Skin Model; also the Vertical and Horizontal Air Gaps comparison by means of Permetest skin model. The procedures are as follow:

1. Materials and Apparatuses
2. R_{ct}/R_{et} - Methods
3. Analysis of the Thermal Manikin and the Permetest Skin Model
4. R_{ct}/R_{et} on the H/V Oriented Permetest Skin Model
5. Analysis of the H/V Oriented Permetest Skin Model
6. Determination for the Best Fit Equation Models for the R_{ct}/R_{et} Data from the H/V Oriented Permetest Skin Model Results

3. Review of the Current State of Problem

Literature related to research employing thermal manikin and hotplate skin model, in general; is divided into three main groups:

- Analysis of clothing for fabric mechanical, thermal and comfort properties and protective clothing using thermal manikin or hot plate skin model [24-36]; in a single layer or multi-layers [37-39]; in dry/wet state [40-46] and different atmospheric conditions to evaluate human behaviour in protective clothing [47-50]. This group is the largest group of research literature using the thermal manikin and the hotplate skin model among the three groups.
- Reports on new development or re-designed on the thermal manikin and the hotplate skin model, for examples; invented a higher temperature range of the hotplate for thermal conductivity tests, better insulation materials and insulation installation of the apparatus, new arrangement of electric wire to stabilized the constant of the heat flow, new material for the hotplate to maintain the perfect flatness of the plate and so on for the sweating guarded hotplate [51-58]. In thermal manikin development, a new invention of the female fabric sweating thermal manikin – Wenda improved breathable manikin for medical purposes and inflatable manikin for thermal properties measurement [59-60].
- Evaluation of sweating guarded hotplate and thermal manikin and comparing these two apparatuses [61-65]. Articles in this group are limited, especially comparing the hotplate skin model to the thermal manikin; like Matusiak et al. compared thermal resistance results of nine different materials between the Alambeta thermal tester model and the thermal manikin, and concluded that "Alambeta could be applied to measure the thermal resistance of the material applied in clothing in situations when no access to the thermal manikin." However, the research is only provided the results from thermal resistance but no evaporative resistance results. Satusumoto et al. compared quasi-clothing heat transfer between a vertical hotplate and the thermal manikin and concluded that "the vertical hot plate was more accurate than the thermal manikin because the manikin could not reproduce

the same setup of construction factors like precise air space sizes." The research is interesting to use the vertical hotplate skin model for the test. Still, only the schematic is shown in the article, which is not enough clearance to understand how this apparatus operates in the experiment. Also, there is no mention of any recognized procedure standard is applied to the vertical skin model test. More, using space bars between the manikin and the clothing to keep the exact air gap distance which is not practical in reality, for gravitation and mechanical properties of the fabric are always exist and influence the drape of the clothing, which are important factors for thermal resistance measurement.

4. Experiments and Results

4.1 Analysis of Air Gap Sizes Related to Free Convection and the Water Vapor Transfer in Air Gaps in Clothing

4.1.1 Air Gap Sizes Related to Free Convection

In thermophysiology, thermal resistance (R_{ct}) when in the steady-state under non-isothermal condition, the total thermal resistance (Rct_t) is equal to the boundary layer of the body (Rct_m) plus the thermal resistance of the air gap (Rct_g) between the body and the clothing, and the thermal resistance of the clothing (Rct_f). It can be defined by equation Eq (5) and the unit of R_{ct} is [$m^2.K/W$]. The air gap resistance (Rct_g) is defined in Eq (6), where h [m] is the thickness and λ [$W/m.K$] is the thermal conductivity of the air.

$$Rct_t = Rct_m + Rct_g + Rct_f \quad (5)$$

$$Rct_g = h/\lambda \quad (6)$$

When the effective thermal resistance (Rct_{eff}) is required, total thermal resistance minus the body boundary layer is the answer as in Eq (7).

$$Rct_{eff} = Rct_t - Rct_m \quad (7)$$

When evaporative resistance (R_{et}) in steady-state under isothermal condition (in non-isothermal conditions, clothing insulation may dramatically change due to moisture absorbent, therefore; isothermal conditions should be used [66-68]), the total evaporative resistance (Ret_t) is similar to Eq (5), the boundary layer of the body (Ret_m) plus the evaporative resistance of the air gap (Ret_g) and the evaporative resistance of the clothing (Ret_f). It can be defined by Eq (8), and their unit is

m²Pa/W. The air gap evaporative resistance (Ret_g) is defined in Eq (9) where Dp [W/m.Pa] is the water vapor thermal diffusivity [69].

$$Ret_t = Ret_m + Ret_g + Ret_f \quad (8)$$

$$Ret_g = h/Dp \quad (9)$$

The effective evaporative resistance (Ret_{eff}) is the total evaporation resistance minus the body boundary layer of the evaporative resistance as in Eq (10).

$$Ret_{eff} = Ret_t - Ret_m \quad (10)$$

When heat is transferred in natural convection, Rayleigh number*³ (Ra) is applied. Rayleigh number is a dimensionless number associated with free or natural convection [70-71]. When the Rayleigh number is used in fluid mechanics, it characterizes the fluid's flow regime to determine a laminar flow or a turbulent flow. Rayleigh number is defined as Eq (11):

$$Ra = Gr*Pr = [g\beta (T_1 - T_2) L^3 / \nu a] * Pr \quad (11)$$

where g is the acceleration due to the Earth's gravity which is 9.81 [m/s²], β is the thermal expansion coefficient (*equals to 1/T* where T* is the mean absolute temperature [K]*), T_1 [K] is the measuring head temperature, T_2 [K] is the ambient temperature, L [m] is the length, a [m²/s] is thermal diffusivity, ν [m²/s] is the kinematic viscosity. The equation is the product of the Grashof number*³ (Gr), the ratio relationship between buoyancy and viscosity within a fluid, and the Prandtl number*³ (Pr), the ratio relationship between momentum diffusivity and thermal diffusivity [72].

The critical value of Rayleigh number (Ra) is 1708 [73-74], where the flow is unstable and this transition period will turn laminar flow into turbulent flow [75-76]. However, there is no fluid

motion when $Ra < 1000$, and the heat transfer is only by conduction rather than convection [77-78].

In the research experiments, air gap size is from 0 –16mm. $g = 9.81$, $T_1 = 32^\circ\text{C}$ (305K), $T_2 = 22^\circ\text{C}$ (295K), $\beta = 1/T^* = (305+295) / 2\text{K} = 300\text{K}$, $L = (0.004 \text{ to } 0.016 \text{ m})$, $a = 19 \cdot 10^{-6} [\text{m}^2/\text{s}]$, $\nu = 15.7 \cdot 10^{-6} [\text{m}^2/\text{s}]$ (values of a and ν are checked from Tables, both at 300K), and Pr (Prandtl number) is 0.7.

By using the Eq (7); results are in *Table 3*.

**³Similarity Theory [79-82] is when two physical phenomena, processes or systems are similar if, at corresponding moments at corresponding points in space, the variables' values that characterize the state of one system are proportional to the corresponding quantities of the second system. For any set of similar phenomena, all the corresponding dimensionless characteristics have the same numerical values. Rayleigh, Grashof and Prandtl numbers are dimensionless numbers that similarity theory can be applied to.*

Table 3. Rayleigh number for air gap size 0-16mm, values in red are for reference only

unit in [m]	Rayleigh number (<i>Ra</i>)
0	0
0.004	49
0.008	393
0.010	767
0.011	1021
0.012	1326
0.016	3143

Results show that from 0-10 mm, *Ra* is under 1000. When $Ra = 10^3$, conduction is the dominant mechanism for heat transfer, indicating no free convection in these narrow air gaps; then convection is slowly introduced when the air gap size started at 11 or 12 mm.

From Grashof number follows that the uplift driving force (responsible for free convection) is driven by differences in the fluid density. Generally, these density differences of the fluid (here is air) are mostly created by gas expansion expressed as $(T_1 - T_2)/T^*$, where $1/T^*$ is the mean absolute temperature of the gas (here is the air). This driving force in the Grashof number can be directly expressed as the relative difference(s) of densities of the fluid (humid air in our case).

In this study, a very specific situation can be observed. At isothermal water vapour transfer required at R_{et} measurements, the only density difference in the studied system is caused by differences in the density of saturated water vapour in the simulated skin of the Permetest skin model and the density of less saturated water vapour inside the measuring channel of the device.

A similar driving force is managed when testing R_{et} on the thermal manikin. The density of the proper (dry) air keeps unchanged. Thus, in the correct version of the Grashof or Rayleigh numbers, the driving force will be the difference of partial water vapor pressures (very close to the skin and outside the skin). However, for this specific case, no critical GR or *Ra* numbers were found in the literature. Moreover, the mentioned pressure differences (driving force) are small. The low level of the possible free convection in this case confirms the following finding: linear dependences of

determined R_{et} numbers on the air gap size (see Figures 17, 18, 20, 21; page 44, 46, 52, 55) confirm that no free convection effect was observed till the air gap width was 12 mm.

4.1.2 Water Vapor Transfer in Air Gaps in Clothing

As already mentioned, heat in narrow gaps inside clothing systems is transferred by pure conduction unless the Rayleigh number (Ra) exceeds 1000. Due to relatively low-temperature drops in clothing worn under common conditions, heat transfer by radiation is neglected. According to Eq (5), radiation heat flow in these conditions should not exceed 10 to a maximum of 15% of the total heat flow [83]. Regarding the transfer of water vapor in the narrow gaps inside clothing systems, its mechanism should be principally the same; due to the similarity between heat and mass transfer. However, in this study, the water vapor transfer is the driving force in the air given by the difference of water vapor partial pressures is low.

Moreover, testing of evaporative resistance (R_{et}) of clothing by the sweating thermal manikins, as well as the R_{et} tests executed on vertically oriented Permetest skin model in this study, were carried out under isothermal conditions, which means that the thermal manikin shell temperature or the porous hotplate of the Permetest device was holding on the same temperature as the fabric sample, thus creating the air gap characterized by its thickness h [m] and the evaporative resistance Ret_g [$m^2.Pa/W$] which is related to power determined by the modified Ret_g^* [$m^2.s.Pa/kg$] which is related to mass.

The term DP [$kg/m.s.Pa$] presents the water vapor diffusion coefficient in the air related to the water vapor partial pressure, which in some papers is called water vapor diffusion permeability [69]. This term will also be used in the study.

Due to low driving force (low difference of water vapor partial pressures) and isothermal conditions that water vapor transfer in the gaps investigated by the vertical skin model would not be influenced by the free convection based on differences of water vapor density. However, contrary to the common Ra number, where the limit for free convection initiation is known, nothing similar was published to initiate free convection based on differences in water vapor density. At present, there is no dedicated EU standard for measuring this quantity, highlighting the fact that more research is needed in this field.

Hence, for the beginning, let us suppose the water vapor transfer in narrow closed gaps in the vertical skin model is based on pure diffusion. In this case, the water vapor diffusion permeability DP in these gaps should approximate to the standard values published in the literature - Schirmer, R.: Die Diffusionszahl von Wasserdampf-Luft-Gemischen und die Verdampfungsgeschwindigkeit, Beiheft VDI-Zeitschrift, Verfahrenstechnik (1938), H. 6, p. 170-177 [84] .

$$DP = 2306 \cdot 10^{-5} P_o \cdot P_a^{-1} \cdot R_v^{-1} (T/273.15)^{0.81} \text{ [kg/m.s.Pa]}$$

Here:

R_v is water vapor gas constant 4615 [J /kg.K]

T is the ambient temperature in Kelvins [K]

P_a and P_o mean the testing and the ambient pressure in Pascals (100,000 Pa), respectively.

According to EN ISO 13788:2012 for standard laboratory conditions used in the study we get:

$$DP = 2,0 \cdot 10^{-10} \text{ [kg/m.s.Pa]}$$

In the next step, the effective water vapor diffusion permeability level will be determined by measuring the vertically oriented skin model and compared with the theoretical value.

Evaporative resistance Ret_g [$\text{m}^2 \cdot \text{Pa} / \text{W}$] related to thermal effects of the evaporation, which was experimentally determined by a vertical skin model for air gaps varying from 0 to 16 mm, can be converted into evaporative resistance Ret_g^* [$\text{m}^2 \cdot \text{s} \cdot \text{Pa} / \text{kg}$] by Eq (12) according to the ISO 11092:

$$Ret_g^* = R_{et}.L \quad (12)$$

where L presents the heat for evaporation of water, 2 450 000 [J /kg] at 22°C. Thus, for certain gap 10 mm created by the studied fabric sample with $R_{et} = 15$ [m².Pa/W], the Ret_g^* value will be $3,675.10^7$ [m².s.Pa/kg]. This evaporative resistance Ret_g^* shall correspond to the gap of the above thickness h as in Eq (13):

$$Ret_g^* = h/ DP_{eff} \quad (13)$$

where the DP_{eff} [kg/m.s.Pa] is the effective vapor diffusion permeability in the studied gap in clothing, then the DP_{eff} value can be calculated as:

$$DP_{eff} = h/ Ret_g^* = 0,01 / 3,675 .10^7 = 2,72.10^{-10} \text{ [kg/m.s.Pa]}$$

As expected, the theoretical level of water vapor diffusion permeability in pure diffusion is slightly lower than the value of $DP = 2,0.10^{-10}$ [kg/m.s.Pa]. Then it can be concluded that in water vapor transfer in the studied gaps prevails the diffusion, just for the gaps thicker than 12 mm, certain effects of free convection can be observed.

4.2 Materials and Apparatuses

Seven materials were prepared for the research, but only four of them (in shade areas) were used for the thermal manikin tests due to limited access to the facilities. Materials' properties are presented in *Table 4* and their photomicrographic images are shown in *Figure 5a-g*. All materials were washed to get rid of the finishing, hang dried and iron-flatted before use. Two apparatuses were used: Tore – the thermal manikin and the Permetest skin model (in vertical orientation) and their features are presented in *Table 5*.

Table 4. Properties of materials**

	100% Cotton	80/20% Cotton /Polyester	70/30% Cotton /Polyester	50/50% Cotton /Polyester	35/65% Cotton /Polyester	100% Polyester	100% Polypropylene
Structure	Plain Weave	2/2 Basket Weave	Plain Weave	Plain Weave	Plain Weave	Plain Weave	2/2 Right Twill
Thickness [mm]	0.37	0.55	0.58	0.33	0.23	0.43	0.63
Sq. mass [g/m²]	154	225	226	159	102	156	252
Fabric Density Warp/Weft [threads/cm]	26/22	24/14	16/14	26/24	24/28	16/22	32/34
*4 Air Permeability [l/m²/s]	277	234	241	272	523	564	74
*5 Absorption Rate Top/Bottom [%/s]	13/36	21/34	24/43	12/39	8/19	8/20	61/10
*6 Porosity[%]	73	72.8	73.8	66.8	68.8	73.3	55.6
*7 Drapability [%]	34	30	32	39	43	43	10

*⁴Air permeability is measured by FX 3300 Air Permeability Tester, the image in Appendix 1

*⁵Absorption rate is measured by M290 Moisture Management Tester (MMT) image in Appendix 1

*⁶Porosity information of seven fabrics – Appendix 2

*⁷Drapability information of seven fabrics – Appendix 3

** Fibre properties – Appendix 4

4.2.1 Method of Calculating Fabric Porosity

Fabric porosity is presented either by percentage (%) or by index, 1 – 0; 1 means 100% porous material, 0 means non-porous material. To calculate the porosity of the material; fabric density and fibre density are the key values needed to be prepared. The calculation is divided into two parts. Part one is fibre volume of a solid material as in Eq (14). Part two is using fabric porosity index 1 minus fibre volume as in Eq (15).

$$\phi = [\rho_{fabric} / \rho_{fibre}] \quad (14)$$

$$P = (1 - \phi) * 100\% \quad (15)$$

$$\rho_{fabric} = fabric\ square\ mass / h \quad (16)$$

where P (%) is the fabric porosity, ϕ is the fibre volume of solid material, ρ_{fabric} [kg/m^3] is the fabric density, ρ_{fibre} [kg/m^3] is the fibre density, h [m] is the thickness of the fabric. Eq (16) is showing the calculation for fabric density. For example, 70% cotton 30% polyester blend fabric used in the experiment, the calculation is as follow:

Using Eq (16), fabric density of the blend = $226 [\text{kg}/\text{m}^2] / 0.00058 [\text{m}] = 389.7 [\text{kg}/\text{m}^3]$. *Values of fabric square mass and thickness were determined by measurement.*

Using Eq (14), fibre volume of the blend = $389.7 [\text{kg}/\text{m}^3] / 1486 [\text{kg}/\text{m}^3] = 0.2622$.

The fibre density is calculated based on the proportion of 100% cotton density and 100% polyester density (common fibre density values can be found on internet).

Using Eq (15), the fabric porosity = $(1 - 0.2622) * 100 = 73.8\%$

Other fabric weight, thickness and fibre density are in Appendix 2

4.2.2 Method of Calculating Fabric Drapability

Estimating fabric drapability has divided into two parts:

Part 1 is to find out the draped fabric outline and trace it over a lightbox.

Part 2 is to use the Eq (17) to calculate the percentage of drapability. Higher in percentage, better drapability of the fabric.

Part 1

1. Fabric samples are cut into a circular shape with 300 mm in diameter
2. An A3 size paper is put on top of the glass screen over the draping device
3. Trace out the silhouette of the draped shape (the shadow)

Part 2

1. A planimeter is used to measure the draped area (the shadow area)
2. Use equation (17) to calculate the percentage of the sample drapability

$$D (\%) = [A - A_p / A_m] * 100\% \quad (17)$$

where D is the fabric drapability (%)

A is the area of circular fabric sample – $70.69*10^3$ [mm²]

A_p is the area of projection [mm²] – measured by Planimeter

A_m is the area of annulus – $45.24*10^3$ [mm²]

For example, 70% cotton 30% polyester blend, the area of projection A_p [mm²] measured by Planimeter is 56090 [mm²]. Using Eq (17)

$$D (\%) = (70.69*10^3 [mm^2] - 56090 [mm^2]) / 45.24*10^3 [mm^2] * 100\%$$

and the drapability of the cotton/polyester blend is 32%

Below is *Figure 5* of planimeter device tracing out the draped fabric outline, and the total area of the draped fabric area can be read from the measuring roller.

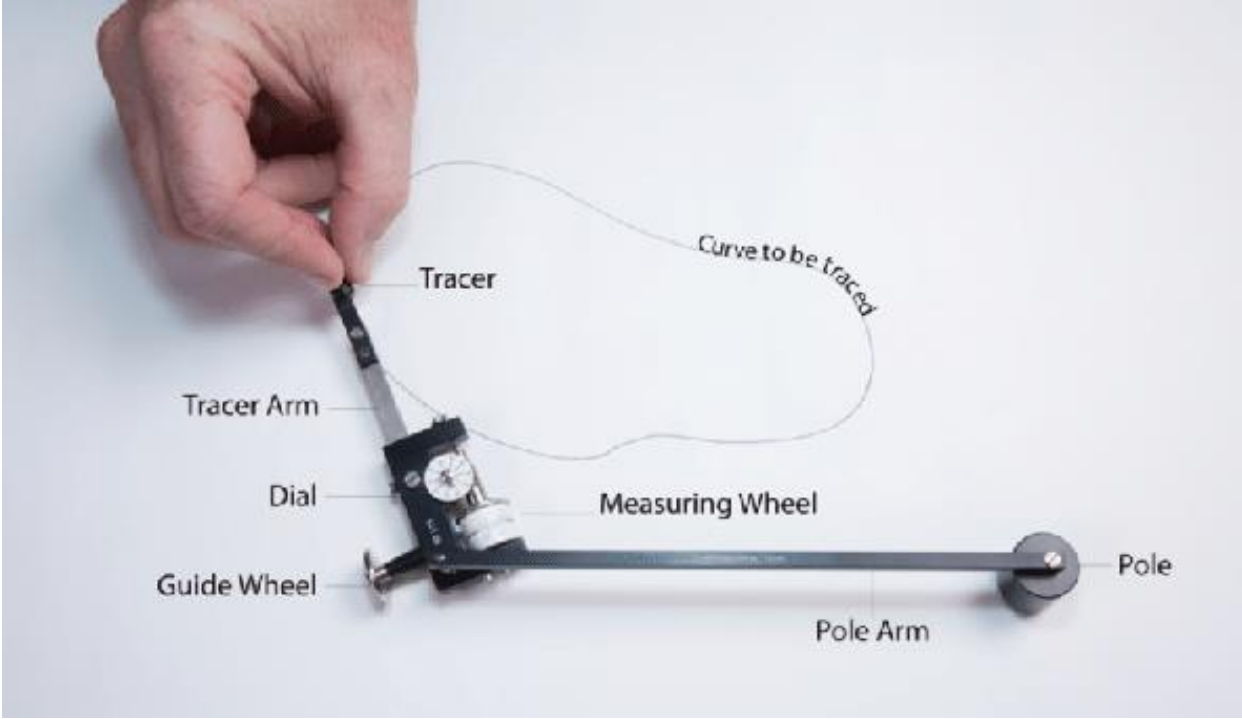
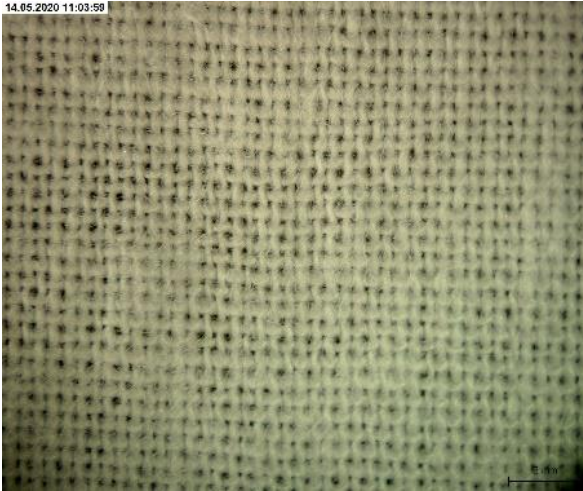


Figure 5. Image of the planimeter device



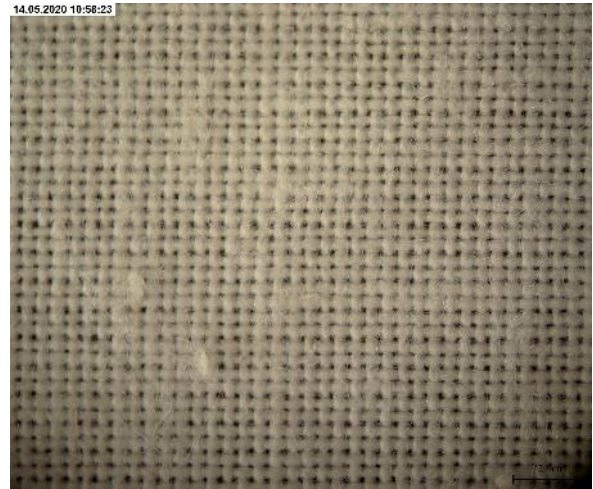
a. 100% Cotton



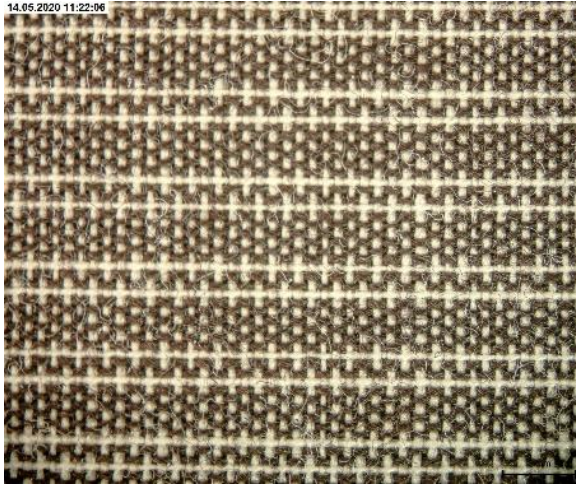
b. 80% Cotton 20% Polyester



c. 70% Cotton 30% Polyester



d. 50% Cotton 50% Polyester



e. 35% Cotton 65% Polyester



f. 100% Polyester



g. 100% Polypropylene

Figure 6a-g. Photomicrographic images of seven materials by Promicra

Table 5. Differences between the thermal manikin and the Permetest skin model

	<i>Tore – Non-Sweating Thermal Manikin</i>	<i>Permetest Skin Model</i>
<i>Shape</i>	Human form	Rectangular form
<i>Dimension</i>	Height-170cm, Chest-94cm, Waist-88cm	Length-54cm, Width-23cm, Height-13cm
<i>Weight</i>	32kg	7kg
<i>Materials</i>	Plastic form shell, inside supported by the metal frame for body parts and joints	Metal
<i>Total heated measured area</i>	1.774 m ²	50.265 cm ²
<i>Measuring Method</i>	3D – Ready-to-wear garments	2D – Flat surface of textile or garments (non-destructive)
<i>Measuring Time</i>	20 minutes of steady-state out of 40 minutes total measuring time in average	1 to 5 minutes in each measurement in average
<i>ISO Standard</i>	15831	11092

Tore (*Figure 7-9*) at Lund University, Sweden is a Swedish-made plastic foam thermal manikin supported by a metal frame underneath the joint and the body. Tore is a male manikin whose height is 170 cm, chest is 94 cm, waist 88 cm with a heated surface area of 1.774 m². The entire figure is divided into 17 segments and each segment is evenly embedded with the wire temperature sensors to measure the surface temperature, which can be adjusted individually for each segment by a computer program to simulate human body heat for heat transfer testing through clothing to the environment (*Figure 13*). The heat input is the heat loss from the manikin [85], and the process is directly recorded by the computer program (Sensirion and Picolog samples are shown in Appendix 5-6) at the adjustable interval of each minute. When testing, Tore will be put inside the climatic chamber where different ambient conditions can be achieved. Wet skin will be put on the manikin when testing for evaporative resistance.



Figure 7. Tore- the dry manikin is in standing mode inside the climatic chamber



Figure 8. Front view of Tore in prewetted suit



Figure 9. Back view of Tore in prewetted suit

The Permetest skin model (developed by L. Hes, *Figure 10-12*) was chosen among all other small-size skin models like the Thermo Labo [86] because of its portability and capability to test materials in horizontal and vertical orientations. The apparatus dimensions are 540 x 230 x 130 mm, net weight 7 kg [87-88].

Permetest skin model is composed of two parts; on one side is the measuring mechanism with digital monitoring panels, control knobs and an electric fan which is responsible for the airflow speed $1,0 \pm 0,1$ [m/s]; on the other side is the wind channel with a sliding opening on the top, and the hotplate is installed at the bottom side. It is connected to a set of lifting mechanisms. Permetest skin model is a non-destructive device with a small diameter (8 cm) testing hotplate featuring a slightly curved surface to allow a very secure and close contact with materials even with air gap distance up to 16 mm and still keeps the material flat for testing. A heat power sensor is embedded beneath the hotplate and data from this sensor are directly recorded using a computer and the device software.

Similar to regular sweating guarded hot plate, the Permetest skin model follows the measuring procedure of ISO 11092. The principle is that the heat power at a constant temperature of the measuring head is measured with and without fabric sample (*Figure 14*) when testing on thermal resistance R_{ct} . When testing R_{ct} , sample textile /clothing, without being cut into a certain testing size like other skin models, is put on the small circular hotplate covered by a thin layer of vapor-permeable membrane function as the wet skin inside the wind channel for testing. The moistened measuring head then measures the evaporation heat (heat power) of distilled water supplied into the measuring head. Due to free water on the porous surface of the measuring head, partial water vapour pressure here reaches its saturation level. The partial pressure of humid air outside of the measuring head, in the measuring channel, is kept mostly at 50% level of the saturated pressure.

The differences in the partial water vapour pressure and temperature of the air in the measuring channel of the Permetest instrument against the partial water vapour pressure and temperature of the air used at calibration procedure of a hydrophobic PP reference fabrics in the Hohenstein

institute are compensated by a special double calibration procedure which belongs to the know-how of this testing instrument. The whole measuring system consisting of the hotplate, the air channel and the axial fans (ventilators) is kept under isothermal conditions ($\pm 1^\circ\text{C}$) when measuring evaporation resistance, or the measuring head is held at the temperature $10^\circ\text{C} \pm 0.1^\circ\text{C}$ higher than the air temperature in the laboratory. The required temperature control is provided by a “clever” (self-reprogramming) OMRON controller.



Figure 10. Permetest skin model in vertical orientation

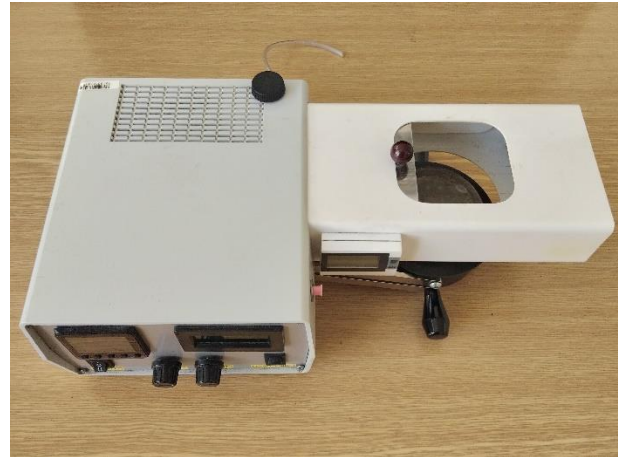


Figure 11. Top view of Permetest skin model



Figure 12. Front view of Permetest skin model in horizontal orientation

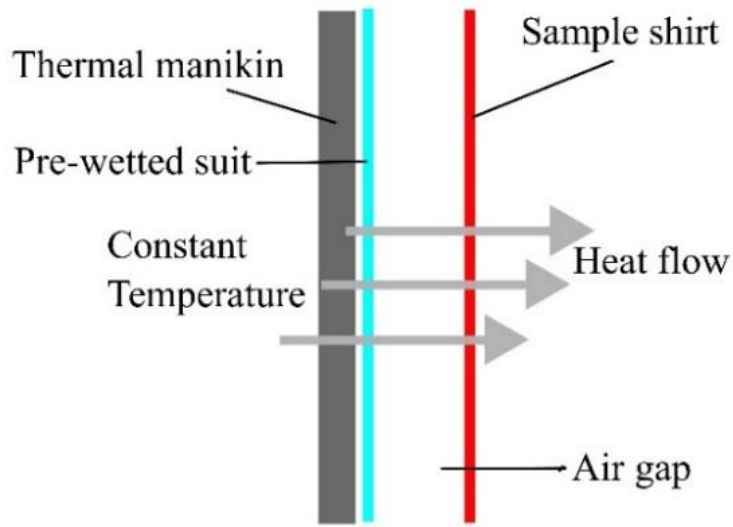


Figure 13. Principle of the thermal manikin

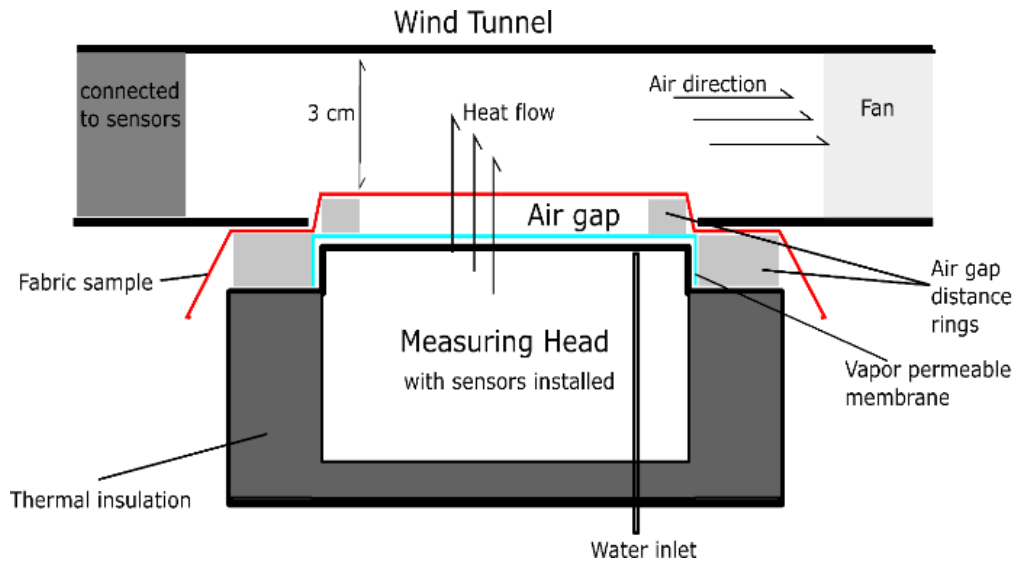


Figure 14. Principle of Permetest skin model

4.3 Rct/Ret – Methods

4.3.1 Thermal Manikin – Samples

Four materials which were 100% cotton, 50/50% cotton/polyester, 100% polyester, and 100% polypropylene that were chosen and were made into long sleeve shirts in five sizes with 1cm overlapping double taped closure center back. Each size was approximately equivalent to a different air gap distance of 0, 4, 8, 12, 16 mm. The first shirt was tight-fitted by the molding method [89], and other shirt sizes were based on the first shirt plus ease allowance (air gap distance).

4.3.1.1 Thermal Manikin Clothing Samples by Molding Method

Using ready-to-wear clothing is not possible to know how much ease allowance (air gap distance) the producer/ designer put into the clothing. Even by the traditional standard in the garment industry for clothing sizing is still difficult to find out the answer because each company will have their variation of the standard of sizing according to their clientele. In such conditions, to know exactly how much of the ease allowance (air gap distance) that built-in the clothing for the R_{ct} and R_{et} tests, the better way is to create a simple regular shirt with the materials for testing. In this way, the researcher will fully control how much ease allowance he needs for the experiment. The procedures are as follow:

1. Observe and analyze the thermal manikin body to determine which parts needed to be cautious and think about the solution. For example, Newton (sweating thermal manikin) has a few hooks in the back arms and legs for the connection for movement. In this case, holes or slits on the sleeves or in the pants needed to be prepared.
2. Take measurements of the manikin for truing the patterns later on.
3. Marking by using small stickers along the contour of the torso of the manikin.
These marks will be the vertical pointers where the front, back, and side seams will be, and the horizontal pointers where the chest level, waist and hips.
4. The first layer is plastic shrinkwrapped around the torso and arms for protection and easy unmolding.

5. The second layer uses duct tape to reinforce the first layer and make sure the markings are correctly transferred to the second layer because the duct tape is usually not see-through.
 6. Connect all the markings using a ruler and marker before cutting along the joined lines and unmold.
 7. Separate the front and back three-dimensional unmolded pieces with different color markers, symbols or numbers to indicate their correct position and order in the front and back moldings.
 8. For pieces with protruded areas, a slit or a cut-through is needed to make all pieces flat and ready for conversion to two-dimensional pattern pieces.
 9. Place unmolded pieces on top of the paper and transfer the shapes onto it using curve and straight rulers. Please do not cut it until after truing (comparing the measurements from the manikin to the drawn pattern outline).
 10. After truing pattern pieces, make sure to add 1 cm seam allowance all around each pattern piece for sewing.
 11. Cut and sew and try it on the manikin, any errors, change and improve the pattern pieces.
- The patternmaking procedures are shown in *Figure 15a-f*.



Figure 15a. Tore – Dry thermal manikin



b. The molding method – duct tape was applied on top of the plastic shrink wrap, which was tightly wrapped around the torso of the manikin for protection and easy unmolding



c. Unmolded front and back pieces and were divided into small segments according to the contour lines on the manikin's torso



d. Unmolded arm piece from shoulder to wrist and cut into small segments



f. The finished shirt was completed with bodice and sleeves and was closed in the center back



e. The arm piece was converted into two-dimensional sleeve patterns

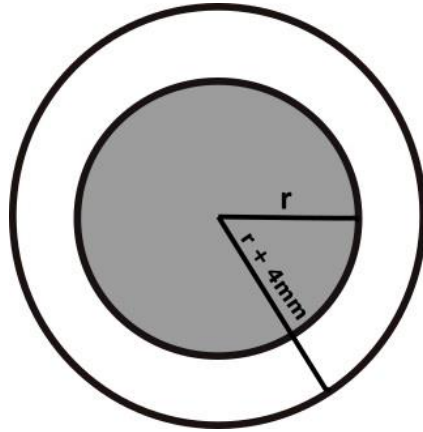


Figure 16. The grey area is the torso of the thermal manikin and air gap distance is added to the radius of the torso that will become the ease allowance of the clothing for the thermal manikin

Based on the first set of shirt patterns, assuming the torso of the thermal manikin was a circular column, ease allowance (air gap distance) would add onto the radius of the circumference of the torso which was then become the ease allowance for the front and back patterns of the shirt and so on (Figure 16).

First size sample (0 mm) by tape measure, the chest circumference of the manikin is 940 mm, hence; using Eq (18) the radius of the chest is 149.68 mm. Based on the clothing pattern of the first sample with 0 mm air gaps, the clothing pattern of other sizes each will have an increase in the radius of the manikin body circumference. The increase in the radius is 0; 4, 8, 12, 16 mm. Hence, the total increase of the pattern sizes is calculated as Eq (19):

$$\text{Manikin Body Circumference (MBC)} = 2\pi.r \tag{18}$$

$$\text{Grading Size of Shirt} = 2\pi(r + i) \tag{19}$$

where: i is the increase of the radius: 0, 4 and 8 mm and so on. The increase of the body circumference from each of the samples will be divided equally and distributed to the front and back on the pattern pieces as shown in Table 6.

Table 6. The total increase in each sample's circumference and the increase in each sample's front and back pattern pieces

<i>Sample number</i>	<i>Radius increase and Total increase in Sample's Circumference</i>	<i>Equal amount increases in the Front piece and Backpiece</i>
<i>Sample 1</i>	<i>r=149.7mm (no increase), 940mm Chest circumference</i>	<i>0</i>
<i>Sample 2</i>	<i>r+4mm=153.7mm, (968.3-940) mm</i>	<i>28.3mm/2=14.1mm</i>
<i>Sample 3</i>	<i>r+8mm=157.7mm, (993.5-940) mm</i>	<i>53.5mm/2=26.8mm</i>
<i>Sample 4</i>	<i>r+12mm=161.7mm, (1018.7-940) mm</i>	<i>78.7mm/2=39.4mm</i>
<i>Sample 5</i>	<i>r+16mm=1mm, (1044-940) mm</i>	<i>104mm/2=52mm</i>

A total of twenty combinations of shirts of four materials with 0, 4, 8, 12, 16 mm built-in air gap distance were made. The air gap distance around the torso when the shirt was put on the manikin might not be the same as desired because of the gravity and the mechanical properties of the materials; for example, on the shoulder areas might have 0 mm air gap distance. All shirts were sewn with a fine 100% polyester thread (Polysheen® No. 40) with a fine machine sewing needle (Schmetz 70/10). The stitched seams were pressed open under a press cloth with high heat to melt/expand the polyester thread to minimize needle holes' size to reduce heat loss.

4.3.2 Thermal Manikin - Climatic Chamber and Experiment Procedures

During the experiment, the thermal manikin was put in the climatic chamber at Lund University (dimensions: 2400 height x 2360 width x 3200 length mm). The chamber can be adjusted from 5 to 60 °C and the temperature standard deviation (SD) from the set value is less than ±2 °C. The relative humidity in this chamber can be adjusted from 10 to 95%, depending on the temperature and the humidity SD from the set value is less than ±5%. Air velocity can be adjusted between 0.1 and 0.7 [m/s]. R_{ct} tests were in non-isothermal condition, the manikin's surface temperature was set and maintained at 34±2 °C. The ambient temperature was set and maintained at 22±2°C (checked against the average of three temperature measurements taken at 0.1, 1.1 and 1.7 m above

the level of the sole of the manikin's foot) with 0.145 ± 0.060 [m/s] air velocity aimed at the manikin's back (measured at 1.2 m above floor level). The relative humidity inside the chamber was maintained at $50 \pm 5\%$. in a hanging/standing position and followed the standard procedures ISO 15831[9]. R_{et} tests were in isothermal condition, thermal manikin skin temperature remained at 34 ± 2 °C and a pre-wet skin would put onto the manikin (wet-skin temperature is difficult to determine); the ambient temperature was $34^\circ\text{C} \pm 2$, the relative humidity inside the chamber was maintained at $50 \pm 5\%$, and wind speed was 0.145 ± 0.060 [m/s].

The experiment for the thermal and evaporative resistance are including two steps: First step for the R_{ct} test, the thermal manikin is measured naked in non-isothermal condition; and for the R_{et} test, a pre-wet skin which is a tight-fitting skin (thickness 0.9 mm, 95% cotton, 5% elastane) covered the manikin's entire body except for the hands and feet, is measured under isothermal condition (despite the pre wet-skin method not being standardized, it has been presented in a variety of publications and was used for sweat simulation [90-92] in heat and mass transfer studies).

The naked manikin or the manikin wearing the pre-wet skin is tested three times to take the mean value for later calculations. Second step is explained in the following: Each of the 20 shirt combinations was tested three times for the thermal insulation (R_{ct}) and the evaporation resistance (R_{et}). For each test, one shirt would be worn on the thermal manikin (or on top of the pre wet-skin in R_{et} tests) and followed the air gap size and material order. For example, 1st round – 1st test, 0 mm/cotton, next 0mm/cotton-polyester blended, next 0mm polyester, next 0mm/polypropylene; then 1st round – 2nd test, 0 mm/cotton and so on until three tests on 0 mm shirts were completed. 2nd round – 1st test, 4 mm/cotton and so on. This order allowed shirts to be recovered, relaxed, and dried before the next test because each test will take about an hour in average.

4.3.3 Thermal Manikin - R_{ct} Results

The heat loss method (using the global calculation method) was used to determine both the total thermal resistance R_{ct_t} [m^2K/W] and the effective thermal resistance $R_{ct_{eff}}$ [m^2K/W]. The resulting data were 20 minutes taken out from the steady-state time, approximately 40 minutes on average (resultant sample in Appendix 7). Eq (20) and (21) are for calculating the R_{ct} results as follow:

$$R_{ct_t} = (T_s - T_o / HL_t) * A \quad (20)$$

$$R_{ct_{eff}} = R_{ct_t} - R_{ct_s} = R_{ct_g} + R_{ct_f} \quad (21)$$

where R_{ct_t} is the total thermal resistance including R_{ct_s} , R_{ct_g} , R_{ct_f} (all in the unit [$m^2.K/W$], which are the boundary layer of the thermal manikin, the thermal resistance of the air gap and the material, respectively. T_s and T_o are the temperature [K] of the thermal manikin shell and the ambient temperature inside the climatic chamber, respectively. HL_t [W] is the total heat loss and A [m^2] is the surface area involved in the experiment. When the effective thermal resistance $R_{ct_{eff}}$ [$m^2.K/W$] is needed, total thermal resistance R_{ct_t} minus the naked thermal manikin resistance is in Eq (21).

Table 7. Effective R_{ct} results from the thermal manikin tests

	Arithmetic Mean of Effective R_{ct} [$m^2.K/W$]							
	100% Cotton	CV %	50/50% Cotton/Polyester	CV %	100% Polyester	CV %	100% Polypropylene	CV %
0mm	0.07	2	0.08	4	0.06	2	0.09	10
4mm	0.1	6	0.09	3	0.08	6	0.11	2
8mm	0.1	6	0.11	1	0.09	4	0.13	6
12mm	0.09	29	0.11	3	0.09	6	0.13	8
16mm	0.12	6	0.12	5	0.11	2	0.14	4

Results of the effective R_{ct} from the combinations of four materials and five air gap distances from 0-16 mm are presented in *Table 7*. Some interesting observations were that one pair of results shared the same mean value from each material and air gap combination. These scenarios may be caused by the shirt draping on the thermal manikin, creating a heterogenous (uneven) air gap between the manikin and the shirt but somehow having the same mean value because the three tests' original values of each sample were all different.

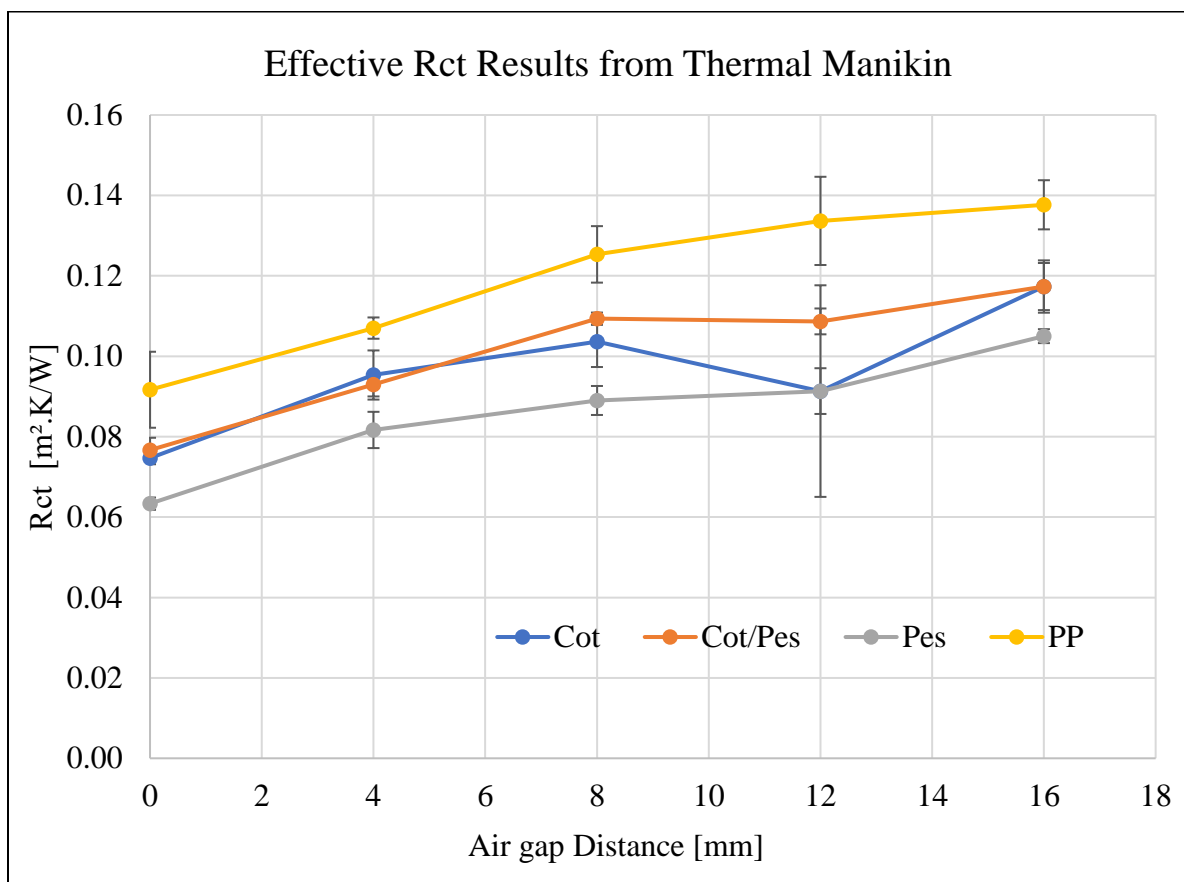


Figure 17. Comparison of the R_{ct} results from the thermal manikin tests of four materials

In *Figure 17*, cotton/polyester blend, 100% polyester, and polypropylene show a similar trend from 0 to 8 mm air gap distance, and R_{ct} is in a linear relation but then slows down after 12 mm. Only 100% cotton reacted differently and slightly dropped at 12 mm the rise quickly at 16mm.

4.3.4 Thermal Manikin - R_{et} Results

The resulting data were 20 minutes taken out from the steady-state time, approximately 40 minutes on average. Eq (22) and (23) are for calculating the R_{et} results as follow:

$$R_{et} = (P_s - P_o / HLt) A \quad (22)$$

$$R_{et_{eff}} = R_{et} - R_{et_s} = R_{et_g} + R_{et_f} \quad (23)$$

where R_{et} [m^2Pa/W] is the total evaporative resistance including R_{et_s} , R_{et_g} , R_{et_f} (all in the unit of [m^2Pa/W]), which are the wet skin layer of the thermal manikin, the evaporative resistance of the air gap and the material, respectively. P_s and P_o are the saturated water vapor pressure (Pa) of the thermal manikin wet skin and the ambient water vapor pressure in the climatic chamber, respectively. When the effective evaporative resistance $R_{et_{eff}}$ [m^2Pa/W] is needed, total evaporative resistance R_{et} minus the wet skin evaporative resistance is in Eq (23).

Table 8. Effective R_{et} results from the thermal manikin tests

Arithmetic Mean of Effective R_{et} [m^2Pa/W]								
	100%	CV	50/50%	CV	100%	CV	100%	CV
	Cotton	%	Cotton/Polyester	%	Polyester	%	Polypropylene	%
0mm	4.9	36	5.87	10	1.73	19	4.63	11
4mm	4.9	21	6.2	9	4.27	12	8.23	6
8mm	10.27	11	10	16	6.47	11	10.73	14
12mm	10.27	27	10.87	5	10.23	10	15.27	17
16mm	11.83	15	13.03	2	12.13	7	13	9

Table 8. presented the effective R_{et} results from the combinations of the air gaps and the materials. However, this time only cotton has one pair of the same result in 0-4 mm and 8-10 mm. Since R_{et} tests were in isothermal condition, there was no temperature difference, only water vapor pressure and it became the cushion layer between the thermal manikin and the shirt. Absorptivity of synthetic fibre like polyester and polypropylene are lower than natural fibre cotton, so when in narrow air gaps, moisture absorbed by the cotton fibre and stick onto the thermal manikin and resulted in similar mean values even though the original R_{et} resulting data of cotton were different from 0 to 16 mm. The cotton properties through the thickness and drapability may also contribute to similar results in different air gap distances.

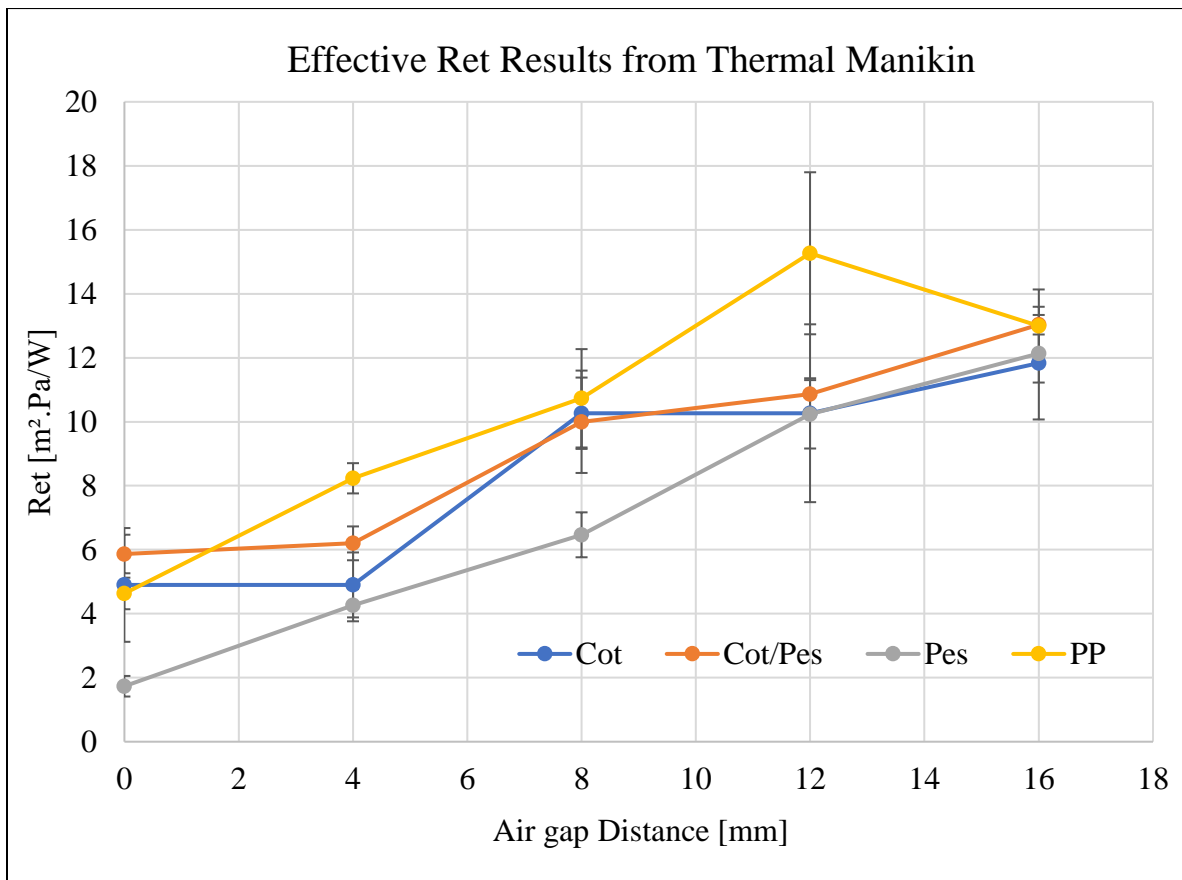


Figure 18. Comparison of the R_{et} results from the thermal manikin of four materials

Two trends were displayed in *Figure 18*: cotton – cotton/polyester and polyester – polypropylene trends. The first trend steady from 0 to 4 mm, then quickly rise to 8 mm and steady at 12 mm then slowly rise to 16 mm; the second trend started to increase steadily from 0 mm until 12 mm then slowed down. Polyester and polypropylene are synthetic fibres, absorptivity is relatively lower than cotton and may not be influenced by the water vapor moisture so that the trend goes steadily; cotton and cotton blends have natural fibres which may have a better absorptivity property that may affect the stability of the vapor pressure between the air gaps from 0 to 16 mm and resulting in rising, stabilized and increasing this regime.

4.3.5 Vertically Oriented Permetest Skin Model – Samples

Like the thermal manikin tests, four materials were used directly without cutting into a particular size and shape. Each test area of the material was randomly chosen and marked after the test not to be used again on the same day.

4.3.6 Vertically Oriented Permetest Skin Model – Climatic Chamber and Experiment Procedures

The experiment was carried out in a climatic chamber and the air parameters were set up on 50-55% of relative humidity, wind speed at 1.0 ± 0.1 [m/s] and ambient temperature at 20-22°C maintaining inside the instrument isothermal conditions for R_{et} tests.

For the R_{ct} tests, the non-isothermal condition was applied, and the hot plate measuring head would increase 10°C more than the ambient temperature. All experiment procedures followed the ISO 11092 [20]. Air gap distance was applied using foamed polyethylene sheet (with low thermal conductivity 0.035 [W/m/K]) serving for preparation of 2.0 / 4.0 and 5.0 mm thickness rings and their combinations (*Figure 19a-c*).

To balance the thickness of the air gap distance created by the stack of rings and to maintain the smooth air current flow inside the wind channel, two types of rings were cut: outer rings were put

around the base of the hotplate for counter thickness; inner rings were placed inside the wind channel on the hotplate to create the air gap distance. The outer ring was 12 cm in diameter on the outer circle and 10 cm on the inner circle, width 2 cm. The inner ring was 8cm in diameter on the outer circle and 6cm on the inner circle, width 2 cm. Each material was tested three times under 0, 4, 8, 12, 16 mm air gap distance in a vertical orientation to simulate the manikin's vertical air gaps.

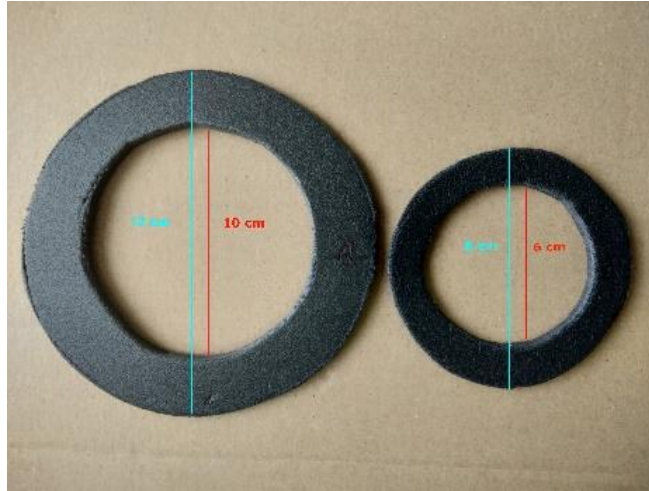


Figure 19a-c. Sizes of outer and inner rings



b. Showing outer rings were stacked on the base of the hotplate



c. Showing inner rings were placed inside the wind channel on the hotplate

4.3.7 Vertically Oriented Permetest Skin Model – R_{ct} Results

Each determination of the R_{ct} of a sample consists of two steps: first test without sample, second test with air gap distance ring of thickness h covered by a sample. When the heat flow q_{eto} [W/m^2] reaches the steady-state, the result of the first step is given by the Eq (24), where R_{cto} [$m^2.mK/W$] presents thermal resistance of the boundary layer above the measuring surface of the apparatus:

$$q_{eto} = (TP_s - TP_o) / R_{cto} \quad (24)$$

Here, TP_s [mK] means the surface temperature of the measuring head, and TP_o [mK] is the ambient temperature in the measuring channel of the Permetest skin model. The second step characterizes the heat flow passing through the measuring head of the apparatus covered by the tested sample:

$$q_{et} = (TP_s - TP_o) / (R_{cto} + R_{ct}) \quad (25)$$

for the case without the distance ring in Eq (25) or with distance ring in Eq (26)

$$q_{etg} = (TP_s - TP_o) / (R_{cto} + R_{ct} + R_{ctg}) \quad (26)$$

which creates the additional air gap resistance R_{ctg} [$m^2.mK/W$]. $R_{ctg} = h/\lambda$, where λ [$W/m.K$] is the thermal conductivity of the air. The required thermal resistance of the sample R_{ct} yields solution of Eq (24) and Eq (25). The required total thermal resistance of the sample R_{ct} plus air gap resistance

R_{ctg} yields the solution of Eq (24) and Eq (26). When the thermal resistance of the sample R_{ct} is deduced from the achieved value, we obtain thermal resistance R_{ctg} of the air gap.

Table 9. Effective R_{ct} results from Permetest skin model in the Vertically Oriented position

Arithmetic Mean Values of Effective R_{ct} [$m^2.mK/W$]								
Vertically Oriented Air gap	100%	CV	50/50%	CV	100%	CV	100%	CV
	Cotton	%	Cotton/Polyester	%	Polyester	%	Polypropylene	%
0mm	8.7	9	11.5	13	7.8	11	12	6
4mm	65.5	14	46.1	3	54.8	2	54.7	15
8mm	94.5	3	69	2	74.9	2	89.5	1
12mm	95.2	2	73.8	5	90.1	3	93	7
16mm	106.5	11	82.2	17	101.1	5	90.2	5

The resulting data in *Table 9* show each material rises from 0 mm quickly to 8 mm, then slows down at 12 mm. *Figure 20* is presenting the visual of the data.

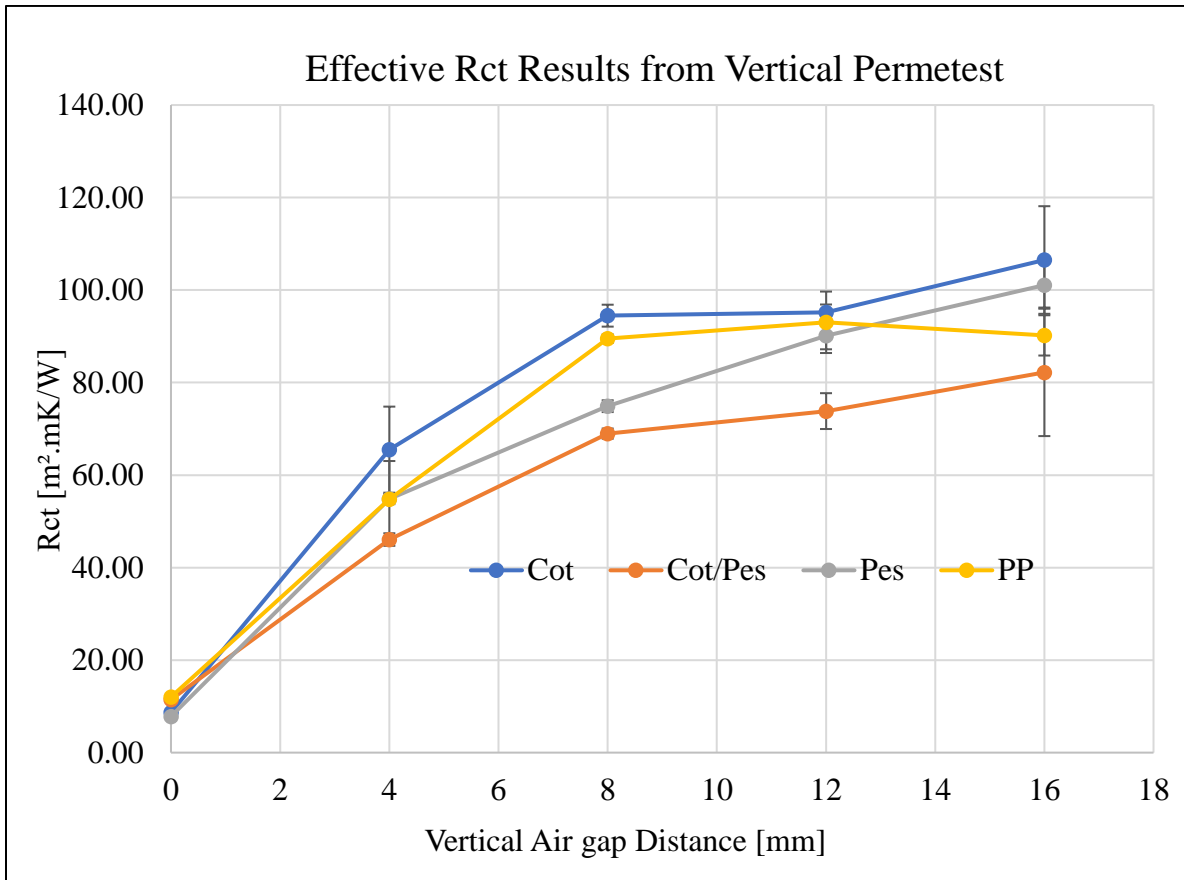


Figure 20. Comparison of the R_{ct} results from Vertically Oriented Permetest of four materials

4.3.8 Vertically Oriented Permetest Skin Model – R_{et} Results

Each determination of the R_{et} of a sample consists of two steps: first test without sample, second test with air gap distance ring of thickness h covered by a sample. When the heat flow q_{eto} reaches the steady-state, the result of the first step is given by the Eq (27), where Ret_o [$m^2 \cdot Pa/W$] presents the evaporative resistance of the boundary layer above the measuring surface of the apparatus:

$$q_{eto} = (PP_s - PP_o) / Ret_o \quad (27)$$

Here, PP_s [Pa] means partial pressure of the saturated water vapor above the hotplate, and PP_o [Pa] is the partial pressure of the water vapor in the measuring tunnel of the testing apparatus. The second step characterizes the heat flow passing through the measuring head of the apparatus covered by the tested sample:

$$q_{et} = (PP_s - PP_o) / (Ret_o + R_{et}) \quad (28)$$

for the case without the distance ring in Eq (28) or with distance ring in Eq (29)

$$q_{etg} = (PP_s - PP_o) / (Ret_o + R_{et} + Ret_g) \quad (29)$$

which creates the additional air gap resistance Ret_g^* [$m^2 Pa \cdot s/kg$]. $Ret_g^* = h/DP$ [$kg/m \cdot Pa \cdot s$] presents the water vapor diffusion coefficient in the air related to the water vapor partial pressure, which had been mentioned in *section 4.1.2*. The required evaporation resistance of the sample R_{et} yields

solution of Eq (27) and Eq (28). The required total evaporative resistance of the sample R_{et} plus air gap resistance Ret_g^* yields solution of v Eq (27) and Eq (29). When the evaporative resistance of the sample Ret is deduced from the achieved value, we obtain evaporation resistance Ret_g^* of the air gap.

Table 10. Effective R_{et} results from Permetest skin model in the Vertical Oriented position

Arithmetic Mean Values of R_{et} [m^2Pa/W]								
Vertically Oriented Air gap	100% Cotton	CV %	50/50% Cotton /Polyester	CV %	100% Polyester	CV %	100% Polypropylene	CV %
0mm	3.4	13	3.6	15	1.5	4	3.2	4
4mm	8.2	2	6.1	4	7.4	3	5.7	2
8mm	12.9	2	11.5	4	14.1	3	9.5	2
12mm	22.5	4	22.2	4	20.7	3	17.3	12
16mm	25.5	11	26.2	4	24.5	10	18.6	7

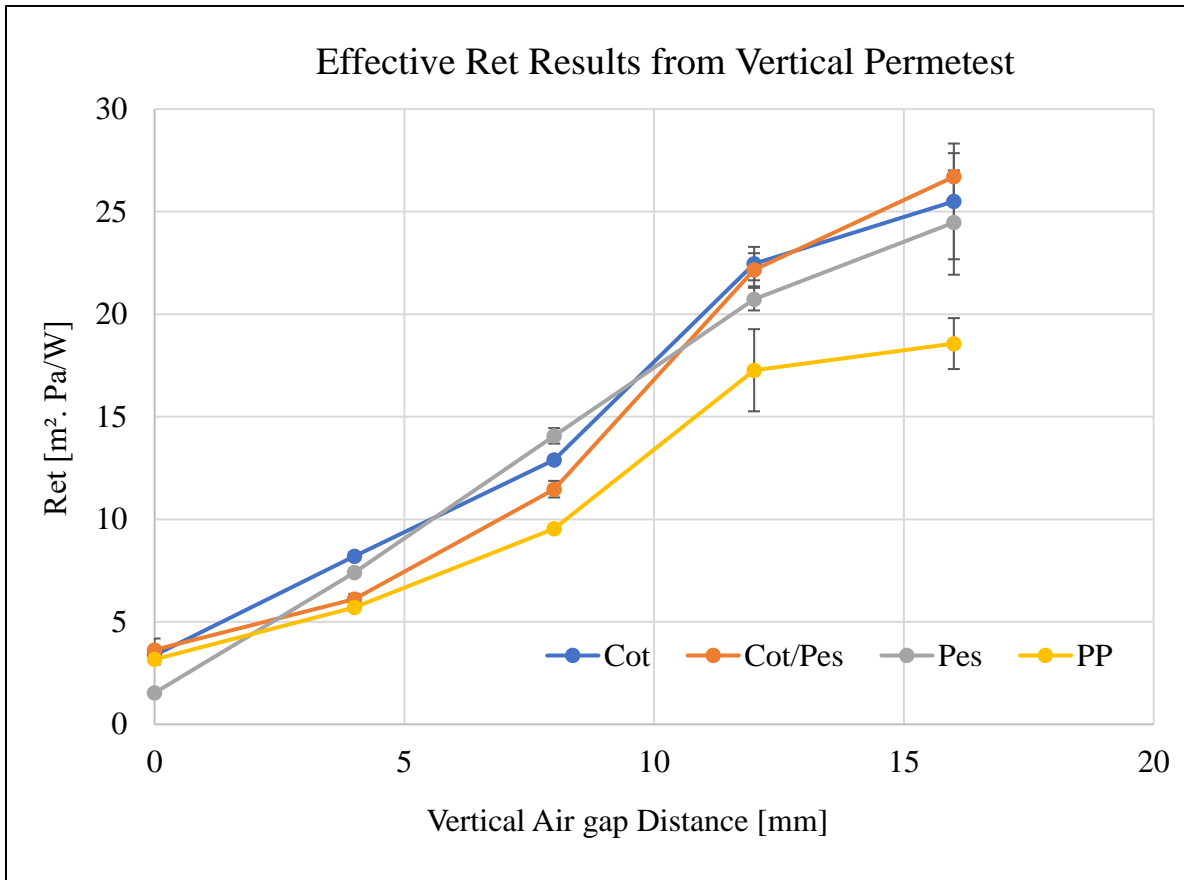


Figure 21. Comparison of the R_{et} results from Vertically Oriented Permetest of four materials

Similar to effective R_{ct} results, effective R_{et} results presented in *Table 10*, showing each material's evaporative resistance rose from 0 mm quickly up to 12 mm then slowed down to 16 mm. When comparing *Figure 17, 18* to *Figure 20, 21*; it seems that the results from the Permetest skin model are more uniformity than the thermal manikin results, and it may cause by the even air gap distances created in Permetest but not the uneven and unpredictable air gap space between the thermal manikin and the shirt.

4.4 Analysis of Thermal Manikin and Permetest Skin Model (Vertical Orientation)

Results from the thermal manikin and the Permetest skin model were analyzed using three statistical methods: correlation coefficient (r), R^2 and two-way ANOVA with replication.

4.4.1 Correlation coefficient (r) -- The Thermal Manikin and the Vertically Oriented Permetest skin model

Table 11. The correlation coefficient (r) of Thermal Manikin Vs. Vertically Oriented skin model

Manikin Vs Permetest (r)	100% Cot	50/50% Cot/Pes	100% Pes	100% PP
R_{ct}	0.83	0.97	0.96	0.97
R_{et}	0.90	0.96	1.00	0.94

Results presented in *Table 11* showing all four materials have a very strong and positive trend (close to +1) between the thermal manikin and the vertically oriented Permetest skin model in both thermal (R_{ct}) and evaporative resistance (R_{et}).

4.4.2 R^2 - Regression between the Thermal Manikin and the Vertically Oriented Permetest skin model

The R^2 results in *Table 12*, each material from thermal and evaporative resistance are showing strong correlations between the thermal manikin and the Permetest skin model, which means that every changing value of thermal manikin can be highly explained by the value of the Permetest skin model or vice versa.

Table 12. The correlation determination (R^2) of Thermal Manikin Vs. Vertically Oriented skin model

Manikin Vs Permetest (R^2)	100% Cot	50/50% Cot/Pes	100% Pes	100% PP
R_{ct}	0.70	0.94	0.91	0.95
R_{et}	0.80	0.91	1	0.88

4.4.3 Two-way ANOVA -- The Thermal Manikin and the Vertically Oriented Permetest skin model

In both R_{ct} and R_{et} results from 100% cotton, 50/50% cotton/polyester blend, 100% polyester, 100% polypropylene showed that the *p-value* < **0.01** means a significant difference between the thermal manikin and the vertically oriented Permetest skin model. The result is logical because the thermal manikin and the vertically oriented Permetest skin model are fundamentally different: from sizes and shapes to test methods, ISO standard and so on (*Table 1-2*).

4.5 R_{ct}/R_{et} on Horizontally/Vertically Oriented Permetest Skin Model

To understand the difference between the vertically and the horizontally oriented air gap distance, the Permetest skin model was chosen for the task because of its versatility of position orientation, portability in size, and the R_{ct}/R_{et} test relatively in shorter time.

4.5.1 Methods and Experiments – Samples

Seven test materials were chosen and their properties were presented in *Table 4*. They were woven and blended fabric between 100% cotton and 100% polyester, plus one polypropylene for counter reference. All test materials were washed, hang-dry, iron flat before used.

4.5.2 Climatic Chamber and Experiment Procedures

Each test material would be tested five times randomly and non-destructively (without cutting into size and shape) for R_{ct}/R_{et} with the combinations of five different air gap distances and the vertical/horizontal orientation in the Permetest skin model. Each test area would be marked after testing to prevent repetition. The experiment would follow ISO 11920 and the climatic chamber set up and apply the air gap distance rings. Please refer to the previous *section 4.3.6*.

Table 13. The arithmetic mean values of 7 materials resulted from R_{ct}/R_{et} and the combinations of Horizontal/ Vertical orientation and air gap distances

100% Cotton								
Air gap Distance	$R_{ct} [m^2.mK/W]$				$R_{et} [m^2.Pa /W]$			
	H	CV %	V	CV %	H	CV %	V	CV %
0mm	10.8	12	9.5	15	2.8	5	2.5	6
4mm	53.5	8	60.4	4	6.2	3	5.4	2
8mm	112.8	3	82.1	4	15.9	10	12.4	2
12mm	147.6	4	130.8	3	22.1	0.4	18	1
16mm	129.2	8	123.8	10	25.4	5	28.6	10
20% Polyester								
Air gap Distance	$R_{ct} [m^2.mK/W]$				$R_{et} [m^2.Pa /W]$			
	H	CV %	V	CV %	H	CV %	V	CV %
0mm	13.2	9	13.3	11	4.1	7	3.7	5
4mm	65.6	6	61.9	2	6.6	2	6.3	2
8mm	116.4	9	80	5	15.9	8	13.5	2
12mm	113.3	8	108.7	2	26.6	4	20	11
16mm	123	7	123.1	10	33	9	30.8	9

30% Pes								
Air gap Distance	$R_{ct} [m^2.mK/W]$				$R_{et} [m^2.Pa /W]$			
	H	CV %	V	CV %	H	CV %	V	CV %
0mm	15.4	11	13.6	9	3.8	8	3.6	3
4mm	68	2	64.5	2	7	6	6	3
8mm	122.3	5	80.2	8	17.8	9	13.3	2
12mm	124.8	3	113.9	4	25.5	6	20.9	5
16mm	131.9	3	132.5	10	26.7	3	26.6	4
50% Polyester								
Air gap Distance	$R_{ct} [m^2.mK/W]$				$R_{et} [m^2.Pa /W]$			
	H	CV %	V	CV %	H	CV %	V	CV %
0mm	13.4	4	13.1	8	2.9	7	2.7	7
4mm	74.1	3	62.9	4	6.1	3	5.4	4
8mm	120.9	5	87.7	4	16.8	8	12.2	2
12mm	140.8	12	113.5	3	24.5	6	18.3	3
16mm	117.4	5	123.8	5	25.8	2	25.6	9

65% Pes								
Air gap Distance	$R_{ct} [m^2.mK/W]$				$R_{et} [m^2.Pa /W]$			
	H	CV %	V	CV %	H	CV %	V	CV %
0mm	11.6	7	11.3	14	2.2	5	2	10
4mm	72.4	3	64.5	4	5.7	4	5.2	2
8mm	131.1	4	91.2	5	15	11	12.2	2
12mm	147.3	9	129.2	9	24.4	7	19.3	5
16mm	121	7	120.3	9	25.7	2	23.4	4
100% Polyester								
Air gap Distance	$R_{ct} [m^2.mK/W]$				$R_{et} [m^2.Pa /W]$			
	H	CV %	V	CV %	H	CV %	V	CV %
0mm	5.8	7	7.4	14	1.7	6	1.3	15
4mm	68.9	11	56.8	8	5.6	4	4.8	2
8mm	116.3	3	90.2	2	13.2	2	12.1	2
12mm	138.2	3	109.4	3	25.6	4	18.3	5
16mm	143.6	7	131.9	6	25.1	2	25	5

<i>100% Polypropylene</i>								
<i>Air gap Distance</i>	<i>R_{ct} [m².mK/W]</i>				<i>R_{et} [m².Pa /W]</i>			
	<i>H</i>	<i>CV %</i>	<i>V</i>	<i>CV %</i>	<i>H</i>	<i>CV %</i>	<i>V</i>	<i>CV %</i>
<i>0mm</i>	15.6	11	15.7	5	4.3	5	3.6	6
<i>4mm</i>	73.6	8	69.8	3	7.5	3	6.5	2
<i>8mm</i>	138.2	5	95.3	5	16	10	14	2
<i>12mm</i>	162.6	2	140.3	12	27.4	0.4	20.4	1
<i>16mm</i>	140.1	5	120.8	3	26.5	5	24.4	10

4.5.3 Results

Results from R_{ct}/R_{et} tests of seven materials in vertically/horizontally oriented air gaps are presented in *Table 13* above. The resulting data show that there are two common trends:

- R_{ct}/R_{et} rises quickly from 0 mm until 12 mm, slowing down or dropping from 12mm air gap distance in both horizontal and vertical orientations. *Table 14 and 15* are presenting the difference between vertically and horizontally oriented air gap results in both R_{ct} and R_{et}. The percentage of difference is calculated by the Eq (30) as follow:

$$(H - V/H) * 100 \quad (30)$$

Where *H* and *V* are horizontal/ vertical air gap results from R_{ct}/R_{et}.

- Vertically oriented test results are slightly lower than the horizontally oriented test results in most cases. Visual comparisons are presenting in *Figure 22-23*.

Table 14. R_{ct} -Difference between Horizontally and Vertically Oriented Air gaps

R_{ct} - Difference between Horizontally and Vertically Oriented Air gaps (%)							
	Cot	20Pes	30Pes	50Pes	65Pes	Pes	PP
0mm	12	-0.8	11.7	2.2	2.6	-27.6	-0.6
4mm	-12.9	5.6	5.1	15.1	10.9	17.6	5.2
8mm	27.2	31.3	34.4	27.5	30.4	22.4	31
12mm	11.4	4.1	8.7	19.4	12.3	20.8	13.7
16mm	4.2	-0.1	-0.5	-5.5	0.6	8.1	13.8

Table 15. R_{et} -Difference between Horizontally and Vertically Oriented Air gaps

R_{et} - Difference between Horizontally and Vertically Oriented Air gaps (%)							
	Cot	20Pes	30Pes	50Pes	65Pes	Pes	PP
0mm	10.7	9.8	5.3	6.9	9.1	23.5	16.3
4mm	12.9	4.5	14.3	11.5	8.8	14.3	13.3
8mm	22	15.1	25.3	27.4	18.7	8.3	12.5
12mm	18.6	24.8	18	25.3	20.9	8.3	25.5
16mm	-12.6	6.7	0.4	0.8	8.9	0.4	7.9

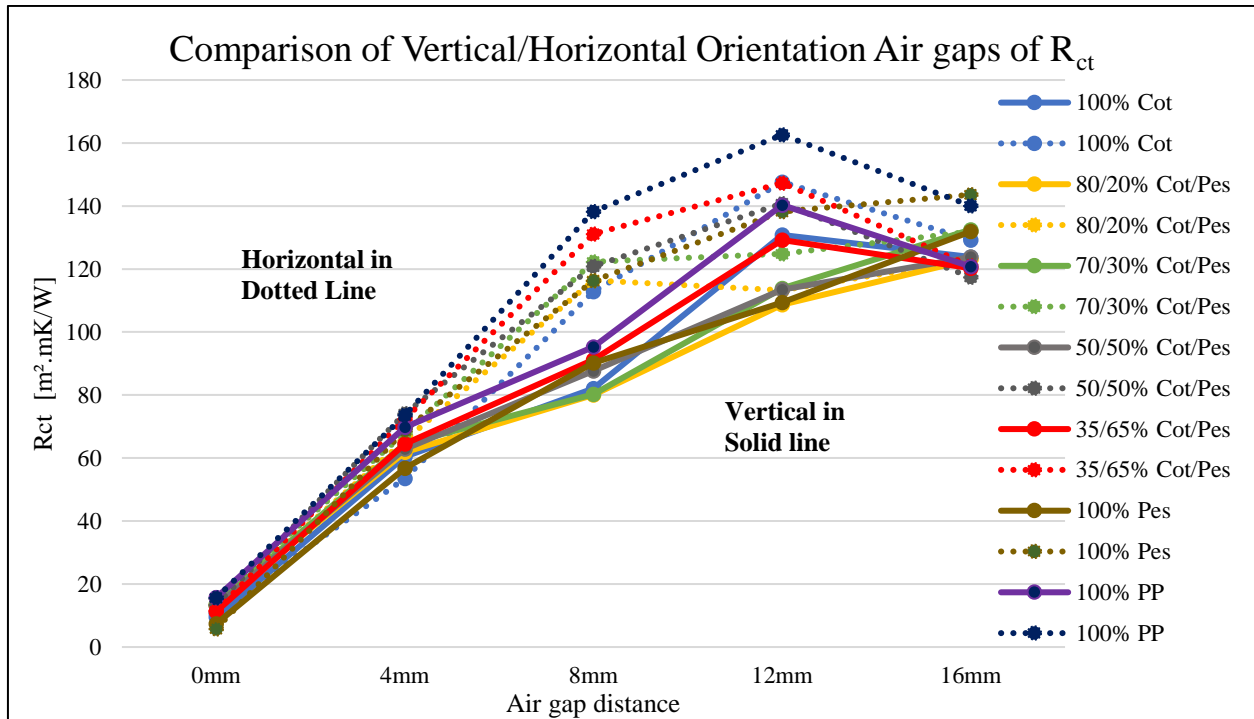


Figure 22. Visual comparison of the vertically and horizontally oriented air gaps of R_{ct}

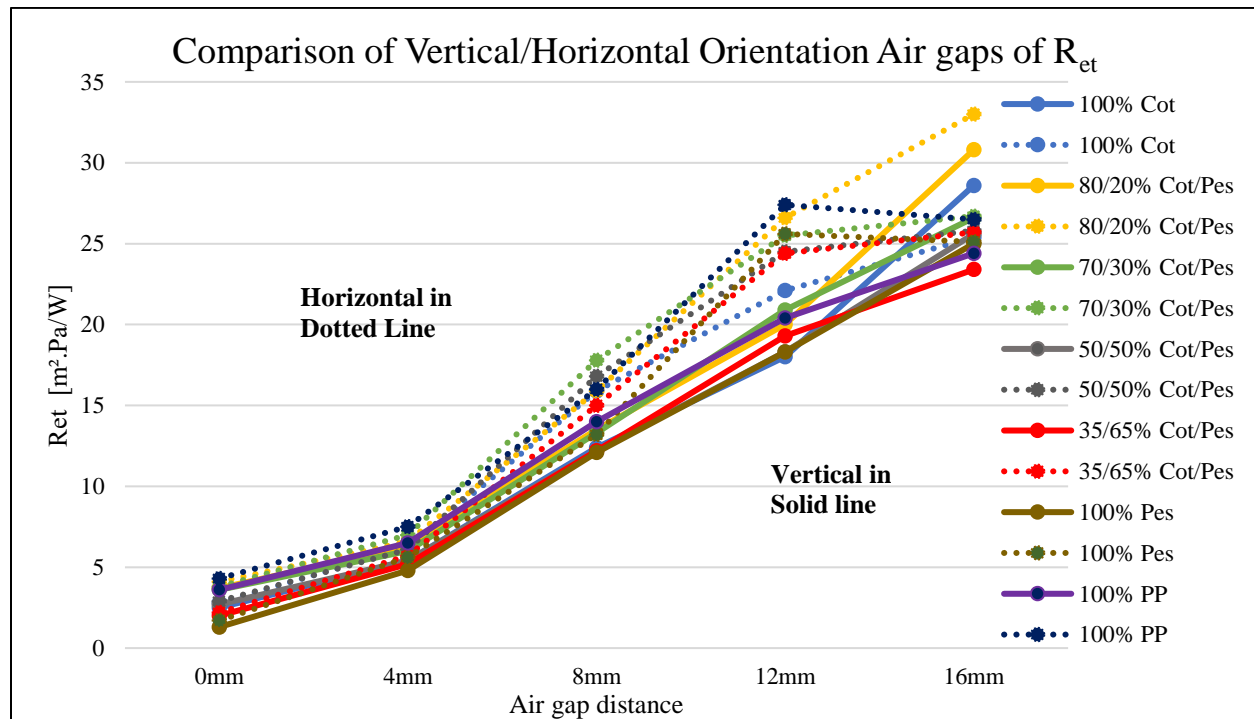


Figure 23. Visual comparison of the vertically and horizontally oriented the air gaps of R_{et}

4.6 Analysis of the H/V Oriented Permetest Skin Mode

Results from the seven tested materials were analyzed using three statistical methods: correlation coefficient (r), R^2 and two-way ANOVA with replication.

4.6.1 The Correlation Coefficient (r) of the Vertically and the Horizontally Oriented Permetest Results from Seven Tested Materials

Each material's correlation coefficient r (*Table 16* on next page) shows a very strong and positive trend from all seven materials; the r is almost +1.

Table 16. Correlation coefficient (*r*) results of *R_{ct}*/*R_{et}* and the combinations of Horizontally/Vertically Oriental air gap distances from 7 materials

100% Cotton				80/20% Cotton/Polyester			
R_{ct}		R_{et}		R_{ct}		R_{et}	
H	V	H	V	H	V	H	V
H	1	H	1	H	1	H	1
V	0.97	V	0.96	V	0.94	V	0.98
70/30% Cotton/Polyester				50/50% Cotton/Polyester			
R_{ct}		R_{et}		R_{ct}		R_{et}	
H	V	H	V	H	V	H	V
H	1	H	1	H	1	H	1
V	0.94	V	0.98	V	0.95	V	0.97
35/65% Cotton/Polyester				100% Polyester			
R_{ct}		R_{et}		R_{ct}		R_{et}	
H	V	H	V	H	V	H	V
H	1	H	1	H	1	H	1
V	0.96	V	0.99	V	0.99	V	1.00
100% Polypropylene							
R_{ct}		R_{et}					
H	V	H	V				
H	1	H	1				
V	0.97	V	0.98				

4.6.2 R² - Regression between the Vertically and the Horizontally Oriented Permetest Results from Seven Tested Materials

Table 17. Regression results of R_{ct}/R_{et} and the combinations of Vertically/Horizontally Oriented air gap distances from 7 materials

Vertical		80/20%	70/30%	50/50%	35/65%		
Vs.	100%	Cotton/	Cotton/	Cotton/	Cotton/	100%	100%
Horizontal	Cotton	Polyester	Polyester	Polyester	Polyester	polyester	polypropylene
R²							
R_{ct}	0.94	0.89	0.88	0.89	0.92	0.98	0.95
R_{et}	0.92	0.97	0.95	0.93	0.99	1	0.96

The regression from the R_{ct}/R_{et} test results (Table 17) from seven materials is very strong, and most of the R² are over 0.9, which means the vertically oriented Permetest can predict the R_{ct}/R_{et} results for the horizontally oriented Permetest or vice versa.

4.6.3 Two-way ANOVA with five repetitions results from Vertically and Horizontally Oriented Permetest from Seven Materials

Results from R_{ct} and R_{et} of all seven materials show that the *p-value* < 0.01 means there is a significant difference between the vertically and the horizontally oriented Permetest skin model. The reason is that even the experiments were done by using the same Permetest skin model. However, the vertical and horizontal orientation of the apparatus was causing some difference in the resulting values. R_{ct} experiments were done under non-isothermal conditions, and the driving force was the temperature difference. Hot air rises and cool air falls naturally in the vertical air gap, but in the horizontal air gap, the air has to travel through a distance inside the wind channel before exiting. R_{et} experiments were done under isothermal conditions, and saturated vapor pressure is the driving force. Water vapor molecules are concentrated at the bottom and rising to the wind channel's top in the horizontal air gap. However, when it is in the vertical orientation, the rising water vapor molecules may escape through the fan that will cause R_{et}'s lower values. It also leads

to the R_{ct}/R_{et} results that the vertically oriented values always seem lower than the horizontally oriented values from the air gap distance 0 - 16mm (*Figure 22-23*).

4.7 Determination for the Best Fit Equation Models for the R_{ct}/R_{et} Data from the H/V Oriented Permetest Skin Model Results

The resulting data from thermal resistance (R_{ct}) of seven materials with the combinations of air gap distances and vertical/horizontal orientations showed a polynomial equation fitted better than the linear equation, $R^2 > 0.95$. However, data from evaporative resistance (R_{et}) of seven materials with the combinations of air gap distances and vertical/horizontal orientations showed that data fitted better in the linear equation and the $R^2 > 0.98$ except 100% polyester $R^2 = 0.90$ (*Figure 24a-n*).

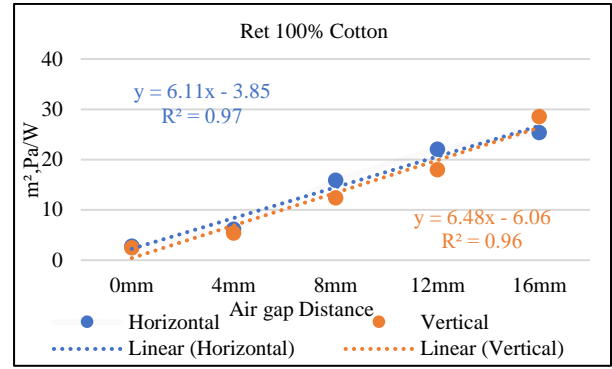
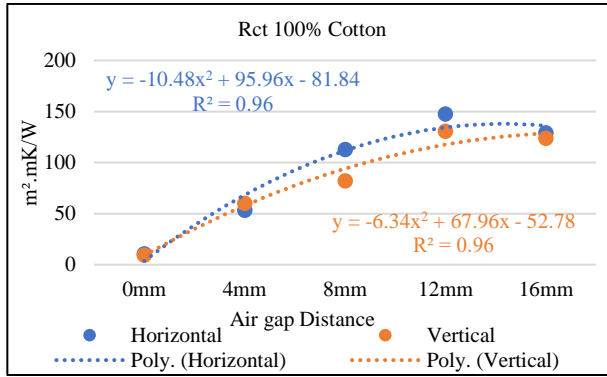
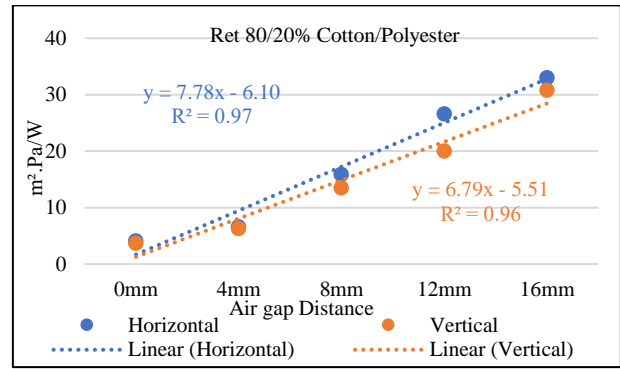
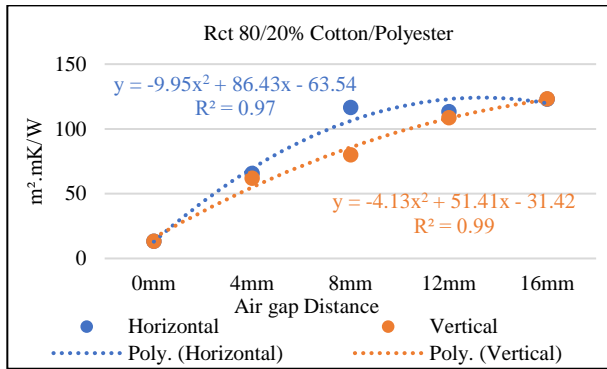
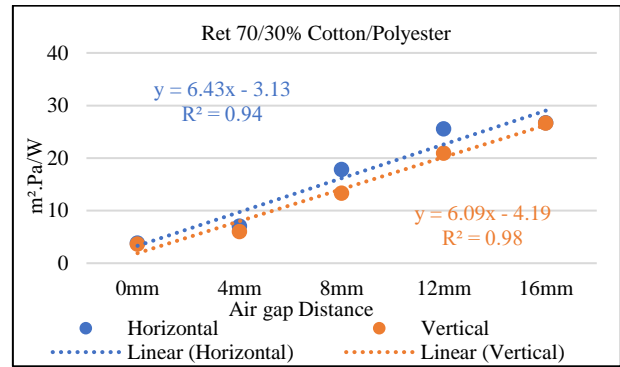
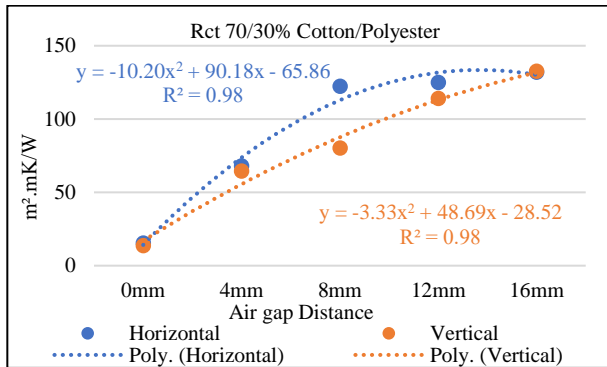


Figure 24a-n a. The best-fit model for data b.
from the R_{ct}/R_{et} of seven materials



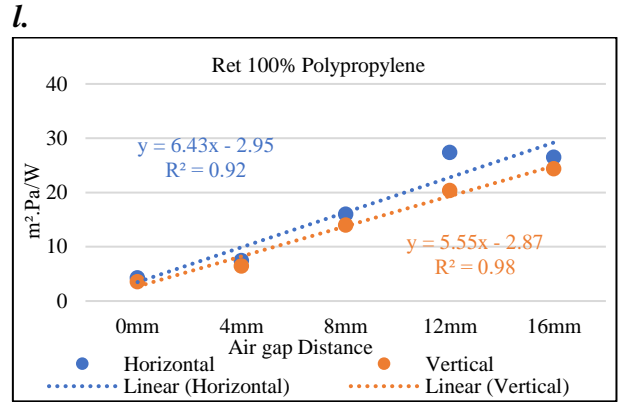
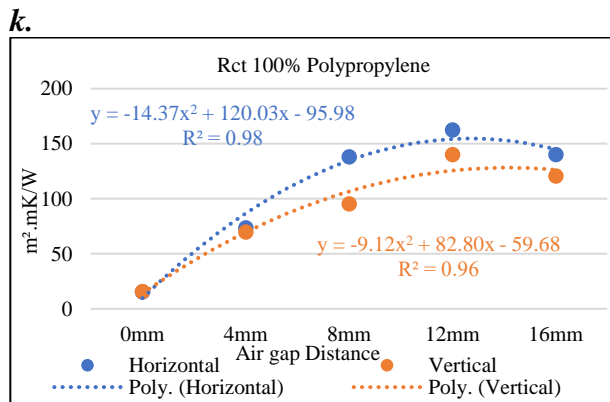
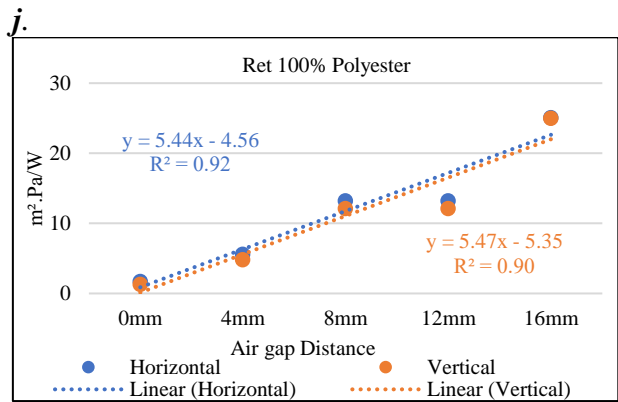
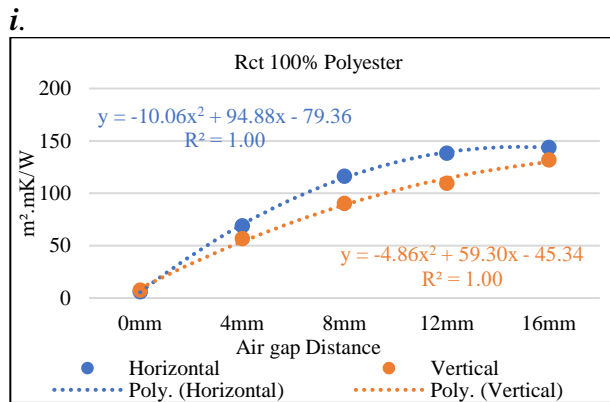
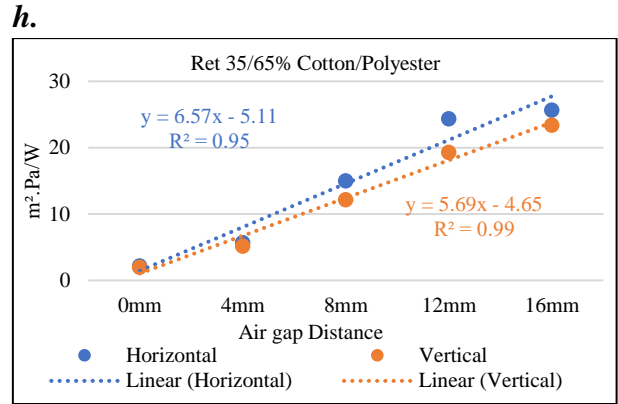
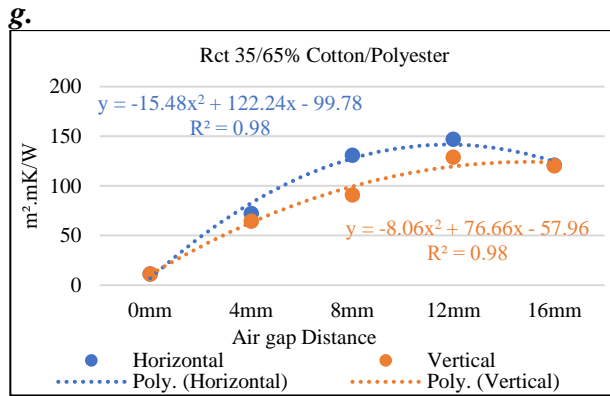
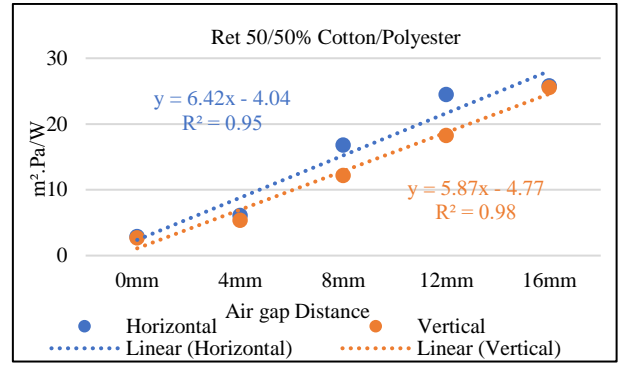
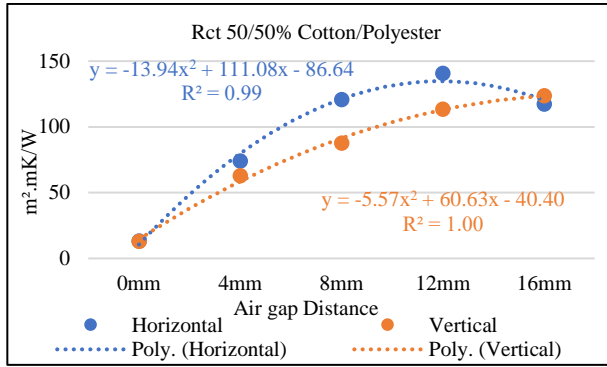
c.

d.



e.

f.



m.

n.

5. Evaluation of Results

The thermal manikin is considered the best apparatus for measuring thermal and evaporative resistance for the clothing system because the apparatus's human form can detect the radiation, conduction, and convection in the 3D environment. However, the expensive cost, the long preparation time for the test, and a big climatic chamber are needed for the apparatus, and not many companies nor researchers can access it. More, the uncertainty of the wet skin temperature of the sweating thermal manikin and error may be caused by wet skin direct contact to clothing; and the condensation build-in under the clothing when in the cold ambient can also cause over or underestimation of the results and so on lead to an alternative method for the thermophysiological measure is needed.

The use of the Permetest skin model in the study is advantageous because of being portable and offering the possibility of its versatile use both in a vertical or horizontal orientation. Moreover, it is a fast thermophysiological comfort measuring device due to its small measuring head. It enables to set up a series of experiments to find out the correlation, R^2 and ANOVA between the thermal manikin and the Permetest skin model, and based on these results; it makes possible to build up a mathematical equation to determine the clothing evaporation resistance R_{et} derived from thermal resistance R_{ct} measured by the dry thermal manikin.

As already mentioned, heat transfer from body skin through an air gap (between the skin and the clothing) and clothing to the environment was executed by conduction, convection and radiation. At the beginning of this research, it was already proved that under isothermal conditions, there is no free convection (see the results for R_{et}) in narrow air gaps under 12 mm. Same results were observed at non-isothermal conditions when determining thermal resistance R_{ct} .

However, besides heat transfer by conduction in relatively narrow air gaps, there is always a certain small component of heat transfer by free convection, caused by local turbulences, despite low levels

of Rayleigh numbers. Moreover, at the non-isothermal thermal resistance measurements on thermal manikins and on the Permetest skin model, there must occur, at least theoretically, a certain level of heat flow $\dot{q}_{rad}[\text{W}/\text{m}^2]$ transferred by radiation, see the commonly known equation (31) for heat transfer by radiation between two large plates with temperatures T_1 and T_2 in [K] and internal surface emissivity levels $\varepsilon_1, \varepsilon_2$. σ is the radiation constant, $5.670 \times 10^{-8} [\text{W}/\text{m}^2\text{K}^4]$.

$$\dot{q}_{rad} = \frac{\sigma(T_1^4 - T_2^4)}{\frac{1}{\varepsilon_1} + \frac{1}{\varepsilon_2} - 1} \quad (31)$$

When considering the possible effects of heat transfer in gaps by radiation, it should be taken into account that the difference between the surface temperature of the manikin body (or the temperature of the hotplate of the Permetest) and the temperature of the outside air (or air temperature in the Permetest channel) was about 10 °C only. From the above equation follows that at these temperature differences, the level of heat transfer by radiation between the studied clothing and the outside air at the room temperature, compared with the total heat flow, will be low, less than 15%. Regarding the level of radiation heat flow between the walls creating the air gaps in manikins or at the Permetest testing, the temperature differences between the air gap walls will be even lower, thus reducing even more the heat flow transferred in air gaps by radiation. To simplify heat transfer analysis in clothing, heat transfer in clothing by radiation is generally neglected [32], which also follows from most published papers dealing with thermal manikins.

When evaluating the achieved results, the experiments showed that a very strong correlation between the thermal manikin and the vertically oriented Permetest skin model in R_{ct}/R_{et} of the combinations of four materials (100% cotton, 50/50% cotton/polyester, 100% polyester and 100% polypropylene) and five air gap distances (0, 4, 8, 12, 16 mm), the R^2 of the R_{ct} is range from 0.70 – 0.95 and R_{et} is range from 0.80 - 1. Also, their arithmetic means of correlation coefficient in R_{ct} and R_{et} are both over 0.9. With these results, correlation tests between vertically and horizontally oriented Permetest skin model were set up with the combinations of seven materials and five air

gap distances (0, 4, 8, 12, 16 mm), and the R^2 of the R_{ct} is range from 0.88 – 0.98, and R_{et} is range from 0.92 - 1; their arithmetic means of correlation coefficient in R_{ct} and R_{et} are both over 0.9. The correlation coefficient and R^2 showed that the vertically and horizontally oriented Permetest experiments have a strong relationship and a strong positive trend. Since a strong relationship between thermal manikin and the vertically oriented Permetest skin model and a strong correlation between the vertically and horizontally oriented Permetest skin model implying that the horizontally oriented Permetest skin model also has a strong relationship with the thermal manikin.

To further develop the relationship between the thermal manikin and the Permetest skin model, the best-fit equation for the R_{ct}/R_{et} must be determined.

From **Section 4.7** R_{ct} data fit better in polynomial so that:

$$R_{ct} = a_1X^2 + b_1X + c_1, \text{ when}$$

$$0 = a_1X^2 + b_1X + (c_1 - R_{ct}), \text{ then}$$

$$X = -b_1 + [b_1^2 - 4a_1(c_1 - R_{ct})]^{1/2} / 2a_1 \quad (32)$$

Here, X is the hypothetical height (h) in millimetre

From **Section 4.7**, R_{et} data fit better in linear so that:

$$R_{et} = a_2X + b_2, \text{ when substitute (32) to X}$$

$$R_{et} = a_2\{-b_1 + [b_1^2 - 4a_1(c_1 - R_{ct})]^{1/2} / 2a_1\} + b_2 \quad (33)$$

$$R_{et} = 1/2(a_2/a_1)\{[b_1^2 - 4a_1(c_1 - R_{ct})]^{1/2} - b_1\} + b_2 \quad (34)$$

5.1 Validation

First, using the **Eq (34)**, constants from the vertically oriented Permetest equations (*Table 22*) and the actual R_{ct} results from the thermal manikin to calculate the R_{et} . The results are presented in *Table 19* and *Table 18* is showing the Mean values are regulated without the three outliers (in red).

Second, comparing the actual R_{et} test results to the calculated results and analysis. *Table 20* is presented the comparing results. Sample shirts were made of four materials which were 100% cotton, 50/50% cotton/polyester blend, 100% polyester and 100% polypropylene.

Values in red are the outliers from the original data in *Table 19*. Without them the results will look as following:

Table 18. R_{et} calculated results without the outliers

COT	Test 1 [m ² ·Pa/W]	Test 2 [m ² ·Pa/W]	Test 3 [m ² ·Pa/W]	Mean [m ² ·Pa/W]	SD	CV %
12mm	(6.84)	10.98	10.73	10.86	0.18	2
Cot/PES	Test 1	Test 2	Test 3	Mean	SD	CV %
8mm	(16.59)	10.75	10.84	10.80	0.06	1
12mm	10.92	10.51	(16.59)	10.72	0.29	3

Table 19. R_{et} calculated results by using Eq (34), R_{ct}^* results from the thermal manikin (Table 7) and constants from the Vertically Oriented Permetest skin model

* Unit which is used in thermal manikin software Kevin [K] is converted to milli-Kevin [mK] before calculation, and the resulting unit is in [m^2Pa/W]

COT	Test 1 [m^2Pa/W]	Test 2 [m^2Pa/W]	Test 3 [m^2Pa/W]	Mean [m^2Pa/W]	SD	CV %
4mm	10.47	9.06	9.79	9.77	0.71	7.2
8mm	11.23	10.3	10.3	10.61	0.54	5.1
12mm	6.84	10.98	10.73	9.52	2.32	24.4
16mm	11.72	11.23	12.3	11.75	0.54	4.6
Cot/PES	Test 1	Test 2	Test 3	Mean	SD	CV %
4mm	9.51	9.76	9.26	9.51	0.25	2.6
8mm	16.59	10.75	10.84	12.73	3.35	26.3
12mm	10.92	10.51	16.59	12.67	3.40	26.8
16mm	12.04	11.16	11.32	11.51	0.47	4.1
PES	Test 1	Test 2	Test 3	Mean	SD	CV %
4mm	8.15	8.58	8.91	8.55	0.38	4.5
8mm	9.08	9.49	8.91	9.16	0.30	3.3
12mm	8.83	9.49	9.74	9.35	0.47	5.0
16mm	10.38	10.62	10.38	10.46	0.14	1.3
PP	Test 1	Test 2	Test 3	Mean	SD	CV %
4mm	5.98	5.68	5.92	5.86	0.16	2.7
8mm	6.98	6.52	7.32	6.94	0.40	5.8
12mm	6.92	7.21	8.11	7.41	0.62	8.4
16mm	7.27	7.94	7.72	7.64	0.34	4.5

Table 20. The comparison of the actual R_{et} values [$m^2.Pa/W$] calculated from the Eq (34) (based on the Skin model experiments) and R_{et} values measured on thermal manikin wearing a pre-wetted suit

*By the ISO 15634,2004, the comparative precision of total arithmetic mean: Serial model 6.8%, Parallel model 5.3%

	Arithmetic Mean		*Difference	
COT	Manikin [$m^2.Pa/W$]	Eq 34 [$m^2.Pa/W$]	in (%)	Eq 34/Manikin [$m^2.Pa/W$]
4mm	4.9	9.77	99	4.87
8mm	10.27	10.61	3	0.34
12mm	10.27	9.52	7	0.75
16mm	11.83	11.75	1	0.08
	Arithmetic Mean		Difference	
Cot/PES	Manikin [$m^2.Pa/W$]	Eq 34 [$m^2.Pa/W$]	in (%)	Eq 34/Manikin [$m^2.Pa/W$]
4mm	6.2	9.51	53	3.31
8mm	10	12.73	27	2.73
12mm	10.87	12.67	17	1.8
16mm	13.03	11.51	12	1.52
	Arithmetic Mean		Difference	
PES	Manikin [$m^2.Pa/W$]	Eq 34 [$m^2.Pa/W$]	in (%)	Eq 34/Manikin [$m^2.Pa/W$]
4mm	4.27	8.55	100	4.28
8mm	6.47	9.16	42	2.69
12mm	10.23	9.35	9	0.88
16mm	12.13	10.46	14	1.67
	Arithmetic Mean		Difference	
PP	Manikin [$m^2.Pa/W$]	Eq 34 [$m^2.Pa/W$]	in (%)	Eq 34/Manikin [$m^2.Pa/W$]
4mm	8.23	5.86	29	2.37
8mm	10.73	6.94	35	3.79
12mm	15.42	7.41	52	8.01
16mm	13	7.64	41	5.36

The difference is calculated by Eq (35),

$$(\bar{R}_{et} - \bar{V}/\bar{R}_{et}) * 100 \quad (35)$$

where \bar{R}_{et} is the arithmetic mean of the actual R_{et} test results, \bar{V} is the arithmetic mean of the calculated test results. In general, the 4 mm air gap has the largest difference between the actual and the calculated values; then, the difference becomes smaller at 8 and 12 mm. In a 16 mm air gap, free convection starts to introduce to the air gap. Hence, the value of the difference is difficult to predict.

Reasons for 4 mm has the biggest difference may be caused by the following explanations:

- 1- Air gap spacing (*Figure 25*). When the sample shirt was draped on top of the pre-wetted suit, a narrower air gap (smaller shirt size) had a higher possibility to contact the pre-wetted suit directly due to the properties of the material; like stiffness, resiliency, moisture absorbent, porosity and so on that would cause creasing or wrinkles which would increase the contact point/area. Contact points or areas influence spacing between the sample shirt and the pre-wetted suit that will decrease the actual evaporative resistance R_{et} of the shirt. On the other hand, a bigger size shirt has a bigger air gap. This air spacing between the pre-wetted suit and the sample shirt acted like a cushion layer that would prevent the material stick to the pre-wetted suit layer to create contact areas. However, from 10 mm to 12mm, the air gap spacing is big enough that free convection will start. This phenomenon will influence the results on R_{et} and make it unpredictable.

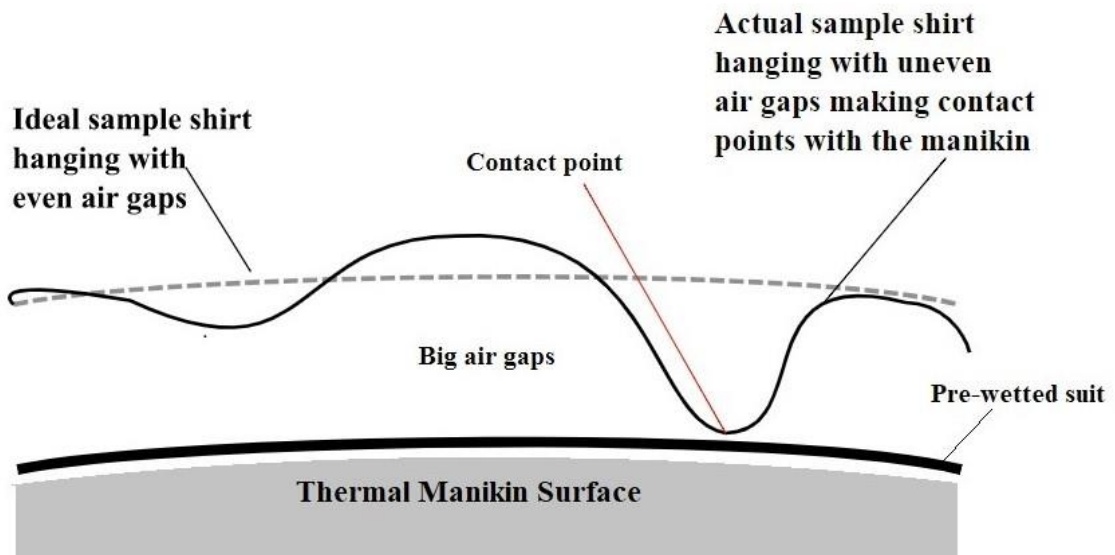
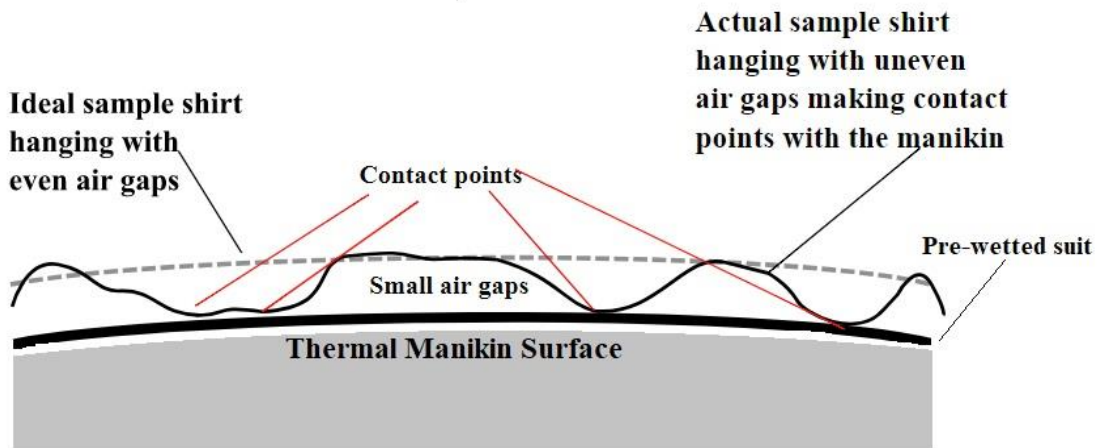


Figure 25. Cross-sections of a small and a big air gap between the thermal manikin wearing a pre-wetted suit and a sample shirt

- 2- The air gap thermal conductivity (λ) of 4mm is about 0.025; however, the average λ of materials used in the experiment is 0.04, which is higher than the air gap that may cause unpredictable outcomes when the air gap is small. *Table 21* presented the results of thermal conductivity of each material by means of Alambeta device.
- 3- Smaller air gap increases the probability of sample shirt contact directly to the thermal manikin wearing the pre-wetted suit, which will moisten the sample shirt and wetness will decrease the water vapor permeability, hence; decreases the evaporative resistance R_{et} [16].
- 4- First validation, labor errors may involve.

The above reasons conclude that the **Eq (34)** may not be suitable for air gap size 4mm or smaller. Further validation is needed.

Table 21. Thermal conductivity of four materials tested by Alambeta device

unit in [W/m·K]	Test 1	Test 2	Test 3	Test 4	Test 5	Mean
100% Cot	0.037	0.037	0.036	0.037	0.04	0.037
50/50% Cot/Pes	0.041	0.042	0.039	0.038	0.037	0.039
100% Pes	0.043	0.045	0.045	0.046	0.044	0.045
100% PP	0.052	0.047	0.048	0.05	0.05	0.049

Table 22. Constants from Polynomial of R_{ct} and Linear of R_{et}

$R_{ct} [m^2 \cdot mK/W] = a_1 X^2 + b_1 X + c_1$							$R_{et} [m^2 \cdot Pa/W] = a_2 X + b_2$			
Constant	a₁		b₁		c₁		a₂		b₂	
Orientation	H	V	H	V	H	V	H	V	H	V
100% Cotton	-	-	95.96	67.96	-	-	6.11	6.48	-	-
	10.48	6.34			81.84	52.78			3.85	6.06
80/20% Cotton/ Polyester	-	-	86.43	51.41	-	-	7.78	6.79	-	-
	9.95	4.13			63.54	31.42			6.10	5.51
70/30% Cotton/ Polyester	-	-	90.18	48.69	-	-	6.43	6.09	-	-
	10.20	3.33			65.86	28.52			3.13	4.19
50/50% Cotton/ Polyester	-	-	111.08	60.63	-	-	6.42	5.87	-	-
	13.94	5.57			86.64	40.40			4.04	4.77
35/65% Cotton/ Polyester	-	-	122.24	76.66	-	-	6.57	5.69	-	-
	15.48	8.06			99.78	57.96			5.11	4.65
100% Polyester	-	-	94.88	59.30	-	-	5.44	5.47	-	-
	10.06	4.86			79.36	45.34			4.56	5.35
100% Polypropylene	-	-	120.03	82.80	-	-	6.43	5.55	-	-
	14.37	9.12			95.98	59.68			2.95	2.87

6. Conclusion

This Thesis deals with a new method of determination of thermal and evaporation resistance of clothing by means of thermal manikins. The so called dry thermal manikins serve for the determination of thermal resistance of clothing, whereas the very costly sweating manikins measure the clothing evaporation resistance. Due to irregular moisture distribution absorbed in clothing, which also reduces thermal resistance and water vapour permeability of the tested clothing, the experimental results achievable in these manikins suffer from low reproducibility.

In the study, the mentioned method in which thermal resistance data measured on dry manikins are transformed into evaporation resistance of clothing, was theoretically analysed and experimentally verified. The transformation procedure is based in comparative measurements of thermal and evaporation resistances in special vertical Skin model, which enables to evaluate heat and mass transfer in simulated vertical air gaps corresponding to real air gaps in the worn clothing. The achieved results then were statistically treated, theoretically analysed and then presented as transformation equations, specific to all tested woven fabrics.

The evaporation resistance data determined by these equations then were correlated with data achieved by testing of clothing (made of the studied fabrics) on real sweating manikin in the Lund University in Sweden. For air gaps in the range of 8 to 14 mm (the mostly occurring gaps) the differences did not exceed 15%, which can be accepted as a good result when considering the complexity of the measurements.

It should be emphasized, that no study on similar topic was found in the literature, despite many papers published on manikins. The achieved results were presented on a few conferences and in several papers. Till now, no negative comments to this new method were observed. Application of the presented method may extend the use of cheaper and easy operable dry manikins in many textile laboratories in the world, despite certain limitations of this new method.

7. Future Scope of Work

- Phrase 2 – Second validate, same materials (only cotton and polyester due to limited access time to the manikin lab) with the same setup, procedures and apparatuses. Air gap distance/shirt allowance will be 5mm and 10mm. Each shirt will be tested five times for R_{ct} and R_{et} . Results will be used in **Eq (34)** for the validation and the comparison to the first validation and analysis.
- Phrase 3 -- Same setup, procedures, apparatuses and air gap distance/shirt allowance will be 0, 4, 8, 12, 16mm. Each shirt will be tested five times for R_{ct} and R_{et} . Thicker natural and synthetic materials will be chosen, for example, denim and broadcloth versus synthetic corduroy and satin. Results will be analyzed and compared to the first experiment.

8. References

- [1] Choudhury, R., Majumdar, A. K., P. K., Datta, C. “Factors Affecting Comfort: Human Physiology and the Role of Clothing”. In *Improving Comfort in Clothing*, edited by Song, G.; 3–60. Woodhead Publishing Series in Textiles. Woodhead Publishing, 2011. <https://doi.org/10.1533/9780857090645.1.3>.
- [2] “HSE - Thermal Comfort: The Six Basic Factors”. Accessed 14 June 2020. <https://www.hse.gov.uk/temperature/thermal/factors.htm>.
- [3] Holmér, I., “Thermal Manikin History and Applications”. *European Journal of Applied Physiology* 92, no. 6(September 2004): 614–18. <https://doi.org/10.1007/s00421-004-1135-0>.
- [4] Lu, Y., Kuklane, K., Gao, C., “2 - Types of Thermal Manikin”. In *Manikins for Textile Evaluation*, edited by Rajkishore Nayak and Rajiv Padhye, 25–54. Woodhead Publishing Series in Textiles. Woodhead Publishing, 2017. <https://doi.org/10.1016/B978-0-08-100909-3.00002-9>.
- [5] Thermal Manikin “423 Operator’s Manual Pdf” by Measurement Technology, Northwest.
- [6] International Organization for Standardization (ISO), “Clothing--Physiological Effects—Measurement of Thermal Insulation by Means of a Thermal Manikin” (ISO 15831: 2004)’, 2004.
- [7] “Manikin History | Thermetrics”, Accessed 21 June 2020. <https://www.thermetrics.com/solutions/manikin-history>.
- [8] “Thermal Manikin”, in *Wikipedia*, 18 May 2020. https://en.wikipedia.org/w/index.php?title=Thermal_manikin&oldid=957275718.
- [9] “USARIEM: Thermal Manikin History”. Accessed 5 July 2020. https://www.usariem.army.mil/index.cfm/about/divisions/bbmd/thermal_manikin
- [10] Wang, F., Kuklane, K., Gao, C., Holmér, I., “Development and Validity of a Universal Empirical Equation to Predict Skin Surface Temperature on Thermal Manikins”. *Journal of Thermal Biology* 35, no. 4 (1 May 2010): 197–203. <https://doi.org/10.1016/j.jtherbio.2010.03.004>.
- [11] Hes, L., Araujo, M. de, “Simulation of the Effect of Air Gaps between the Skin and a Wet Fabric on Resulting Cooling Flow”. *Textile Research Journal* 80, no. 14 (9 January 2010): 1488–97. <https://doi.org/10.1177/0040517510361797>.
- [12] Hes, L., “Analysis and Experimental Determination of Effective Water Vapor Permeability of Wet Woven Fabrics”. *Journal of Textile and Apparel, Technology and Management*. 2014 May 29 <http://ojs.cnr.ncsu.edu/index.php/JTATM/article/view/5317>
- [13] ASTM F2370-16. Standard test method for measuring the evaporative resistance of clothing using a sweating manikin. West Conshohocken, PA: Author, 2016.
- [14] Havenith, George, Richards, M., “Use of Clothing Vapour Resistance Values derived from Manikin Mass Losses or Isothermal Heat Losses may cause severe Under or Over Estimation of Heat Stress”, 2008, 2.
- [15] Havenith, George, Richards, M., Wang, X. , Bröde, P., Candas, V., Hartog, E. den, Holmér, I., Kuklane, K., Meinander, H., Nocker. W., “Apparent Latent Heat of Evaporation from Clothing: Attenuation and “Heat Pipe” Effects”. *Journal of Applied Physiology* 104, no. 1 (1 January 2008): 142–49. <https://doi.org/10.1152/jappphysiol.00612.2007>.

- [16] “Breathability in Quality Control at Hohenstein Institute”. Accessed 9 July 2020. <https://www.innovationintextiles.com/breathability-in-quality-control-at-hohenstein-institute/>.
- [17] “Sweating Guarded Hotplate | Thermetrics”. Accessed 22 June 2020. <https://www.thermetrics.com/products/guarded-hotplates/sweating>.
- [18] Huang, Jianhua, “Sweating Guarded Hot Plate Test Method”. *Polymer Testing* 25, no. 5 (1 August 2006): 709–16. <https://doi.org/10.1016/j.polymertesting.2006.03.002>.
- [19] ISO, EN. “11092: 2014 Textile”. *Physiological Effects. Measurement of Thermal and Water-Vapour Resistance under Steady-State Conditions (Sweating Guarded-Hotplate Test)*, n.d.
- [20] Fourier1878.pdf [Internet]. [cited 2021 May 12]. Available from: <https://www3.nd.edu/~powers/ame.20231/fourier1878.pdf>
- [21] Špelić, I., Mihelić-Bogdanić, A., Šajatović, A.H., “Standard Methods for Thermal Comfort Assessment of Clothing”. *CRC Press*; 2019. <https://doi.org/10.1201/9780429422997>
- [22] Huang, J., “Review of Heat and Water Vapor Transfer through Multilayer Fabrics”, 2016 Available from internet: <https://journals.sagepub.com/doi/full/10.1177/0040517515588269>
- [23] Reiners P, Kyosev Y., “About the Thermal Conductivity of Multi-layer Clothing.” *Hochschule Niederrhein – University of Applied Sciences Faculty of Textile and Clothing Technology Mönchengladbach, Germany* * priscilla.reiners@hs-niederrhein.de
- [24] Zarr, Robert R., “A History of Testing Heat Insulators at the National Institute of Standards and Technology”. *Ashrae Transactions* 107 (2001): 661.
- [25] Stoffberg, M. E., Hunter, L. Botha, A., “The Effect of Fabric Structural Parameters and Fiber Type on the Comfort-Related Properties of Commercial Apparel Fabrics”, *Journal of Natural Fibers*, 2015, 12:6, 505-517, DOI: 10.1080/15440478.2014.967370
- [26] Akalović, J., Skenderi, Z., FirštRogale, S., Zdraveva, E., “Water Vapor Permeability of Bovine Leather for Making Professional Footwear, *Leather & Footwear*” 67, 2018, Original Scientific Paper UDC:675.14.031.1.017.6:685.345.
- [27] Fung, F. T., Hes, L. Bajzik, V. “A Study of Air Permeability Influences on Pattern Cutting”, *Vlakna a Textil – Fibres and Textiles*, volume 26, December 2019.
- [28] Hes, L. “Optimisation of Shirt Fabrics” Composition from the Point of View of Their Appearance and Thermal Comfort’. *International Journal of Clothing Science and Technology* 11, no. 2/3 (1 January 1999): 105–19. <https://doi.org/10.1108/09556229910276250>.
- [29] Kaczmarek, F., Joanna, A., Psikuta, Bueno, M. A , Rossi. R. M., “Air Gap Thickness and Contact Area in Undershirts with Various Moisture Contents: Influence of Garment Fit, Fabric Structure and Fiber Composition”. *Textile Research Journal* 85, no. 20 (1 December 2015): 2196–2207. <https://doi.org/10.1177/0040517514551458>.
- [30] Pavlinic', Z., Daniela, Geršak, J., “Investigations of the Relation between Fabric Mechanical Properties and Behaviour”. *International Journal of Clothing Science and Technology* 15, no. 3/4 (1 January 2003): 231–40. <https://doi.org/10.1108/09556220310478332>.
- [31] Bassett, Richard J., Postle, R., Pan, N., “Experimental Methods for Measuring Fabric Mechanical Properties: A Review and Analysis”. *Textile Research Journal* 69, no. 11 (1 November 1999): 866–75. <https://doi.org/10.1177/004051759906901111>.
- [32] Baczek M., Hes L., “Determination of heat transfer by radiation in textile fabrics by means of method with known emissivity of plates“ *Journal of Industrial Textiles* 44(1):115-129, 2014

- [33] Oglakcioglu, N., Celik, P., Bedez T., Ute, A., Marmarali, H., Kadoglu, “Thermal Comfort Properties of Angora Rabbit/Cotton Fiber Blended Knitted Fabrics –2009”. Accessed 8 July 2020. <https://journals.sagepub.com/doi/abs/10.1177/0040517508099396>.
- [34] Chen, Y.S., Fan, J., Qian, X., Zhang, W., “Effect of Garment Fit on Thermal Insulation and Evaporative Resistance – 2004”. Accessed 9 July 2020. <https://journals.sagepub.com/doi/abs/10.1177/004051750407400814>.
- [35] Nayak, R K, Punj, S. K., Chatterje, K. N., “Comfort Properties of Suiting Fabrics”. *INDIAN J. FIBRE TEXT. RES.*, 2009, 7.
- [36] Verdu P., Jose M., Rego, J., Nieto, Blanes, K. N., “Comfort Analysis of Woven Cotton/Polyester Fabrics Modified with a New Elastic Fiber, Part 1 Preliminary Analysis of Comfort and Mechanical Properties”. *Textile Research Journal* 79, no. 1 (1 January 2009): 14–23. <https://doi.org/10.1177/0040517508090888>.
- [37] Stull, Jeffrey O. “American Society for Testing and Materials”. *Performance of Protective Clothing: Sixth Volume*. ASTM International, 1997.
- [38] Rego, Jose M., Verdu, P., Nieto, J., Blanes, M., “Comfort Analysis of Woven Cotton/Polyester Fabrics Modified with a New Elastic Fiber, Part 2: Detailed Study of Mechanical, Thermo-Physiological and Skin Sensorial Properties”. *Textile Research Journal* 80, no. 3 (1 February 2010): 206–15. <https://doi.org/10.1177/0040517508099910>.
- [39] Reiners, P., Kyosev, Y., “About the Thermal Conductivity of Multi-layer Clothing”, Hochschule Niederrhein – University of Applied Sciences Faculty of Textile and Clothing Technology Mönchengladbach, Germany.
- [40] Ding, D., Tang, T., Song, G., McDonald, A., “Characterizing the Performance of a Single-Layer Fabric System through a Heat and Mass Transfer Model - Part I: Heat and Mass Transfer Model”. *Textile Research Journal* 81, no. 4 (1 March 2011): 398–411. <https://doi.org/10.1177/0040517510388547>.
- [41] Hes, L., Araujo, M., “Simulation of the Effect of Air Gaps between the Skin and a Wet Fabric on Resulting Cooling Flow”. *Textile Res. Journal*, Vol. 80, No. 14, pp. 1488–1497, 2010, ISSN 1746-5175
- [42] Fukazawa, T., Lee, G., Matsuoka, T., Kano, K., Tochiyama, Y., “Heat and Water Vapour Transfer of Protective Clothing systems in a Cold Environment, Measured with a Newly Developed Sweating Thermal Manikin”, *Eur J Appl Physiol*, 2004, 92: 645–648, DOI: 10.1007/s00421-004-1124-3
- [43] Bogusławska-Bączek, M., Hes, L., “Effective Water Vapour Permeability of Wet Wool Fabric and Blended Fabrics”, *Fibres & Textiles in Eastern Europe*, 2013, Vol. 21, No. 1 (97).
- [44] Wang, L., “Heat, Moisture and Air Transfer Properties of Selected Woven Fabrics in Wet State”. *Journal of Fiber Bioengineering and Informatics* 2, no. 3 (June 2009): 141–49. <https://doi.org/10.3993/jfbi12200901>.
- [45] Gibson, P.W., “Factors Influencing Steady-State Heat and Water Vapor Transfer Measurements for Clothing Materials”. *Textile Research Journal* 63, no. 12 (1 December 1993): 749–64. <https://doi.org/10.1177/004051759306301208>.
- [46] Hes, L., Dolezal, I., “Indirect Measurement of Moisture Absorptivity of Functional Textile Fabrics”. *Journal of Physics: Conference Series* 1065 (August 2018): 122026. <https://doi.org/10.1088/1742-6596/1065/12/122026>.
- [47] “Methods of Evaluating Protective Clothing Relative to Heat and Cold Stress: Thermal Manikin, Biomedical Modeling, and Human Testing”. Accessed 10 August-2020. <https://www.tandfonline.com/doi/full/10.1080/15459624.2011.613291>.

- [48] Wyon; David P., “Use of Thermal Manikins in Environmental Ergonomics”. *Scandinavian Journal of Work, Environment & Health* 15 (1989): 84–94.
- [49] “Comparative Evaluation of Clothing Thermal Insulation Measured on a Thermal Manikin and on Volunteers”. Accessed 8 July 2020. http://www.fibtex.lodz.pl/61_17_73.pdf.
- [50] Hassan, M., Qashqary, K., Hassan, H. A., Shady, E., Alansary, M, “Influence of Sportswear Fabric Properties on the Health and Performance of Athletes”. *Fibres & Textiles in Eastern Europe* Nr 4 (93) (2012). <http://yadda.icm.edu.pl/baztech/element/bwmeta1.element.baztech-article-BPW7-0023-0062>.
- [51] Wang, F., “A Comparative Introduction on Sweating Thermal Manikins “Newton” and “Walter””, 2008, 8.
- [52] Salmon, D., “Thermal Conductivity of Insulations Using Guarded Hot Plates, Including Recent Developments and Sources of Reference Materials”. *Measurement Science and Technology* 12, no. 12 (2001): R89.
- [53] Healy, W. M, “Using Finite Element Analysis to Design a New Guarded Hot Plate Apparatus for Measuring the Thermal Conductivity of Insulating Materials” Accessed 17 July 2020. https://tsapps.nist.gov/publication/get_pdf.cfm?pub_id=860852.
- [54] Scoarnec, V., Hameury, J., Hay, B., “A New Guarded Hot Plate Designed for Thermal-Conductivity Measurements at High Temperature”. *International Journal of Thermophysics* 36, no. 2–3 (March 2015): 540–56. <https://doi.org/10.1007/s10765-014-1794-y>.
- [55] Reddy, K. S., Jayachandran, S., “Investigations on Design and Construction of a Square Guarded Hot Plate (SGHP) Apparatus for Thermal Conductivity Measurement of Insulation Materials”. *International Journal of Thermal Sciences* 120 (2017): 136–147.
- [56] Zarr, Robert R., “A History of Testing Heat Insulators at the National Institute of Standards and Technology”. *Ashrae Transactions* 107 (2001): 661.
- [57] Nayak, Rajkishore, Padhye, R., “Manikins for Textile Evaluation”. Woodhead Publishing, 2017.
- [58] Lei, Z., “Review of Application of Thermal Manikin in Evaluation on Thermal and Moisture Comfort of Clothing – 2019”. Accessed 5 July 2020. <https://journals.sagepub.com/doi/full/10.1177/1558925019841548>.
- [59] “Thermal Manikin Testing 1997”. Accessed 10 August 2020. http://www.lth.se/fileadmin/eat/Termisk_miljoe/ArbLivsRapp1997_9.PDF#page=37.
- [60] Matsunaga, Kazuhiko, F., Sudo, S., Tanabe, Madsen, T. L., “Evaluation and Measurement of Thermal Comfort in the Vehicles with a New Thermal Manikin”. SAE Technical Paper. Warrendale, PA: SAE International, 1 November 1993. <https://doi.org/10.4271/931958>.
- [61] Anttonen; Hannu, J., Niskanen, H., Meinander, V., Bartels, K., Kuklane, Randi E., Reinertsen, S., Varietas; Sołtyński, K., “Thermal Manikin Measurements—Exact or Not?” *International Journal of Occupational Safety and Ergonomics* 10, no. 3 (January 2004): 291–300. <https://doi.org/10.1080/10803548.2004.11076616>.
- [62] Sun, C., Fan, “Comparison of Clothing Thermal Comfort Properties Measured on Female and Male Sweating Manikins”. *Textile Research Journal* 87, no. 18 (1 November 2017): 2214–23. <https://doi.org/10.1177/0040517516669071>.
- [63] Mijovic, Budimir, Skenderi, Z., Camara, J. A., “Inflatable Mannequin for Testing Thermal Properties of Clothing”. In *Proceedings of the 17 Th World Congress on Ergonomics. Beijing, IEA, 2009*.

- [64] Matusiak, Małgorzata, Sybilska, W., “Thermal Resistance of Fabrics vs. Thermal Insulation of Clothing Made of the Fabrics”. *The Journal of The Textile Institute* 107, no. 7 (2 July 2016): 842–48. <https://doi.org/10.1080/00405000.2015.1061789>.
- [65] Satsumoto, Yayoi, K., Ishikawa, Takeuchi, M., “Evaluating Quasi-Clothing Heat Transfer: A Comparison of the Vertical Hot Plate and the Thermal Manikin”. *Textile Research Journal* 67, no. 7 (1 July 1997): 503–10. <https://doi.org/10.1177/004051759706700705>.
- [66] Xiaohong Z, Chunqin Z, Yingming Q, et al. “The Thermal Insulation Difference of Clothing Ensembles on the Dry and Perspiration Manikins”. *Meas Sci Technol* 2010; 21: 85203.
- [67] Chen YS, Fan JT, Zhang W. “Clothing Thermal Insulation during Sweating”, *Text Res J*, 2003; 73: 152–157.
- [68] Wang FM, Kuklane K, Gao CS, et al. “Effect of Temperature Difference between Manikin and Wet Fabric Skin Surfaces on Clothing Evaporative Resistance: How Much Error is There?” *Int J Biometeorol* , 2012; 56: 177–182.
- [69] Richter, Jan; Stanek, K., “Measurements of Water Vapour Permeability – Tightness of Fibreglass Cups and Different Sealants and Comparison of μ -Value of Gypsum Plaster Boards”. *Procedia Engineering* 151 (2016): 277–83. <https://doi.org/10.1016/j.proeng.2016.07.377>.
- [70] Nuclear Power. “What Is Rayleigh Number”. Accessed 23 August 2020. <https://www.nuclear-power.net/nuclear-engineering/heat-transfer/introduction-to-heat-transfer/characteristic-numbers/what-is-rayleigh-number/>.
- [71] Pirobloc. “How Rayleigh’s Number Links Conduction and Convection”, 24 April 2018. <https://www.pirobloc.com/en/blog-en/how-the-rayleigh-number-links-conduction-convection/>.
- [72] Rayleigh Number | Definition, Formula & Calculation | nuclear-power.net [Internet]. Nuclear Power. [cited 2021 Apr 16]. Available from: <https://www.nuclear-power.net/nuclear-engineering/heat-transfer/introduction-to-heat-transfer/characteristic-numbers/what-is-rayleigh-number/>
- [73][cited 2021 Apr 16]. Available from: <http://hmf.enseeiht.fr/travaux/CD9900/travaux/optmfn/gpfmho/99-00/grp13/chap2.htm>
- [74] Kerr RM. “Rayleigh number scaling in numerical convection”. *Journal of Fluid Mechanics*. 310(1):139.
- [75] Nuclear Power. “Thermal Diffusivity”. Accessed 23 August 2020. <https://www.nuclear-power.net/nuclear-engineering/heat-transfer/thermal-conduction/heat-conduction-equation/thermal-diffusivity/>.
- [76] Nuclear Power. “Flow Regime”. Accessed 23 August 2020. <https://www.nuclear-power.net/nuclear-engineering/fluid-dynamics/flow-regime/>.
- [77] “Rayleigh Number - an Overview | ScienceDirect Topics”. Accessed 8 September 2020. <https://www.sciencedirect.com/topics/chemistry/rayleigh-number>.
- [78] Smith R., Inomata H., Peters C., “Chapter 8 - Heat Transfer and Finite-Difference Methods”. *Supercritical Fluid Science and Technology [Internet]. Elsevier; 2013 [cited 2021 Apr 16]. p. 557–615. <https://www.sciencedirect.com/science/article/pii/B9780444522153000088>*
- [79] Durst F. editor, “In Fluid Mechanics: An Introduction to the Theory of Fluid Flows.” *Springer*, 2008 Berlin, Heidelberg p. 193–219. Available from: https://doi.org/10.1007/978-3-540-71343-2_7
- [80] Similarity theory - Encyclopedia of Mathematics [Internet]. Available from: https://encyclopediaofmath.org/wiki/Similarity_theory

- [81] Theories of Similarity [Internet]. [cited 2021 May 16]. Available from: <http://www.pigeon.psy.tufts.edu/avc/dblough/theory.htm>
- [82] Similarity Theory - TheFreeDictionary.com. Available from: <https://encyclopedia2.thefreedictionary.com/Similarity+Theory>
- [83] ResearchGate. “Determination of Heat Transfer by Radiation in Textile Fabrics by Means of Method with Known Emissivity of Plates”. Accessed 13 September 2020. https://www.researchgate.net/publication/264200451_Determination_of_heat_transfer_by_radiation_in_textile_fabrics_by_means_of_method_with_known_emissivity_of_plates.
- [84] Schirmer, R.: Die Diffusionszahl von Wasserdampf-Luft-Gemischen und die Verdampfungsgeschwindigkeit, Beiheft VDI-Zeitschrift, Verfahrenstechnik (1938), H. 6, p. 170-177)
- [85] “Thermal Manikin Testing”. Accessed 8 July 2020. http://www.lth.se/fileadmin/eat/Termisk_miljoe/ArbLivsRapp1997_9.PDF#page=37.
- [86] “KES-F7 Thermo Labo | KATO TECH CO., LTD. | Pioneer of Texture Testers and Electronic Measuring Instruments”. Accessed 6 July 2020. <https://english.keskato.co.jp/archives/products/kes-f7>.
- [87] Permetest Manual 09.’. Accessed 6 July 2020. <http://www.sensora.eu/PermetestManual09.pdf>.
- [88] Hes, L. “Permetest Instrument”. *Liberec: Sensora Instrument and Consulting*, 2005.
- [89] Fung, F. T., Krucinska, I., Draczynski, Z, Hes, L., Bajzik, V., “Method of Patternmaking for Sweating Thermal Manikin for Research Purposes”, *Vlakna a Textil – Fibres and Textiles*, VaT 1, volume 27, March 2020.
- [90] Wang FM, Lai DD, Shi W, et al., “Effects of Fabric Thickness and Material on Apparent ‘Wet’ Conductive Thermal Resistance of Knitted Fabric ‘Skin’ on Sweating Manikins”. *J Therm Biol* 2017; 70: 69–76.
- [91] Wang FM, Zhang CJ and Lu YH., “Correction of the Heat Loss Method for Calculating Clothing Real Evaporative Resistance”. *J Therm Biol* 2015; 52: 45–51.
- [92] Wang FM, Ji EL, Zhou XH, et al., “Empirical Equations for Intrinsic and Effective Evaporative Resistance of Multi-layer Clothing Ensembles”. *Ind Text* 2010; 61: 176–180.

9. List of Tables

Table 1	Properties comparison among the thermal manikin, sweating guarded hotplate and Permetest skin model	8
Table 2	The sweating thermal manikin is in wet-skin (in blue) prepared for water vapor resistance tests and sweating guarded hotplate is put inside the climatic chamber before any sample testing; and Permetest skin model is in the vertical orientation	9
Table 3	Rayleigh number for air gap size 0-16mm, values in red are for reference only	19
Table 4	Properties of materials **	24
Table 5	Differences between the thermal manikin and the Permetest skin model	30
Table 6	The total increase in each sample's circumference and the increase in each sample's front and back pattern pieces	41
Table 7	Effective R_{ct} results from the thermal manikin tests	43
Table 8	Effective R_{et} results from the thermal manikin tests	45
Table 9	Effective R_{ct} results from Permetest skin model in the Vertically Oriented position	51
Table 10	Effective R_{et} results from Permetest skin model in the Vertically Oriented position	54
Table 11	The correlation coefficient (r) of Thermal Manikin Vs. Vertically Oriented skin model	56
Table 12	The correlation determination (R^2) of Thermal Manikin Vs. Vertically Oriented skin model	57
Table 13	The arithmetic mean values of 7 materials resulted from R_{ct}/R_{et} and the combinations of Horizontal/ Vertical orientation and air gap distances	59-62
Table 14	R_{ct} -Difference between Horizontally and Vertically Oriented Air gaps	63
Table 15	R_{et} -Difference between Horizontally and Vertically Oriented Air gaps	63
Table 16	Correlation coefficient (r) results of R_{ct}/R_{et} and the combinations of Horizontally/Vertically Oriented air gap distances from 7 materials	66

Table 17	Regression results of R_{ct}/R_{et} and the combinations of Vertically/Horizontally Oriented air gap distances from 7 materials	67
Table 18	R_{et} calculated results without the outliers	74
Table 19	R_{et} calculated results by using Eq (29), R_{ct}^* results from the thermal manikin (Table 7) and constants from the Vertically Oriented Permetest skin model	75
Table 20	The comparison of the actual R_{et} values ($m^2.Pa/W$) calculated from the Eq (29) (based on the Skin model experiments) and R_{et} values measured on thermal manikin wearing a pre-wetted suit	76
Table 21	Thermal conductivity of four materials tested by Alambeta device	79
Table 22	Constants from Polynomial of R_{ct} and Linear of R_{et}	80
Table 23	Fibre density– values are found based on open sources on internet	97
Table 24	Fabric weight and thickness by measurement	98
Table 25	Color code and measured area of each draped-sample shape	101
Table 26	A collection of microscopic, physical, chemical, biological, thermal properties of fibres; and the functional group and fibre content	102-103
Table 27	Thermal resistance data from the thermal manikin	107
Table 28	Evaporation resistance data from the thermal manikin	108
Table 29	Thermal resistance data from Permetest skin model-1	109
Table 30	Thermal resistance data from Permetest skin model-2	110
Table 31	Evaporation resistance data from Permetest skin model-1	111
Table 32	Evaporation resistance data from Permetest skin model-2	112
Table 33	Thermal resistance data from Permetest skin model of seven fabrics	113-115
Table 34	Evaporative resistance data from Permetest skin model of seven fabrics	116-118

10. List of Figures

Figure 1	Sweating thermal manikin-Newton (<i>Figure 1. is downloaded from thermetrics.com</i>)	5
Figure 2	Newton in wet-suit and walking mode (<i>Figure 2. is downloaded from thermetrics.com</i>)	5
Figure 3	Sweating guarded hot plate and software (<i>Figure 3. is downloaded from mesdan.it</i>)	6
Figure 4	Permetest skin model	6
Figure 5	Image of the planimeter device (<i>Figure 5. is downloaded from researchgate.net</i>)	27
Figure 6a-g	Photomicrographic images of seven materials by Promicra	28-29
Figure 7	Tore- the dry manikin is in standing mode inside the climatic chamber	31
Figure 8	Front view of Tore in prewetted suit	31
Figure 9	Back view of Tore in prewetted suit	31
Figure 10	Permetest skin model in vertical orientation	34
Figure 11	Top view of Permetest skin model	34
Figure 12	Front view of Permetest skin mode in horizontal orientation	34
Figure 13	Principle of the thermal manikin	35
Figure 14	Principle of Permetest skin model	35
Figure 15a-f	a. Tore - Dry thermal manikin	38

	b. The molding method -- duct tape was applied on top of the plastic shrink wrap which was tightly wrapped around the torso of the manikin for protection and easy unmolding	38
	c. Unmolded front and back pieces and were divided into small segments according to the contour lines on the manikin's torso	38
	d. Unmolded arm piece from shoulder to wrist and cut into small segments	39
	e. The arm piece was converted into two-dimensional sleeve patterns	39
	f. The finished shirt was completed with bodice and sleeves and was closed in the center back	39
Figure 16	The grey area is the torso of the thermal manikin and air gap distance is added to the radius of the torso that will become the ease allowance of the clothing for the thermal manikin	40
Figure 17	Comparison of R_{ct} results from the thermal manikin tests of four materials	44
Figure 18	Comparison of R_{et} results from the thermal manikin of four materials	46
Figure 19a-c	a. Sizes of outer and inner rings	49
	b. Showing outer rings were stacked on the base of the hotplate	49
	c. Showing inner rings were placed inside the wind channel on the hotplate	49
Figure 20	Comparison of the R_{ct} results from the Vertically Oriented Permetest of four materials	52
Figure 21	Comparison of the R_{et} results from Vertically Oriented Permetest of four materials	55
Figure 22	Visual comparison of the vertically and horizontally oriented air gaps of R_{ct}	64
Figure 23	Visual comparison of the vertically and horizontally oriented air gaps of R_{et}	64
Figure 24a-n	The best-fit model for data from the R_{ct}/R_{et} of seven materials	69-70

Figure 25	The cross-section of a small and a big air gap between the thermal manikin wearing a pre-wetted suit and a sample shirt	78
Figure 26	Image of the M290 Moisture Management Tester (MMT)	96
Figure 27	Image of the FX 3300 Air Permeability Tester	96
Figure 28	Schematic diagram of the draping test <i>device (Figure 28. is downloaded from Indiantextilejournal.com)</i>	99
Figure 29	Image of the draping shape of the sample	99
Figure 30	Image of the planimeter device <i>(Figure 5. is downloaded from researchgate.net)</i>	100
Figure 31	Draped outlines of seven material samples	100
Figure 32	Sensirion (screenshot) is monitoring heat loss in every heat zone involved in the experiment in adjustable time period. Here is every 2 minutes 30 seconds	104
Figure 33	Sensirion (screenshot) is monitoring temperature changing in every heat zone involved in the experiment in adjustable time period. Here is every 2 minutes	104
Figure 34	Picolog recording temperature changing of heat zones in every 10 seconds during the thermal resistance experiment	105
Figure 35	The screenshot is showing part of the results of thermal resistance tests from Sensirion and Picolog softwares	106

11. List of Publications by the Author

List of Publications in Research Journals

- Fung, F. T., Hes, L., Unmar, R., Bajzik, V., “Thermal and Evaporative Resistance measured in a Vertically and Horizontally Oriented Air Gap by Permetest Skin Model” *Industria Textila Journal*, April 2021. **Impact factor: 0.784**
- Fung, F. T., Hes, L., Bajzik, V., “A Study of Air Permeability Influences on Pattern Cutting”, *Vlakna a Textil – Fibres and Textiles*, VaT 4, volume 26, December 2019. Recorded in **Scopus**
- Fung, F. T., Krucinska, I., Draczynski, Z, Hes, L., Bajzik, V., “Method of Patternmaking for Sweating Thermal Manikin for Research Experiment Purposes”, *Vlakna a Textil – Fibres and Textiles*, VaT 1, volume 27, March 2020. Recorded in **Scopus**
- Fung, F. T., Kalaoglu, F., Altay, P., Hes, L., Bajzik, V., “Measuring Movement Ease for Clothing Pattern by means of Special made Shirt”, *Vlakna a Textil – Fibres and Textiles*, VaT 2, volume 27, June 2020. Recorded in **Scopus**
- Fung, F. T., Hes, L., Bajzik, V., “Review of Men’s Shirt Pattern Development for the Last 100 Years – Part 1. The Bodice” *Vlakna a Textil – Fibres and Textiles*. VaT 3, volume 27, September 2020. Recorded in **Scopus**
- Fung, F. T., Gao, C., Hes, L., Bajzik, V., “Water Vapor Resistance Measured on Sweating Thermal Manikin and Permetest Skin Model in the Vertical Orientation”, *Journal of Communications in Development and Assembling of Textile Products, (CDATP)*, September 2020. **DOI:** <https://doi.org/10.25367/cdatp.2020.1>
- Fung, F. T., Hes, L., and Bajzik, V., “Review of Men’s Shirt Pattern Development for the Last 100 Years – Part 2. Sleeve and Cuff” *Vlakna a Textil – Fibres and Textiles*. VaT 4, volume 28, March 2021. Recorded in **Scopus**

List of Publications in International Conferences

- Fung, F. T., Havelka, A., “Small Increase in Clothing Pattern Relates to Thermal Insulation in Clothing of Woven Fabric”, International Ph.D. Students Day, CEC 2017, Liberec, Czech Republic.
- Fung, F. T., Havelka, A., “Effect of Air Permeability on Grainlines, Aged, Washed and Moistened Woven Fabric” won the **3rd prize** of poster presentation, International Ph.D. Students Day, 22nd Strutex 2018, Liberec, Czech Republic.
- Fung, F. T., Hes, L., Bajzik, V., “Review of Men’s Shirt Pattern Development” 47th Textile Research Symposium 2019, Liberec, Czech Republic.

Research Projects

- Member of the student grant competition (SGS) project 2017, “Increase in Clothing Pattern Relates to Thermal Insulation in Clothing of Woven Fabric”, Faculty of Textile Engineering, Technical University of Liberec, Czech Republic.
- Member of the student grant competition (SGS) project 2018- number 21246, “Estimate Wearing Ease for Movement for Clothing Pattern of Men’s Shirt of Woven Fabric”, Faculty of Textile Engineering, Technical University of Liberec, Czech Republic.

12. Appendices

Appendix 1- Images of devices



Figure 26. Image of the M290 Moisture Management Tester (MMT)

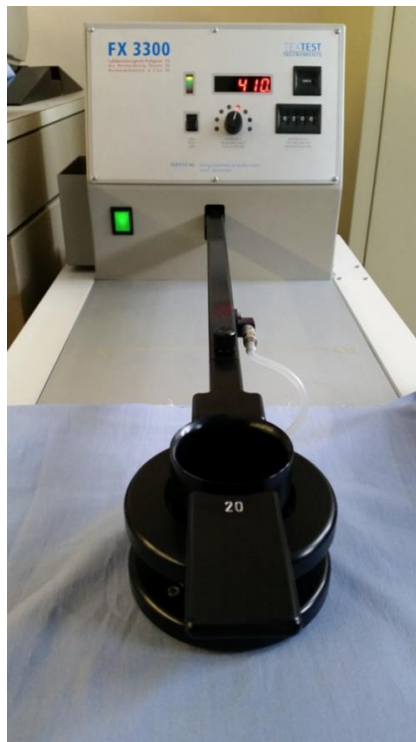


Figure 27. Image of the FX 3300 Air Permeability Tester

Appendix 2 – Porosity Information of Seven Fabrics

$$\phi = [\rho_{fabric} / \rho_{fibre}] \quad (14)$$

$$\rho_{fabric} = \text{Fabric square mass} / h \quad (15)$$

$$P = (1 - \phi) * 100\% \quad (16)$$

where P (%) is the fabric porosity

ϕ is the fibre volume of solid material

ρ_{fabric} [kg/m^2] is the fabric density

ρ_{fibre} [kg/m^3] is the fibre density

h [m] is the thickness of the fabric

Table 23. Fibre density – values are found based on open sources on internet

	100% Cotton	100% Polyester	100% Polypropylene
[kg/m^3]	1540	1360	900

The following fibre density is calculated based on the proportion of 100% cotton density and 100% polyester density

	80% Cotton 20% Polyester	70% Cotton 30% Polyester	50% Cotton 50% Polyester	35% Cotton 65% Polyester
[kg/m^3]	1504	1486	1450	1423

Table 24. Fabric square mass and thickness by measurement

	100% Cotton	100% Polyester	100% Polypropylene	80% Cotton 20% Polyester	70% Cotton 30% Polyester	50% Cotton 50% Polyester	35% Cotton 65% Polyester
Fabric weight [g/m ²]	154	156	252	225	226	159	102
<i>h</i> [mm]	0.37	0.43	0.63	0.55	0.58	0.33	0.23

Appendix 3 - Drapability Information of Seven Fabrics

1. Fabric samples are cut into a circular shape with 300mm in diameter
2. An A3 size paper is put on top of the glass screen over the draping device as shown in Figure 20-21
3. Trace out the silhouette of the draped shape
4. A planimeter is used to measure the draped area (Figure 22-23)
5. Use equation (27) to calculate the percentage of the sample drapability

$$D (\%) = [A - A_p / A_m] * 100\% \quad (17)$$

where D is the fabric drapability (%)

A is the area of circular fabric sample – $70.69 * 10^3$ [mm²]

A_p is the area of projection [mm²] – measured by Planimeter

A_m is the area of annulus – $45.24 * 10^3$ [mm²]

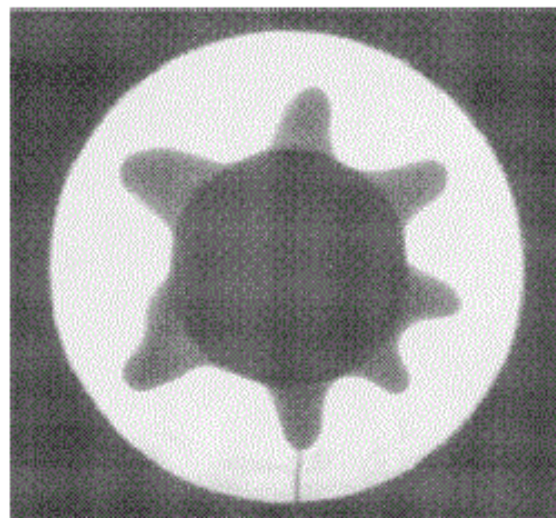
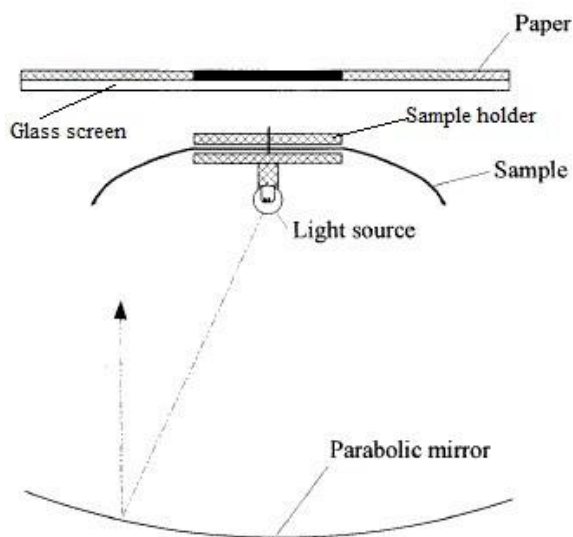


Figure 29. Image of the draping shape of the sample

Figure 28. Schematic diagram of the draping test device

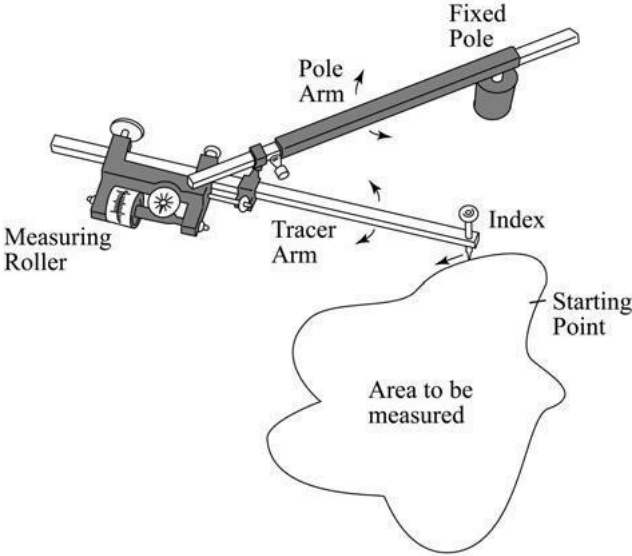


Figure30. Image of the planimeter device

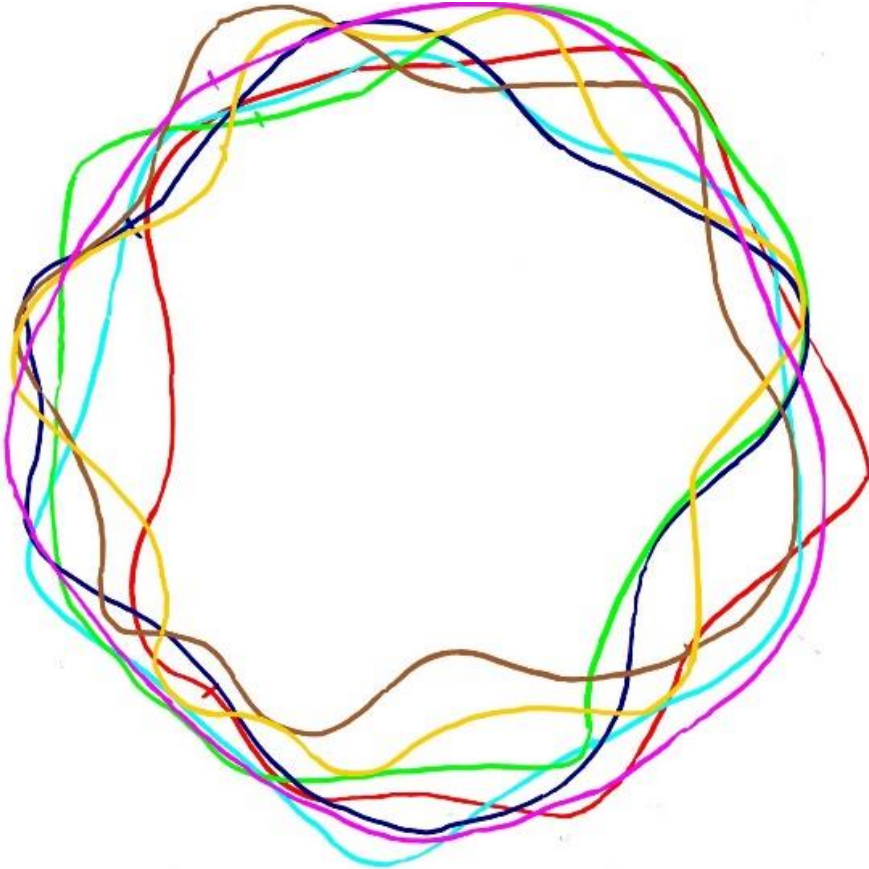


Figure 31. Draped outlines of seven material samples

Table 25. Color code and measured area of each draped-sample shape



100% Cotton
55240 mm²



80% Cotton
20% Polyester
57060 mm²



70% Cotton
30% Polyester
56090 mm²



50% Cotton
50% Polyester
53090 mm²



35% Cotton
65% Polyester
51280 mm²



100% Polyester
51060 mm²



100% Polypropylene
66060 mm²

Appendix 4 – Fibre properties

Table 26. A collection of microscopic, physical, chemical, biological, thermal properties of fibres; and the functional group and fibre content

Microscopic properties	Cotton	Polyester	Polypropylene
Cross-section and Shape	Kidney-shaped cross-section, flat and twisted ribbon-like structure. Convolutions are 150-400 per inch	Cross-section shapes, length and thickness are controlled by spinnerets	
Physical properties	Cotton	Polyester	Polypropylene
Length Thickness	20-30 mm 12-20 μm	Cross-section shapes, length and thickness are controlled by spinnerets	
Luster	Low, mercerization increases luster	Can be adjusted by chemical finish	Low
Tenacity Dry/Wet (gram/denier)	D 3-5/ W 3.3-6	D/W 5-7	D/W 3.5-5
Break Elongation Dry/Wet (%)	D 25-35 W 25-50	D 19-23 W 19-23	D 25-75 W 25-75
Resiliency	Low - wrinkles easily	90% wrinkles resistant	Low
Moisture Regain Dry/ Wet (%)	8/15-25	0.04	0.1
Density (kg/m^3)	1540	1350	900
Chemical properties	Cotton	Polyester	Polypropylene
Effect of Alkali	Highly resistant	<ul style="list-style-type: none"> - high alkali resistance - chemically resistant to acid, bases, salts and most solvents - Outstanding fibre dispersibility - biogenic origin - industrial biodegradable 	
Effect of Acids	Easily damaged by strong mineral acids Hot diluted acids will cause disintegration faster than cold diluted acids		
Effect of Organic Solvents	Highly resistant		
Biological properties	Cotton	Polyester	Polypropylene
Effect of Mildew	Affected in dam condition	No	
Effect of Moth	No		
Effect of Sunlight	Prolong sunlight weaken fibre	It can withstand 12 months of exposure	The chemical structure of

		to sunlight and still retain over 67% of its strength	polypropylene causes a high degradation rate when exposed to UV light
Thermal properties	Cotton	Polyester	Polypropylene
Effect of Flame	It burns readily and quickly and smells like burning paper, and leaves a small amount of fluffy gray ash.	It will shrink from the flame and burn slowly with black smoke and a sweet chemical odor. Its residue is a soft, sticky black ash.	It burns very well and smells like charred wood, and will continue to burn slowly, producing drips even the flame source is removed
Static Charge	No	Yes	Yes
Melting Point and Glass Transitional Temperature	Over 150 °C fibre decompose, and glass transitional temperature is Tg 220 °C	-Melting point 250 °C - Tg 75 °C	-Soften at 150°C -Melting point 165 °C
Conductivity (W/mK)	0.026-0.065	0.218	0.172
Functional Group	Cotton	Polyester	Polypropylene
	Natural polymer Cellulosic (C ₆ H ₁₀ N ₅) _n	Ester group O = C – O (C ₁₀ H ₈ O ₄) _n	Methyl group R– CH ₃ (C ₃ H ₆) _n
Fibre Content	Cotton	Polyester	Polypropylene
	Cellulose 90% Water 8% Pectin 0.55% Wax/Fat 0.4% Others 0.2%	Made from the mixture of dicarboxylic acid and dialcohol	Made from the combination of propylene monomers

Appendix 5 – Sensirion software samples

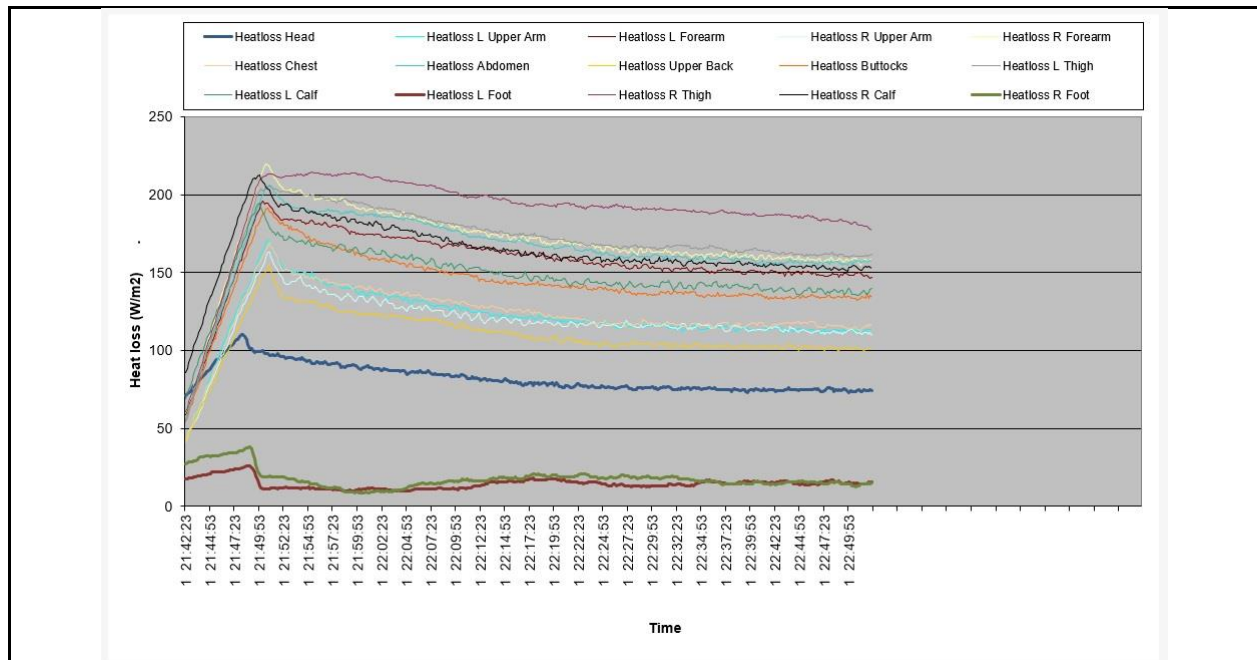


Figure 32. Sensirion (screenshot) is monitoring heat loss in every heat zone involved in the experiment in adjustable time period. Here is every 2 minutes 30 seconds

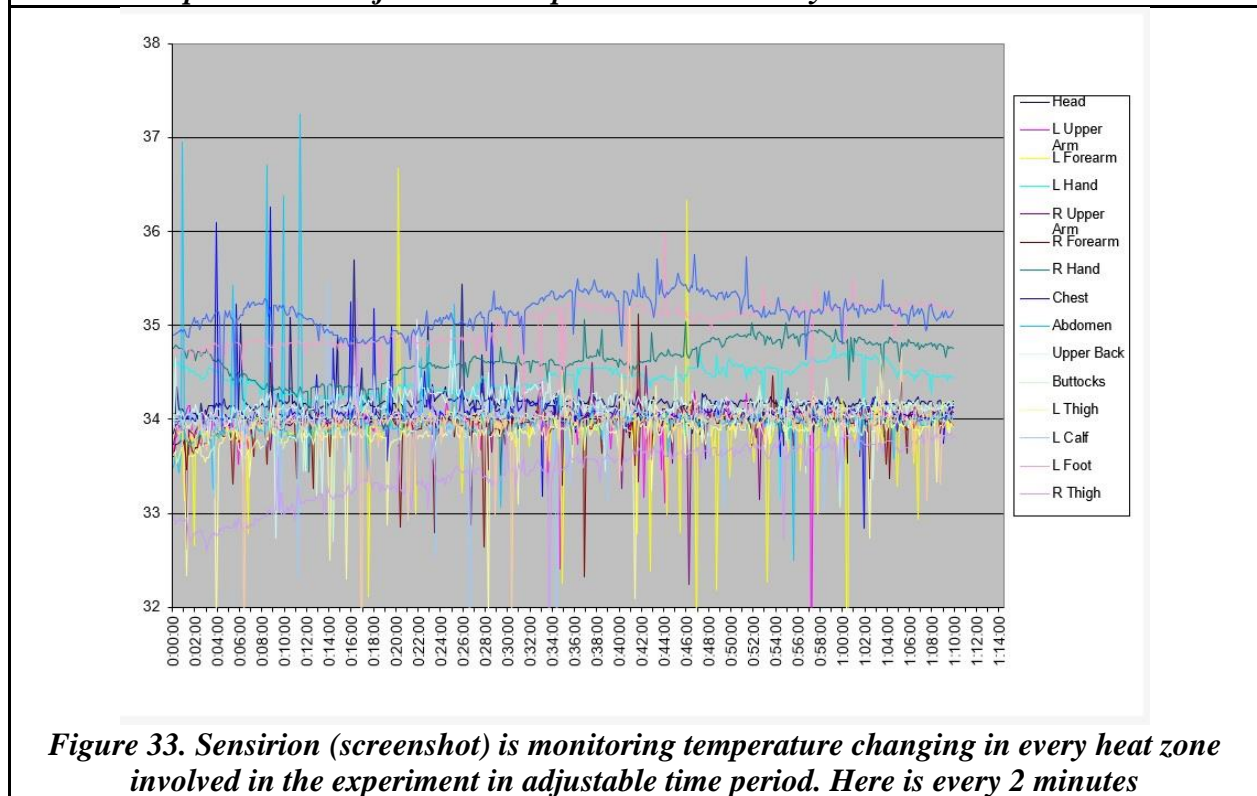


Figure 33. Sensirion (screenshot) is monitoring temperature changing in every heat zone involved in the experiment in adjustable time period. Here is every 2 minutes

Appendix 7 – Sensirion and Picolog resultant sample

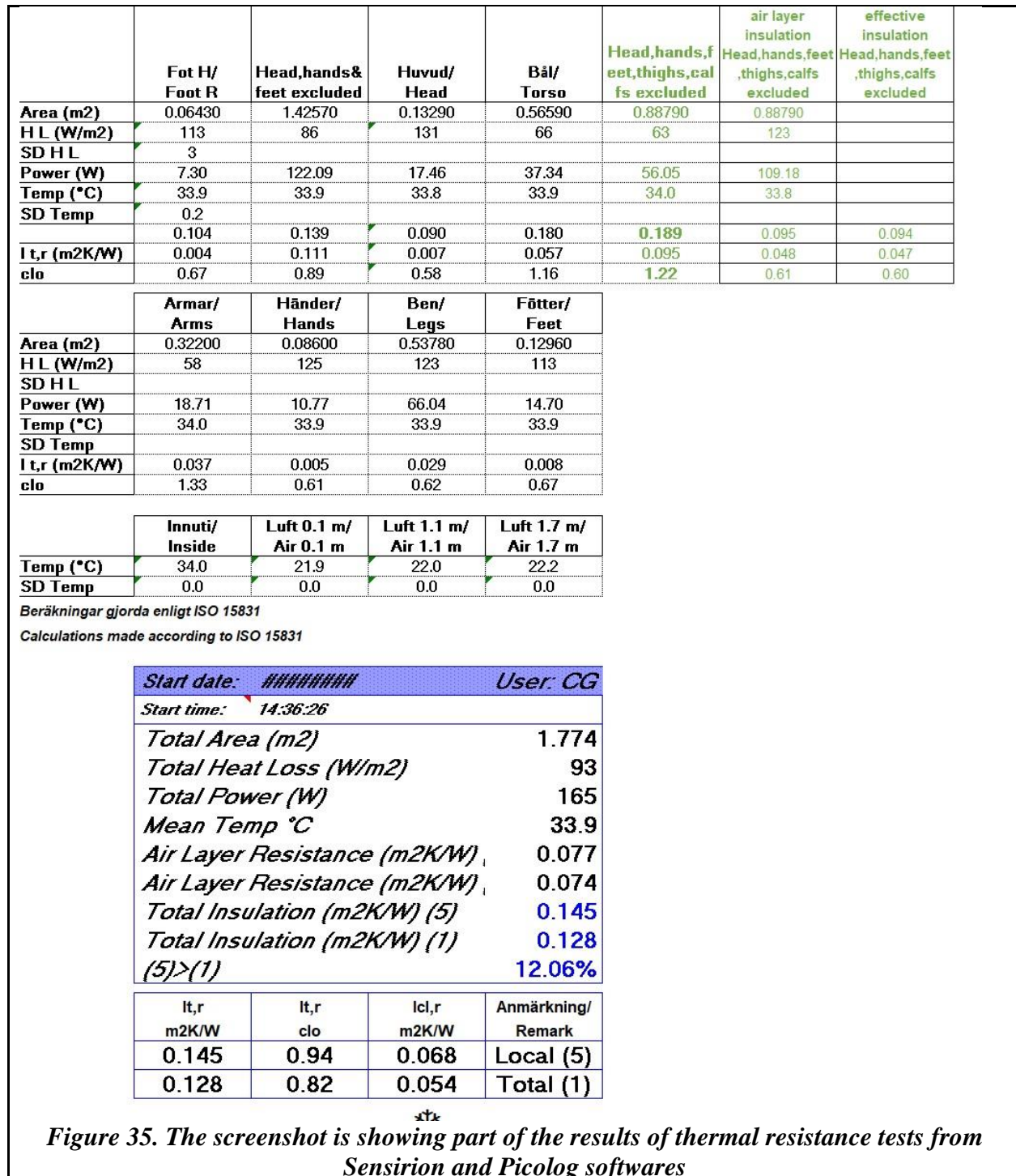


Figure 35. The screenshot is showing part of the results of thermal resistance tests from Sensirion and Picolog softwares

Appendix 8 - Original Data from Thermal Manikin

(A combination of 3 tests for each material sample, 4 materials and 5 air gap distances)

Thermal Manikin - Thermal Resistance Data

Table 27. Thermal resistance data from the thermal manikin

Thermal Resistance (Rct) Thermal Manikin	100% Cotton [m ² .K/W]	50% Cotton 50% Polyester [m ² .K/W]	100% Polyester [m ² .K/W]	100% Polypropylene [m ² .K/W]
0mm air gap Test 1	0.075	0.08	0.062	0.081
Test 2	0.076	0.074	0.063	0.099
Test 3	0.073	0.076	0.065	0.095
4mm air gap Test 1	0.102	0.093	0.077	0.109
Test 2	0.09	0.096	0.082	0.104
Test 3	0.094	0.09	0.086	0.108
8mm air gap Test 1	0.111	0.111	0.088	0.126
Test 2	0.1	0.108	0.093	0.118
Test 3	0.1	0.109	0.086	0.132
12mm air gap Test 1	0.061	0.11	0.085	0.125
Test 2	0.108	0.105	0.093	0.13
Test 3	0.105	0.111	0.096	0.146
16mm air gap Test 1	0.117	0.124	0.104	0.131
Test 2	0.111	0.113	0.107	0.143
Test 3	0.124	0.115	0.104	0.139

Thermal Manikin - Evaporative Resistance Data

Table 28. Evaporation resistance data from the thermal manikin

Evaporative Resistance (Ret) Thermal Manikin	100% Cotton [m ² .Pa/W]	50% Cotton 50% Polyester [m ² .Pa/W]	100% Polyester [m ² .Pa/W]	100% Polypropylene [m ² .Pa/W]
0mm air gap Test 1	5.5	5.8	2.1	5.2
Test 2	2.9	6.5	1.6	4.4
Test 3	6.3	5.3	1.5	4.3
4mm air gap Test 1	5.1	6.6	4.2	7.7
Test 2	3.8	6.4	3.8	8.4
Test 3	5.8	5.6	4.8	8.6
8mm air gap Test 1	10.7	8.4	5.8	12.5
Test 2	9	10	7.2	9.7
Test 3	11.1	11.6	6.4	10
12mm air gap Test 1	9.3	10.3	9.3	18
Test 2	8.1	11.2	11.4	13
Test 3	13.4	11.1	10	14.8
16mm air gap Test 1	10.4	13.3	12.8	14.3
Test 2	13.8	12.7	12.5	12.2
Test 3	11.3	13.1	11.1	12.5

Appendix 9 - Original Data from Permetest Skin Model

(A combination of 3 tests for each material sample, 2 orientations, 4 materials and 5 air gap distances)

Permetest Skin Model - Thermal Resistance Data

Table 29. Thermal resistance data from Permetest skin model-1

Thermal Resistance (Rct) Permetest Skin Model	100% Cotton		50% Cotton 50% Polyester	
	Vertical Orientation [m ² .mK/W]	Horizontal Orientation [m ² .mK/W]	Vertical Orientation [m ² .mK/W]	Horizontal Orientation [m ² .mK/W]
0mm air gap Test 1	8	11.3	11.7	9.9
Test 2	9.6	10.2	12.8	9.8
Test 3	8.5	9.7	9.9	11.7
4mm air gap Test 1	54.9	68.1	45.9	48.8
Test 2	72.3	74.5	44.8	46.7
Test 3	69.3	70.1	47.5	47.3
8mm air gap Test 1	97.2	96.8	67.7	83.9
Test 2	93.2	87.4	69.5	71.5
Test 3	93	96	69.7	64.9
12mm air gap Test 1	93.6	112.3	69.6	94
Test 2	94.9	98.7	77.2	88.9
Test 3	97	102.9	74.7	85.6
16mm air gap Test 1	105.5	108.1	67.5	94.2
Test 2	118.6	106.8	84.3	79.6
Test 3	95.4	100.2	94.8	95

Table 30. Thermal resistance data from Permetest skin model-2

Thermal Resistance (Rct) Permetest Skin Model	100% Polyester		100% Polypropylene	
	Vertical Orientation [m ² .mK/W]	Horizontal Orientation [m ² .mK/W]	Vertical Orientation [m ² .mK/W]	Horizontal Orientation [m ² .mK/W]
0mm air gap Test 1	7.1	8	12.9	11.9
Test 2	8.8	8.7	11.8	13.7
Test 3	7.6	7.8	11.4	13
4mm air gap Test 1	54	69.3	45.5	61.6
Test 2	56.1	58.1	57.5	58
Test 3	54.4	59.2	61.2	59.5
8mm air gap Test 1	75.2	82	88.7	86.6
Test 2	76	85.6	90.5	89.2
Test 3	73.5	83.9	89.3	91
12mm air gap Test 1	89.9	96.4	88.9	91.4
Test 2	87.3	101.9	89.5	106.5
Test 3	93.1	100.5	100.7	101.8
16mm air gap Test 1	105.9	107.3	94.5	94.9
Test 2	96.2	106.6	90.3	92.2
Test 3	101.1	104.6	85.8	91.4

Permetest Skin Model - Evaporative Resistance Data

Table 31. Evaporation resistance data from Permetest skin model-1

Evaporative Resistance (Ret) Permetest Skin Model	100% Cotton		50% Cotton 50% Polyester	
	Vertical Orientation [m ² .Pa/W]	Horizontal Orientation [m ² .Pa/W]	Vertical Orientation [m ² .Pa/W]	Horizontal Orientation [m ² .Pa/W]
0mm air gap Test 1	3.4	3.8	4.2	2.8
Test 2	2.9	2.7	3.6	2.7
Test 3	3.8	2.9	3.1	2.9
4mm air gap Test 1	8.2	8.8	5.8	4.9
Test 2	8.4	8.9	6.3	5.3
Test 3	8	8.6	6.2	5.7
8mm air gap Test 1	12.9	13	11.7	11.7
Test 2	12.7	13	11.7	11.1
Test 3	13.1	15.7	11	11.1
12mm air gap Test 1	23.4	21.6	22.3	20.8
Test 2	22.1	22.6	22.9	21.5
Test 3	21.9	32.1	21.3	25.8
16mm air gap Test 1	25.1	28.1	26.3	19.9
Test 2	28.5	23.1	25.8	29.9
Test 3	22.9	33.7	28	36.4

Table 32. Evaporation resistance data from Permetest skin model-2

Evaporative Resistance (Ret) Permetest Skin Model	100% Polyester		100% Polypropylene	
	Vertical Orientation [m ² .Pa/W]	Horizontal Orientation [m ² .Pa/W]	Vertical Orientation [m ² .Pa/W]	Horizontal Orientation [m ² .Pa/W]
0mm air gap Test 1	4.2	2.8	1.5	1.4
Test 2	3.6	2.7	1.6	1.5
Test 3	3.1	2.9	1.5	1.5
4mm air gap Test 1	5.8	4.9	7.2	5.7
Test 2	6.3	5.3	7.4	7.6
Test 3	6.2	5.7	7.6	7.5
8mm air gap Test 1	11.7	11.7	14.5	17.8
Test 2	11.7	11.1	13.9	17.7
Test 3	11	11.1	13.8	15.8
12mm air gap Test 1	22.3	20.8	20.2	20.8
Test 2	22.9	21.5	20.7	20.3
Test 3	21.3	25.8	21.3	20.5
16mm air gap Test 1	26.3	19.9	23.1	26.2
Test 2	25.8	29.9	27.4	23.4
Test 3	28	36.4	22.9	21

Appendix 10 - Original Data from the Vertical/Horizontal Permetest Skin Model

(A combination of 5 tests for each material sample, 7 materials, 5 air gap distances and 2 orientations)

Permetest Skin Model - Thermal Resistance Data

Table 33. Thermal resistance data from Permetest skin model of seven fabrics

Thermal Resistance (R _{ct}) Permetest Skin Model	100% Cotton		80% Cotton 20% Polyester	
	Vertical Orientation [m ² .mK/W]	Horizontal Orientation [m ² .mK/W]	Vertical Orientation [m ² .mK/W]	Horizontal Orientation [m ² .mK/W]
0mm air gap Test 1	8.3	9.6	15.1	12.5
Test 2	10.2	9.6	13.6	15.3
Test 3	9	10.7	11.8	12.7
Test 4	8.1	12.6	14.4	12.7
Test 5	11.6	11.6	11.8	12.7
4mm air gap Test 1	59.3	52.1	62.6	69.8
Test 2	57.1	46.7	63.1	64.6
Test 3	60.3	56.4	63.1	65.4
Test 4	61.6	55.2	59.9	69.1
Test 5	63.8	56.9	60.9	59.2
8mm air gap Test 1	82.9	111.8	78.7	130.1
Test 2	79.4	113	80.1	102.2
Test 3	86.7	108.5	85.7	122.6
Test 4	81.6	114.6	81.2	118.2
Test 5	80.2	116.1	74.2	109
12mm air gap Test 1	129.6	144.3	107.5	122.9
Test 2	131.7	143.5	108.8	122.9
Test 3	137	156.5	110.9	109.5
Test 4	127.2	143.4	105.9	102.9
Test 5	128.3	150.1	110.2	108.3

16mm air gap Test 1	126.5	140	127.3	130.9
Test 2	106.5	134.6	131.5	127.2
Test 3	135.3	124.4	127.4	117.5
Test 4	135.9	132.9	129.2	111.1
Test 5	114.8	114.1	100.3	128.5
Thermal Resistance (Rct) Permetest Skin Model	70% Cotton 30% Polyester		50% Cotton 50% Polyester	
	Vertical Orientation (m ² .mK/W)	Horizontal Orientation (m ² .mK/W)	Vertical Orientation (m ² .mK/W)	Horizontal Orientation (m ² .mK/W)
0mm air gap Test 1	12.5	16.7	12	13.4
Test 2	15.4	16.5	12	13.8
Test 3	12.4	16.3	14.5	14
Test 4	13.9	12.6	13.4	12.9
Test 5	13.6	14.7	13.8	12.8
4mm air gap Test 1	64.9	66.5	65.3	76.1
Test 2	65.4	69.4	62.5	74.5
Test 3	65.3	67.1	59.5	71.1
Test 4	62.7	69.8	62.3	73.5
Test 5	64.2	66.9	65.1	75.4
8mm air gap Test 1	77.1	122.4	91.8	127
Test 2	76.1	111.5	82.2	123.8
Test 3	91.3	126.6	89.9	114
Test 4	75.6	122.8	88.5	115.7
Test 5	81.1	128.2	86	124.2
12mm air gap Test 1	108.7	122.4	109.7	113.3
Test 2	113.8	125.9	110	136.8
Test 3	120.3	131	115.8	150.3
Test 4	110.7	120.4	117	154.8
Test 5	116	124.2	114.8	148.8
16mm air gap Test 1	133.1	129.3	125.7	119.4
Test 2	123.9	127.7	120.1	121.6
Test 3	149.1	137.4	116.5	122.7
Test 4	114.2	131	130.9	108.6
Test 5	142.1	134.1	125.7	114.7

Thermal Resistance (Rct) Permetest Skin Model	35% Cotton 65% Polyester		100% Polyester		100% Polypropylene	
	Vertical Orientation (m ² .mK/W)	Horizontal Orientation (m ² .mK/W)	Vertical Orientation (m ² .mK/W)	Horizontal Orientation (m ² .mK/W)	Vertical Orientation (m ² .mK/W)	Horizontal Orientation (m ² .mK/W)
0mm air gap Test 1	9.3	12	8.8	5.6	15.2	14.5
Test 2	13.3	10.3	7.4	5.5	16.3	16.5
Test 3	11	12.2	6.4	6.6	16.7	13.4
Test 4	12.5	11.3	7.2	5.8	15.2	17.7
Test 5	10.7	12.1	5.9	5.7	15	16
4mm air gap Test 1	64.9	76.5	55.6	69.6	69.2	64.9
Test 2	61.1	70.4	55.9	56.4	72	73.8
Test 3	66.8	71.6	55.1	74.2	71.1	77.8
Test 4	66.2	72.6	52.7	74.4	66.2	78.2
Test 5	63.4	71.1	64.9	70.1	70.7	79
8mm air gap Test 1	98.6	137.8	89.4	112.3	97.3	132.5
Test 2	92.2	124.5	91.9	116.8	98.5	146.8
Test 3	89.7	129.1	91	114.1	100.1	131.8
Test 4	89.3	134.9	88.1	119.1	88.4	144.1
Test 5	86.3	129.1	90.6	119.1	92.3	135.9
12mm air gap Test 1	114.8	157	105.1	136.2	148.9	167
Test 2	130.2	127.3	107.1	142.9	111.4	164
Test 3	140.5	153.2	110.5	140.7	142	157.1
Test 4	121.2	156.8	109.2	132	149.2	161.3
Test 5	139.6	142.3	115.2	139.1	149.9	163.9
16mm air gap Test 1	106.4	120	130	140.2	115.7	141.9
Test 2	126.5	115	121.1	161	125.1	128.4
Test 3	111.3	121.2	141	141.2	123.3	139.7
Test 4	133.6	135.2	137.2	141.7	122.1	149.5
Test 5	123.8	113.4	130.3	134	117.6	140.8

Permetest Skin Model - Evaporative Resistance Data

Table 34. Evaporative resistance data from Permetest skin model of seven fabrics

Evaporative Resistance (Ret) Permetest Skin Model	100% Cotton		80% Cotton 20% Polyester	
	Vertical Orientation [m ² .Pa/W]	Horizontal Orientation [m ² .Pa/W]	Vertical Orientation [m ² .Pa/W]	Horizontal Orientation [m ² .Pa/W]
0mm air gap Test 1	2.5	2.9	3.5	3.9
Test 2	2.7	2.8	3.8	4.2
Test 3	2.5	2.7	3.9	4.5
Test 4	2.5	2.7	3.6	3.9
Test 5	2.3	2.8	3.9	4.1
4mm air gap Test 1	5.4	6	6.1	6.6
Test 2	5.7	6	6.3	6.4
Test 3	5.3	6.2	6.2	6.7
Test 4	5.4	6.3	6.4	6.6
Test 5	5.3	6.6	6.2	6.7
8mm air gap Test 1	12.5	16.7	13.4	15.5
Test 2	12.6	16.1	13.7	15.2
Test 3	12.2	16	13.8	17.7
Test 4	12.1	15.9	12.9	14.5
Test 5	12.5	15	13.5	16.4
12mm air gap Test 1	18.1	23.8	23.5	26.9
Test 2	17.4	20.7	19.7	27.2
Test 3	17.9	23.8	19.7	24.8
Test 4	18.5	19.7	19.4	27
Test 5	18.1	22.4	18	27
16mm air gap Test 1	32.9	27.3	30	30.8
Test 2	31.9	24.9	33.3	29.4
Test 3	24.8	23.9	34.4	34.2
Test 4	27.9	24.4	28.1	36.9
Test 5	25.7	26	28.2	33.5

Evaporative Resistance (Ret) Permetest Skin Model	70% Cotton 30% Polyester		50% Cotton 50% Polyester	
	Vertical Orientation [m ² .Pa/W]	Horizontal Orientation [m ² .Pa/W]	Vertical Orientation [m ² .Pa/W]	Horizontal Orientation [m ² .Pa/W]
0mm air gap Test 1	3.7	3.4	2.8	2.7
Test 2	3.6	4	3	3
Test 3	3.6	4.1	2.7	2.8
Test 4	3.5	4	2.6	2.8
Test 5	3.4	3.5	2.6	3
4mm air gap Test 1	6.1	6.7	5.6	6.4
Test 2	6	6.8	5.4	6.4
Test 3	6.1	7.6	5.4	6.1
Test 4	6.2	7.2	5.6	5.9
Test 5	5.7	6.9	5.3	5.9
8mm air gap Test 1	13.7	19.3	12.3	15.8
Test 2	13.3	17.8	12.2	18.4
Test 3	13.1	16.3	11.9	15.1
Test 4	13.2	16	12.3	17.2
Test 5	13.1	19.3	12.2	17.6
12mm air gap Test 1	22.1	27.1	18.9	26.4
Test 2	21	27.3	18.4	23
Test 3	21.7	24.1	18.4	23.4
Test 4	19.5	23.8	17.8	24
Test 5	20	25.4	17.8	25.7
16mm air gap Test 1	26.4	26.7	23.8	25.7
Test 2	27.7	26.7	25.8	25.2
Test 3	26.6	27.1	29.3	25.7
Test 4	25.1	27.4	23.6	26.3
Test 5	27.1	25.3	25.7	26

Evaporative Resistance (Ret) Permetest Skin Model	35% Cotton 65% Polyester		100% Polyester		100% Polypropylene	
	Vertical Orientation [m ² .Pa/W]	Horizontal Orientation [m ² .Pa/W]	Vertical Orientation [m ² .Pa/W]	Horizontal Orientation [m ² .Pa/W]	Vertical Orientation [m ² .Pa/W]	Horizontal Orientation [m ² .Pa/W]
0mm air gap Test 1	2	2	1.5	1.6	3.7	4.4
Test 2	2.2	2.1	1.2	1.8	3.8	4.2
Test 3	1.7	2.1	1.1	1.8	3.7	4.1
Test 4	1.9	2.2	1.4	1.6	3.4	4.3
Test 5	2.1	2.3	1.2	1.7	3.4	4.6
4mm air gap Test 1	5.3	5.6	4.6	5.5	6.6	7.6
Test 2	5.1	5.8	4.9	5.4	6.5	7.8
Test 3	5.2	6.1	4.8	5.7	6.4	7.2
Test 4	5.2	5.5	4.7	5.5	6.4	7.4
Test 5	5.2	5.7	4.9	5.8	6.3	7.3
8mm air gap Test 1	11.7	13.9	12.1	13.1	13.9	14.6
Test 2	12.4	15.7	12.2	13.6	13.7	15.8
Test 3	12.2	15.2	12.3	13.2	14.5	14.4
Test 4	12.5	12.9	11.9	12.8	14	16.8
Test 5	12.3	17.1	12.1	13.2	14	18.3
12mm air gap Test 1	19.8	23.6	18.6	24.5	20.5	27.3
Test 2	20.5	22	18.5	26.5	20.5	27.3
Test 3	18.2	25.8	17.2	26.4	20	27.6
Test 4	19.4	25.1	17.7	25.8	20.4	27.2
Test 5	18.5	25.4	19.6	24.9	20.4	27.4
16mm air gap Test 1	23.8	25.9	24.4	25.6	22.6	24.6
Test 2	24.6	25.3	24.9	24.7	23.4	26
Test 3	22.5	25.7	25.1	25.2	23.7	26.4
Test 4	22.4	26.6	27	24.7	28.8	28.2
Test 5	23.5	24.9	23.5	25.3	23.4	27.3